UNDERSTANDING THE PHYSICOCHEMICAL PROPERTIES OF SOME IMIDAZOLIUM AND MORPHOLINIUM IONIC LIQUIDS BY STUDYING PHOTOPHYSICAL PROCESSES IN THESE MEDIA

A Thesis
Submitted for the Degree of

DOCTOR OF PHILOSOPHY

by

Dinesh Chandra Khara

School of Chemistry
University of Hyderabad
Hyderabad 500 046
INDIA

March 2013

Contents

STATEMENT i

CERTIFICATE ii

Acknowledgement iii

List of Publication v

Conference Presentation vii

Thesis Layout viii

Chapter 1. Introduction

1.1. Room temperature Ionic Liquids 1

1.1.1. A Brief Introduction 1

1.1.2. Properties of RTILs 4

1.1.3. Structural features and Heterogeneity 8

1.1.4. RTILs and Mixed Solvents 9

1.1.5. Application of RTILs 10

1.2. Photoinduced Conformational Change in the Excited State 13

1.3. Solvation Dynamics

1.3.1. Solvation Dynamics in Conventional Solvents 16

1.3.2. Solvation Dynamics in Confined Media 17

1.3.3. Solvation Dynamics in RTILs 17

1.4. Rotational Dynamics 18

1.4.1. Rotational Dynamics in Conventional Solvents 19

1.4.2. Rotational Dynamics in Confined Media 20
1.4.3. Rotational Dynamics in RTILs 20
1.5. Motivation Behind thesis 21
References 26

Chapter 2. Materials, Methods and Instrumentation

2.1. Materials 37
2.2. Purification of conventional solvents 39
2.3. Synthesis and purification of RTILs 40
2.4. Instrumentation 41
2.4.1. Picosecond time-correlated single-photon counting setup 42
2.5. Sample preparation for spectral measurements 42
2.6. Measurement of emission quantum yields and rate constant for reverse intersystem crossing 43
2.7. Data analysis 45
2.8. Construction of time-resolved emission spectra (TRES) 46
2.9. Time-resolved Anisotropy decay profiles 48
2.10. Estimation of polarity 49
2.11. Standard error limits 50
References 51

Chapter 3. Excited State Process of Bianthryl in Imidazolium Ionic Liquids

3.1. Introduction 53
3.2. Steady-state behavior 55
3.3. Time-resolved behavior 57
3.4. Conclusion 66
References 67

Chapter 4. Photophysical Processes of Benzil in Imidazolium Ionic Liquids

4.1. Introduction 69
4.2. Steady-state absorption 71
4.3. Steady-state emission 72
4.4. Temperature dependence of the delayed emission 76
4.5. Emission at 77 K 80
4.6. Conclusion 82
References 84

Chapter 5. Solute Rotation and Solvation Dynamics of Charged Solutes in Imidazolium Ionic Liquids

5.1. Introduction 87
5.2. Steady-State Behavior 91
5.3. Time-Resolved Measurements 92
5.3.1. Rotational Dynamics 92

5.3.2. Solvation Dynamics 102
5.4. Conclusion 107
References 108

Chapter 6. Solvation and Rotational Dynamics of C153 in N-alkyl-N-methylmorpholinium Ionic Liquids

6.1. Introduction 111
6.2. Steady-state Measurement 114
6.2.1. Steady-state absorption and emission 114
6.2.2. Temperature dependence of the emission spectra 116
6.2.3. Excitation wavelength dependence of the emission spectra 120
6.3. Time-Resolved Measurement 123
6.3.1. Rotational Dynamics 123
6.3.2. Solvation Dynamics 128
6.4. Conclusion 133
References 134

Chapter 7. Rotational Dynamics of Dipolar and Nonpolar Solutes in N-alkyl-N-methylmorpholinium Ionic Liquids

7.1. Introduction 139
7.2 Results and Discussion 144

7.3. Concluding Remark 158
References 160

Chapter 8. Concluding Remarks

8.1. Overview 165
8.2. Future scope and challenges 169

STATEMENT

I hereby declare that the matter embodied in the thesis entitled "***Understanding the Physicochemical Properties of Some Imidazolinium and Morpholinium Ionic Liquids by Studying Photophysical Processes in These Media***" is the result of investigations carried out by me in the School of Chemistry, University of Hyderabad, Hyderabad, India under the supervision of **Prof. Anunay Samanta**.

In keeping with the general practice of reporting scientific investigations, due acknowledgements have been made wherever the work described is based on the findings of other investigators. Any omission or error that might have crept in is regretted.

March 2013 **Dinesh Chandra Khara**

SCHOOL OF CHEMISTRY
UNIVERSITY OF HYDERABAD
HYDERABAD-500 046, INDIA

Phone: +91-40-2313 4813 (O)
+91-40-2313 0715 (R)
Fax: +91 40 2550 1532
Email: assc@uohyd.ernet.in
anunay.samanta@gmail.com

Professor Anunay Samanta,

CERTIFICATE

Certified that the work embodied in the thesis entitled ***"Understanding the Physicochemical Properties of Some Imidazolinium and Morpholinium Ionic Liquids by Studying Photophysical Processes in These Media"*** has been carried out by **Mr. Dinesh Chandra Khara** under my supervision and that the same has not been submitted elsewhere for any degree.

Anunay Samanta
(Thesis Supervisor)

Dean
School of Chemistry
University of Hyderabad

Acknowledgement

First and foremost I express my sincere gratitude to Prof. Anunay Samanta, my research supervisor for his constant encouragement and invaluable guidance. He has been quite helpful to me both the academic and personal fronts.

I gratefully acknowledge the Council of Scientific and Industrial Research (CSIR, New Delhi, India) for financial assistance.

I would like to thank present and formal Deans, school of chemistry, for their constant inspiration and for the available facilities. I am extremely thankful individually to all the faculty member of the school for their help, cooperation and encouragements at various stages of my stay in the campus. I am also grateful to all my former teachers for their help and encouragements.

I value my association with my former lab-mates: Moloy, Aniruddha, Bhaswati and Ravi from whom I have learned many valuable aspects of research. I am extremely thankful to Moloy for not only helping me in academically but also otherwise. I acknowledge my present colleagues, Santhosh, Sanghamitra, Satyajit, Soumya, Ashoke, Chandrasekher, Tanmoy, Praveen and Navendu for maintaining friendly, cooperative and cheerful atmosphere in the lab. I am really happy to have them as lab-mates.

I thank all non-teaching staff of school for their timely help. I am also thankful to all my colleagues in the school for helping me with various things.

I would like express my sincere thanks to all my senior dadas; Moloy, Manb, Saikat, Subhas, Prasant, Tejendar, Aniruddha, Ghana, Pradip, Utpal, Abhijit, Pati, Ghanta, Arindam, Tapta, Tonmoy, and Sandip.

I am really luck for my close association with the colorful friends which include Rishi, Maity, Susrata, Paromita, Sandip, Bubai, Santanu, Nayan, Anup, Raja, Satyajit, Koushik, Navendu, Ganesh and many others.

Without their cheerful company, the campus life would have been trifle easier but a lot of boring and worn out. I am also thankful to Hari, Gupta, Balaswamy, Tridip, Palash, Tonmoy, Mona, Raju, Kamle, Meheboob, Subhadeep, Sunny, Abu, Prdip, Rajib, Arun, Bipul, Sanjib, Naba, Ranjit, Monima, Mousumi, Tulika, Supratim, Pramithi, Sutanuka, Suman, Rudra, Sugata, Debparna, Malkappa and many others.

I am also grateful for the valuable friendship of Tapas, Debu, Goutam, Deba, Srikanta, Subrata, Bidus, Avijit, Sibaprasad, Mahadev, Ashok, Srijit, Dipankar, Amal, Suvendu, Sadhan, Shubhadeep, Giridhari, Santanu, Biman, Narul, Subodh, Monobilash, Santanu, Partha, Dipak, Biswajit, Dibyendu, Gouri, Mritunjoy, Sourav, Rajesh, Suvendu, Rajib, Sanak, Tapas, Nilanjan, Vade, Nimai, Santu, Nandan, Rahul, Shayama, Krinananda, Kalayan and many others.

Last but not the least I would also like to thank my entire family members for their supports and freedom.

Dinesh

List of publications

1. **D. C. Khara,** J. P. Kumar, N. Mondal & A. Samanta. Effect of the Alkyl Chain Length on the Rotational Dynamics of Nonpolar and Dipolar Solutes in a series of N-Alkyl-N-Methylmorpholinium Ionic Liquids. (Manuscript Under Revision)

2. **D. C. Khara** & A. Samanta. Fluorescence Response of Coumarin-153 in N-alkyl-N-methylmorpholinium Ionic Liquids: Are these Media More Structured Than the Imidazolium Ionic Liquids? *J. Phys. Chem. B* **2012,** 116, 13430–13438.

3. **D. C. Khara** & A. Samanta. Fluorescence, Phosphorescence, and Delayed Fluorescence of Benzil in Imidazolium Ionic Liquids. *Aust. J. Chem.* **2012**, 65, 1291–1297.

4. K. Santhosh, S. Patra, S. Soumya, **D. C. Khara,** & **A.** Samanta. Fluorescence Quenching of CdS Quantum Dots by 4-Azetidinyl-7-Nitrobenz-2-Oxa-1,3-Diazole: A Mechanistic Study. *ChemPhysChem* **2011,** 12, 2735 – 2741.

5. **D. C. Khara** & A. Samanta. Solvation Dynamics and Red-edge Effect of two Electrically Charged Solutes in an Imidazolium Ionic Liquid. *Ind. J. Chem.* **2010,** 49A, 714-720.

6. **D. C. Khara** & A. Samanta. Rotational Dynamics of Positively and Negatively Charged Solutes in Ionic Liquid and Viscous Molecular Solvent Studied by Time-resolved Fluorescence Anisotropy Measurements. *Phys. Chem. Chem. Phys.* **2010,** 12, 7671-7677.

7. **D. C. Khara, A.** Paul, K. Santhosh, & A. Samanta. Excited State Dynamics of 9,9′-Bianthryl in Room Temperature Ionic Liquids as Revealed by Picosecond Time-Resolved Fluorescence Study. *J. Chem. Sci.* **2009,** 121, 309-315.

8. A. Paul, M. Sarkar, **D.C. Khara,** T. Kamijo, A. Yamaguchi, N. Teramae, & A. Samanta. Solvation Dynamics of a Surfactant Probe in Mesostructured Silica-Surfactant Nanocomposites. *Chem. Phys. Lett.* **2009,** 469, 71–75.

Talk and Poster Presentations

- Excited state dynamics of bianthryl in different imidazolium ionic liquids, National Symposium on Radiation and Photochemistry (NSRP), Nainital, Uttarakhanda, 2009 (Poster Presentation).
- Rotational Dynamics of Positively and Negatively Charged Solutes in Ionic Liquid and Viscous Molecular Solvent Studied by Time-resolved Fluorescence Anisotropy Measurements, ChemFest-2012, 7th Annual In-House symposium of the school of chemistry, university of Hyderabad, February 25th, 2010 (Poster Presentation).
- Photophysical Behavior of Benzil in Imidazolium Ionic Liquids, Trombay Symposium on Radiation and photochemistry (TSRP) Lonavala, Maharashtra, September 16th - 19th 2010 (Poster Presentation).
- Effect of alkyl chain of cation on the solute rotation and solvation dynamics in N-alkyl-N-methylmorpholinium ionic liquids, ChemFest-2012, 9th Annual In-House symposium of the school of chemistry, university of Hyderabad, February 24th - 25th, 2012 (Oral and Poster Presentation).
- A time-resolved fluorescence anisotropy study in N-alkyl-N-methylmorpholinium ionic liquids, Seminar at Tokyo Institute of Technology, Tokyo, Japan. December 5th, 2012 (Oral Presentation).

Thesis Layout

The thesis has been divided into eight chapters. ***Chapter 1*** describes a brief introduction on room temperature ionic liquids (RTILs), the fundamentals of the photophysical processes which have been studied in this thesis. This is followed by the motivation of the thesis has also been outlined. ***Chapter 2*** provides the experimental procedure and methodology and necessary instrumental details relevant to this work. Various kinds of data analysis and calculations have also been discussed in this chapter. ***Chapter 3*** deals with the excited state dynamics of Binanthryl (**BA**) in three imidazolium ionic liquids differing in their polarity and viscosity. ***Chapter 4*** describes the photophysical processes of a well-studied system, benzil, in different imidazolium ionic liquids which differ in their viscosity and polarity. ***Chapter 5*** delivers the solute rotation and solvation dynamics of charged solutes in imidazolium ionic liquid. ***Chapter 6*** describes the fluorescence response of C153 in a series of N-alkyl-N-methylmorpholinium ionic liquids by using a steady-state and time-resolved techniques. ***Chapter 7*** deals with solute rotation of dipolar and nonpolar solutes in a series of N-alkyl-N-methylmorpholinium ionic liquids by using a time-resolved fluorescence depolarization technique. ***Chapter 8*** summarizes the findings of the present works and looking into the future scopes.

Chapter 1

Introduction

A brief introduction on room temperature ionic liquids (RTILs), highlighting the physical and chemical properties as well as structural features and potential applications of these substances in various fields, is provided in this chapter. This is followed by a brief description of some of the photophysical processes with which the present thesis is concerned, such as excited state dynamics, solvation dynamics and rotational dynamics, along with existing literatures. Finally, the motivation of the thesis work has been described at the end of this chapter.

1.1. Room temperature ionic liquids

1.1.1. A brief introduction

Over the last two decades room temperature ionic liquids (RTILs) have been a stimulating topic of research and are now considered as promising and potential candidate to serve the science and society at large.[1-10]

Ionic liquids (ILs) are low melting salts and are entirely composed of ions. In academic literature, the term 'ionic liquids' refers to those substances which are entirely composed of ions and have melting point around or below 100 ^{0}C.[11,12] However, the RTILs are ionic liquids, are liquid at ambient temperature and atmospheric pressure. These are different from the 'molten salt' which are highly corrosive and viscous melt at higher temperatures (803 ^{0}C for NaCl).[13]

Though the RTILs have become popular over the last two decades and presently research has been focusing on the third generation of the RTILs, the

journey of the ionic liquids started more than a century ago. The evolution of the RTILs is shown in Chart 1.1-1.3. Ethanolammonium nitrate (m.p. 52 – 55 ^{0}C) was reported in 1888 by Gabriel and Weiner.[14] In 1914, a true RTIL, ethylammonium nitrate (m.p. 12 ^{0}C) was described by Walden.[15] The pre-modern age of RTILs started in the early 1950s, but did not receive much attention up to 1980s as the ionic liquids were based on haloaluminates (AlX_3Y^-, $Al_2X_6Y^-$, X = Cl & Y = Br) which are highly hygroscopic and reactive towards moisture and need an inert atmosphere to handle.[16,17]

However, the modern age of RTILs started after 1992 when the haloaluminates were replaced by the air and moisture stable RTILs comprising less reactive anions like BF_4^-, PF_6^-, CH_3COO^-, $(CF_3SO_2)_2N^-$ etc. and 1-ethyl-3-methylimidazolium and 1-butyl-3-methylimidazolium cations.[18] In the subsequent years, RTILs were developed mostly based on imidazolium, pyridinium, pyrolidinium, ammonium and phosphonium moieties, which belong to the first generation ionic liquids (Chart 1.1).[19,20] It was found that these inorganic anions are not biodegradable and toxic in nature due to the hydrolysis of the anion in the presence of trace amount of water.[21-25] The disadvantages of first generic RTILs lead to exploration of a second generation, task-specific ionic liquids (Chart 1.2) whose physical properties could also be controlled accordingly. By introducing an ester group or ether linkage to the alkyl group of the cation and organic anion (instead of the inorganic anion), biodegradability and non-toxicity of the ionic liquids are tremendously increased. The latest discovery in this field is a third generation ionic liquids (Chart 1.3) which are a combination of the two pharmaceutical active drug molecules.[2,26-31]

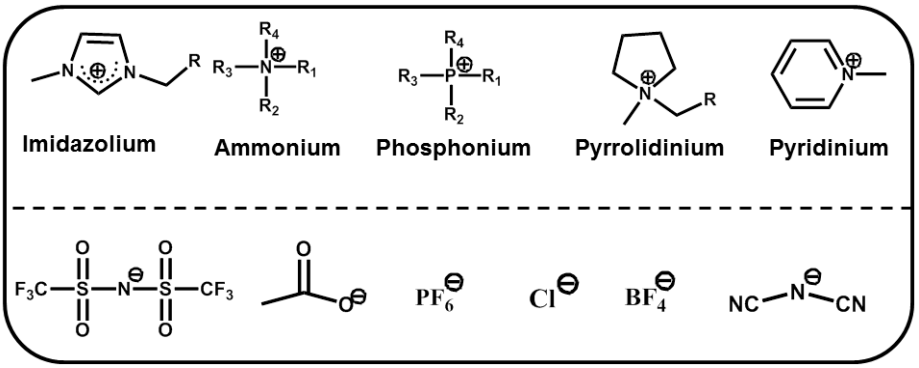

Chart 1.1. Representative cations and anions for the first generation of RTILs

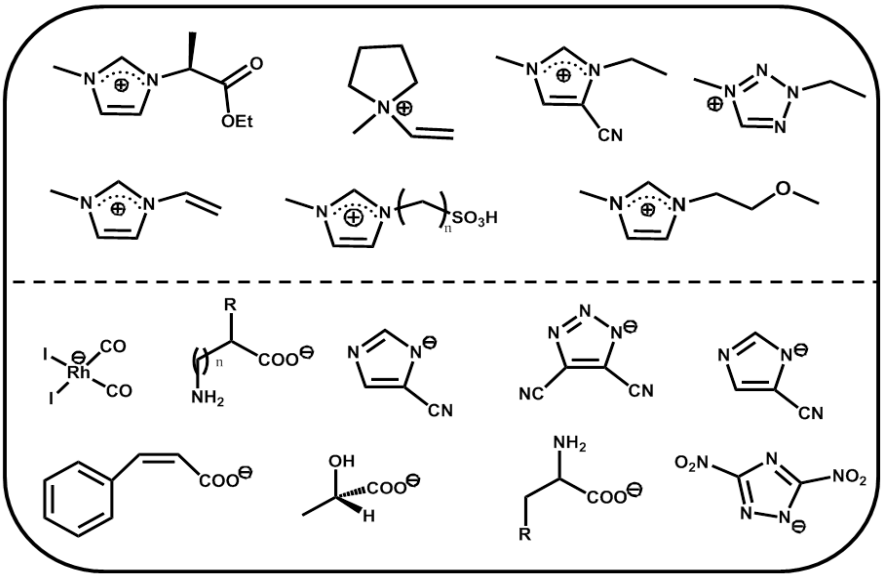

Chart 1.2. Representative cations and anions for the second generation of RTILs

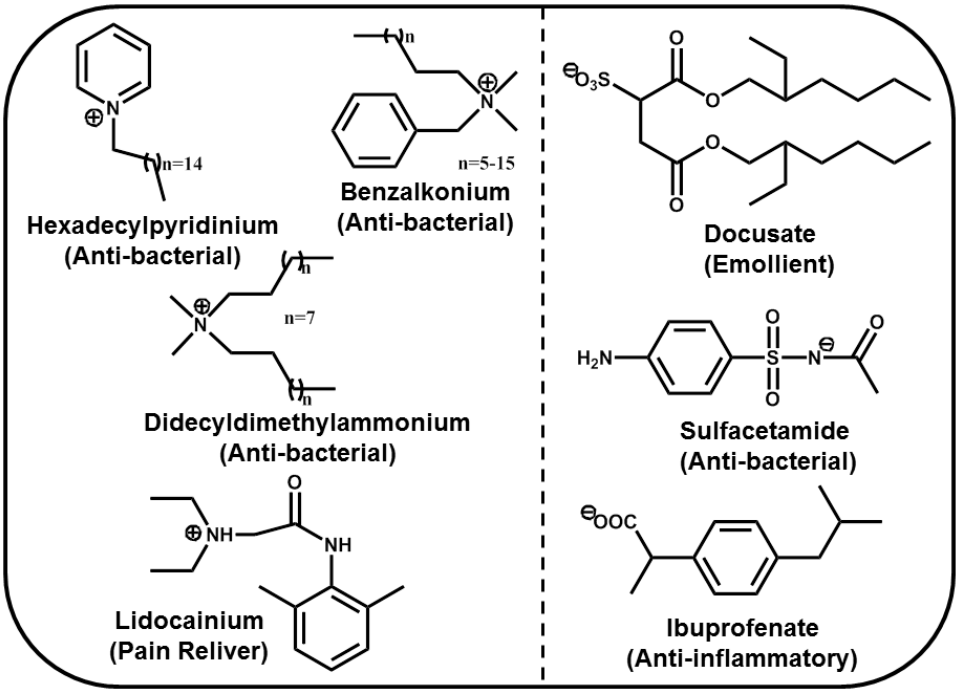

Chart 1.3. Representative cations and anions for the third generation of RTILs

1.1.2. Properties of room temperature ionic liquids

Some unique properties of the RTILs such as non-volatility, good electrical and high thermal stability, non-toxicity and non-flammability, apart from tunable physical properties through structural manipulation, make them ideal alternative to the conventional organic solvents in various fields. Moreover, a large number of RTILs are possible by permutation combination of cations and anions, which can dissolve both the organic and inorganic substances. Since the properties of RTILs are largely dependent on the constituent ions, it is possible to explore them

in various applications. The growing interest in RTILs is reflected in the enormous increase in the number of articles in recent years.

Melting Points: Most of the known RTILs have melting point far below the room temperature (25 ^{0}C). The melting points of the RTILs are uncertain as they undergo considerable super cooling. The phase change can vary significantly depending on whether the sample is being heated or cooled.[32] However, some correlation has been found for specific cations, where it has been seen that the melting point decreases with increasing alkyl chain length of the cation. Moreover, the branching in the alkyl chain increases the melting point.[32] Although the influence of the cation on the melting point is rather straightforward, the anion effect remains quite uncertain. However, hydrogen bonding and delocalization of charge have been invoked to explain the influence of anion.[32]

Polarity: The idea of polarity of a medium is important to be explored in many directions. A variety of solvatochromic probes have been used to understand the microscopic polarity of RTILs in terms of $E_T(30)$ or E_T^N values.[33-36] Some commonly used solvatochromic probes are depicted in Chart 1.4. Apart from the $E_T(30)$ or E_T^N values, Kamlet-Taft parameters[35] and multiple polarity parameters[36] have also been used as measures of the polarity of the RTILs. Studies reveal that the polarity of the RTILs lie between that of acetonitrile and methanol, depending on the chain length of the cation. However, static dielectric constants of some RTILs are very low indicating that the RTILs are much less polar media.[37,38] It has also been found that the dielectric constant of the RTILs decreases as the length of the alkyl chain of the cations increases. The large

difference in polarity of the RTILs measured by different techniques is still unclear.

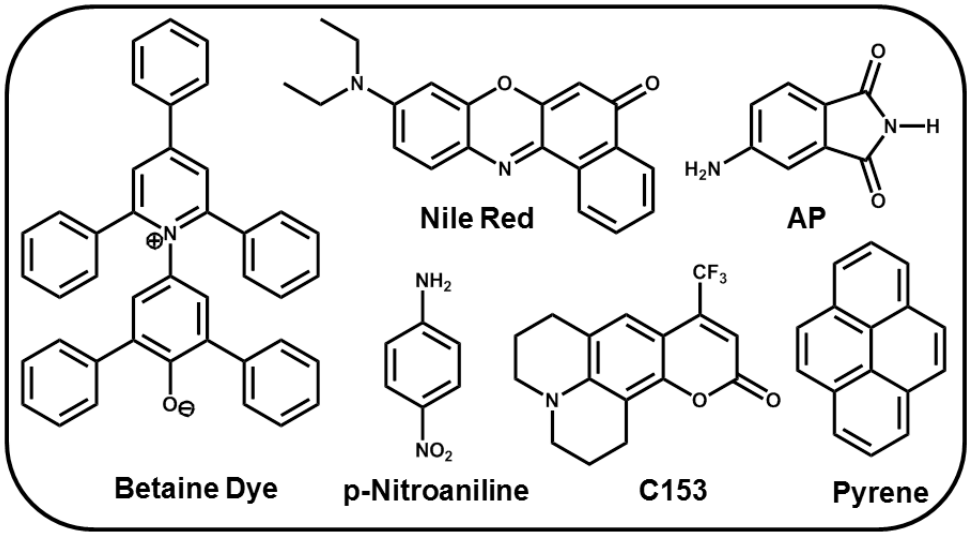

Chart 1.4. Structures of some polarity measurement probes

Viscosity and Density: The viscosity of the RTILs is much higher in comparison to the conventional organic solvents of similar polarity. Even the least viscous RTILs is ~30 times more viscous than water. The viscosity of the RTILs is sensitive to the moisture content and halide impurities. Generally, the viscosity of the RTILs follows a non-Arrhenius type of behaviour.[32] Temperature dependent viscosity data of the RTILs can be well fitted to the Vogel-Tammann-Fulcher (VFT) equation.[32] The viscosity of the RTILs depends on many factors such as the symmetry of the ionic constituents, hydrogen bonding, substituted alkyl chain length on the ions, nature of the functional group present on ions, etc.[32] Hence, it

is difficult to predict the viscosity of a RTIL just by looking at the ions combinations present. However, it has been observed that the viscosity of RTILs increases with increase in chain length of the ion.

The density of the RTILs, which is much higher than the conventional organic solvents, depends on the molar mass of the anions. The density of the RTILs decreases with increase in volume of the anionic component.[32]

Thermal stability and volatility: RTILs have a much higher thermal stability, up to around 400 ^{0}C, in comparison to the conventional organic solvents. However, prolonged heating under a protective atmosphere at comparatively lower temperatures, for example 200 ^{0}C, leads to an appreciable thermal degradation.[32] The decomposition temperature of RTILs increases as the hydrophobicity of anion increases. However, the cations do not have any significant role in this regard.

Generally, it is believed that the RTILs have negligible or no vapour pressure and thus cannot be purified by distillation process. A report however shows that the RTILs can be distilled under reduced pressure without any decomposition.[39] However, the rate of distillation is very slow for RTILs.

Conductivity: Since RTILs are entirely composed of ions, they are expected to have high conductivity due to the availability of mobile charge carriers. However, measurements of ionic conductivities of various RTILs have revealed that these values are considerably lower than those of concentrated aqueous electrolytes. Since, the conductivity is inversely related to the viscosity; the high viscosity could be the reason for the lower conductivity of the RTILs.[32,40] However, it is also found that RTILs of similar viscosity and density show different

conductivity. Hence, the viscosity of RTILs alone cannot account for its conductivity. It is observed that an increase in the length of the alkyl chain results in a higher viscosity and lower conductivity. The conductivities are similar for any of the anions over the same cation whereas an increasing size of the anions lower the viscosity of RTILs.[32,40] Though RTILs show low conductivity, dilution of the neat RTILs in molecular solvents or in the presence of added small cation (Li^+) increases the conductivity of the medium considerably thus making the RTILs suitable for application in batteries or double-layers capacitors.[41]

Other Properties: The surface tension of RTILs is higher than that of the conventional organic solvents. Generally, the surface tension decreases with increase in chain length of the cation. However, the surface tension does not show any clear trend with the variation of the cationic or anionic moiety of the RTILs. Surface tension of the RTILs decreases when alcohol is added to the RTILs, whereas it increases in presence of water.[32]

1.1.3. Structural features and heterogeneity

The structural features of the ionic liquids in the solid and liquid state have been investigated using various techniques. An X-ray diffraction study of the imidazolium salts in the solid state revealed an extended network of cations and anions connected together by hydrogen bond.[42,43] Pyrrolidinium, piperidinium, morpholinium, and piperazinium ionic liquids show a rich mesomorphism, including highly ordered and disordered smectic phases, and hexagonal columnar phases, depending on the alkyl chain length of the cation and anion.[44]

However, the structure of the RTILs in liquid phase is quite complex and is not yet understood clearly. Two independent studies performed by Watanabe and coworkers[45] and Samanta and coworkers[46] indicate that the RTILs are not homogeneous media like conventional organic solvents. Several simulation studies have been carried out to obtain insight into the liquid structure of the RTILs.[56-71] These studies have indeed revealed the presence of local structure of the RTILs thus making them different from the conventional organic solvents. Recently, a large number of simulation studies as well as experimental studies based on optical Kerr effect, small-wide angle X-ray scattering, have shown the evidence of nanoscale ordering and mesoscopic local structure of the RTILs.[47-71] It is found that the mesoscopic structure is prominent in the case of long alkyl chain containing RTILs, and that the presence of hydroxyl or ether linkage disrupts the mesoscopic structure of the RTILs.[48]

1.1.4. RTILs in mixed solvents

It has been observed recently that the mixtures of RTILs and conventional molecular solvents are important media for various processes such as separation and extraction and they also serve as a catalyst for many reactions. This is why it is necessary to understand the physicochemical properties of the mixture of RTILs and conventional molecular solvents. It is found that addition of cosolvent significantly alters the physical properties of the RTILs such as, polarity, viscosity, electrochemical behaviour and solvation dynamics.[40,72-80] The measurements of microscopic polarity of the mixtures of the RTILs and cosolvents employing polarity sensitive probes reveal that these probe molecules

preferentially reside in the RTILs core of most RTILs-cosolvents mixtures. However, the cybotactic region of the probe is mostly surrounded by the cosolvents of the RTILs in the case of polar and protic cosolvent.[78] Viscosity of the RTILs decreases drastically in presence of cosolvents. Electrochemical studies in RTILs and cosolvents mixtures show that the solvents with low dielectric constant stimulate ionic association, whereas solvents having strong hydrogen bonding ability and high dielectric constants stimulate the ionic dissociation of RTILs. It is also found that RTILs and cosolvents mixture show higher conductivity than the pure RTILs.[40]

1.1.5. Application of RTILs

The journey of the RTILs started based mainly on its non-volatility, high thermal stability, large electrochemical windows and liquidity. The use of RTILs is mostly confined as alternative solvent system for a large number of organic and inorganic synthesis, catalysis, electrochemical and separation process. However, a branch of sincere thoughts has led to second and third generation of ionic liquids which are task specific and pharmaceutically active, respectively. The idea of task specific ionic liquids through structural manipulation helped us to improve a vast range of application in various prospects. Brief introductions on the application of RTILs are highlighted below.

Reaction Media. In earlier times, RTILs were used as reaction media for few selective reactions. However, after exploring the task specific ionic liquids, specific organic and inorganic reactions have been developed in specific ionic liquids giving better selectivity and yields. For example, ionic liquids for

heterocyclic synthesis, inorganic synthesis, hydroformylation, oxidation, olefins metathesis reaction, Friedel-Crafts reaction, Heck reaction and in selected name reactions of carbonyl chemistry such as Mannich, Reformatsky, Cannizaro, Streacker, Barbier, Pechmann, etc. have been described.[1,19,81-93]

Catalysis. Task-specific ionic liquids serve as catalysts as well as reaction media for a few reactions.[4,13,89]

Electrochemistry. Ionic liquids are a promising alternative, as their non-volatility, good electrical and thermal stability and non-flammability, in addition to tunable physical properties through structural manipulation, make them ideal for electrochemical applications. These are also been proposed as favorable electrolytes for lithium and lithium ion battery. Ion gel, a binary composition of ionic liquids with polymer, is also an encouraging candidate as new material for electrochemical applications.[5,40,41,94-99]

Biofuel Production. Lignocellulose biomass and vegetable oil or animal fat are important sources of renewable energy for the next generation and RTILs have been found to be a catalyst and a potential medium for the efficient conversion of lignocellulose biomass to bioethanol and vegetable oil or animal fat to biodiesel.[3,100-109]

Gas Adsorption. Task-specific ionic liquids have also been proposed as an alternative solvent platform to aqueous amine solvents for the removal of CO_2 and SO_2 from the fuel gas of coal-fired power plants and the removal of CO_2 and/or H_2S from natural gas. CO_2, which is regarded a greenhouse gas, could be captured by using reactive and reversible ionic liquids and used as a renewable carbon source for making commodity chemicals, fuels, and materials.[6,89,110-116]

Separation Process. Ionic liquids are also found to be good candidates for the separation of specific azeotropic mixture and aromatic hydrocarbon from aliphatic and aromatic mixtures. It is already demonstrated that RTILs are novel media for the extraction and separation of bioactive compounds from the plant sources.[117] Ionic liquids also serve as good candidates for the separation of poly- and disaccharides.[10,117-137]

Metal Extraction. RTILs are found to be potential candidates for the extraction and separation of all kinds of metal.[132-134]

Nuclear Fuel Extraction. Apart from the common physical and chemical properties, the radiation stability of RTILs makes them an alternative to commonly used solvents like, PUREX, SREX, TRUEX, DIAMEX and DIDPA for nuclear fuel reprocessing technologies.[122]

Materials Science. Ionic liquids are also found to be potential candidates for the synthesis of organic, inorganic and carbon nanomaterial and nanomaterial-ionic liquid hybrids which have wide range of applications.[7,98,138-146]

Enzyme Activity. Ionic liquids have shown great potential as alternative solvent media to conventional solvents for many enzymatic reactions with efficient conversion rate. The stereoselectivity and regioselectivity of the reactions are high in comparison to the conventional solvents.[147-152]

Protein Chemistry. Synthesis and stabilization of the proteins and the study of their dynamics has also started in ionic liquids, but this area needs more attention and exploration.[153,154]

Pharmaceutical Drug. The latest recognition in ionic liquids chemistry is the pharmaceutically active ionic liquids, the third generation of ionic liquids. An

ionic liquid and the combination of two active drug molecules lead to new active drug molecules having two different activities. This is now an interesting topic of research and may lead to a revolutionary improvement in the medicinal chemistry.[2,26-31]

1.2. Photoinduced conformational dynamics in the excited state

Photoinduced charge separation in the excited state is responsible for many excited state processes such as electron transfer, proton transfer, conformational dynamics, etc.[155,156] Among these processes, photoinduced conformational dynamics in the excited state is an interesting topic for fundamental research to understand the structure of a molecule in the ground state as well as in the excited state. This can help us in better understanding of the reaction mechanism and their molecular properties.[157] Some solutes which undergo excited state conformational change are collected in Chart 1.5. Since, the molecular spectral properties due to different conformers are entirely different; one can follow the spectral property of evolving species due to excited state processes. In this thesis, we have followed the emission spectral behaviour of different conformers to study their conformational dynamics.

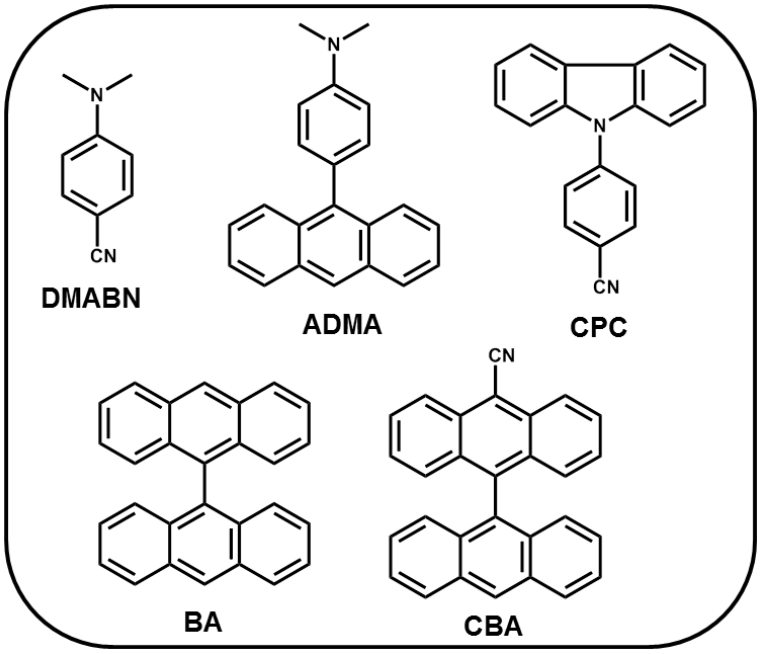

Char 1.5. Structure of some conformational dynamics probes

1.3. Solvation dynamics

Solvation is a process in which the solvent molecules reorganize themselves around the instantly created dipole within the solvent medium. In fluorescence spectroscopy, dipolar probe (Chart 1.6) which undergoes significant change in dipole moment after photoexcitation, are used to follow the solvation dynamics process. There is an instantaneous change in dipole moment of the dipolar solute due to photoexcitation and the equilibrium between the solute and solvent dipole is destroyed. The solvent molecules again rearrange themselves around the newly created dipole to attain the equilibrium. As a result, physical dynamic processes occur among the solvent molecules, called solvation dynamics. This process of

reorganization is also called solvent relaxation and the time required for this relaxation process is known as solvation time. Solvation time depends on temperature, solvent's molecular structure and viscosity. Solvation time in conventional solvents is typically less than the fluorescence lifetime of the probe.[155] This shows the attainment of excited state equilibrium prior to fluorescence. However, the scenario alters in viscous solvents and organized molecular assemblies such as micelles, protein or membrane. In these media the emission can be observed from various stages of solvent relaxation and monitored by studying the time-dependent dynamic shifts of the emission spectra, known as dynamic Stokes shift, shown in Chart 1.7. The method of studying solvation dynamics using dynamic Stokes shift technique is discussed in detail in Chapter 2.

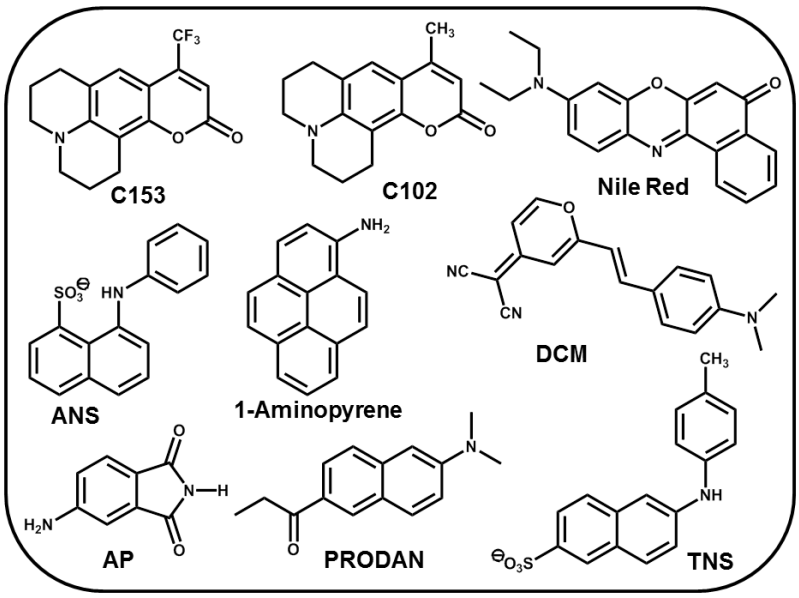

Chart 1.6. Structure of some solvation probes

1.3.1. Solvation dynamics in conventional solvents

Solvation dynamics has been studied extensively to understand the effect of macroscopic solvent property such as viscosity, polarity during the stabilization of an electronically excited dipolar solute by its solvent surroundings. Solvation dynamics in conventional polar solvent is extremely fast and it occurs in the sub-picosecond time scale at room temperature.[158,159] It has been observed that solvation is non-exponential and average solvation time is greater than the longitudinal relaxation time.[158,159] The experimental results are not adequately described by the continuum model. However, in another study, a nice correlation between longest longitudinal relaxation and average solvation time is observed when solvation dynamics is studied in alcoholic solvents as a function of pressure.[160] This study reveals that the continuum model adequately provides the solvent response.

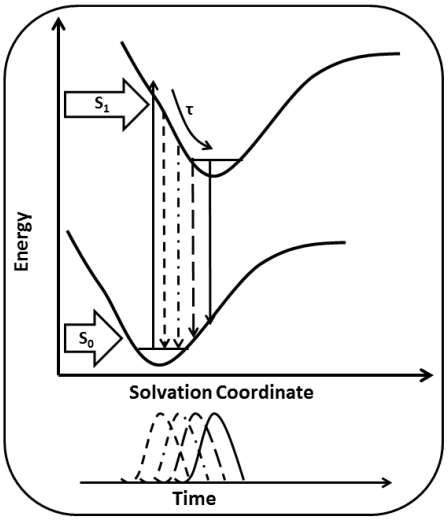

Chart 1.7. Schematic diagram of dynamic Stokes shift

1.3.2. Solvation dynamics in confined environment

Solvation dynamics of water confined in organized molecular assemblies such as micelles, reverse micelles, cyclodextrin, vesicles, proteins, DNA, membrane etc. is quite slow compared to pure water.[161-167] In pure water the solvation dynamics is biphasic in nature with time constants 126 fs and 880 fs, respectively.[168] The faster component is due to vibrational relaxation and the relatively slower component is due to librational motion. The dynamics of confined water is also found to be biphasic in nature, an ultrafast component is associated with a slow component in the sub-nanosecond to nanosecond region. These slow components have been attributed to the dynamic exchange of the free and bound water molecules in such media.[165]

1.3.3. Solvation dynamics in RTILs

Since the early work of Karmakar and Samanta,[169,170] several groups have studied the solvation dynamics in different RTILs using dipolar fluorescence probe molecules to understand the mechanism and dynamics of solvation following an instantaneous separation of charge in the dipolar probe molecule. These studies reveal that the dynamic process is quite slow compared to the conventional molecular solvents. It is believed that the slow dynamics is due to high viscosity of these media. However, despite the slow dynamics, a large part of the dynamics, nearly 30-50%, are found to be missed with the finite time resolution of the time-correlated single-photon counting technique (TSCPC) setup, typically 25 ps. The unseen part of the dynamics is called ultrafast or

missing component which is independent of the viscosity of the media.[80,171,172] Recently, femtosecond nonlinear spectroscopic techniques such as optical Kerr effect and three-photon echo spectroscopy have been used to understand the dynamics of RTILs.[61,173-175] Very recently, combined techniques of broadband fluorescence upconversion spectroscopy (FLUPS) having a time resolution of 80 fs and TCSPC to cover times upto 20 ns, have been used to capture the complete dynamics in several RTILs.[176] The complete study reveals that the dynamic process is biphasic in nature, consisting of a sub-picosecond component which contributes to 10 – 40 % of the dynamics and a slower component relaxing over the nanosecond time scale. The slower component of the dynamics depends on the viscosity of the medium indicating that its origin lies in the diffusive and structural reorganization of the solvent molecules. Whereas, the time constant associated with the fast component is found to be correlated with ion mass, specifying its origins in inertial solvent motions, which has been demonstrated by the earlier simulation studies.[80,171,172]

1.4. Rotational dynamics

Rotational dynamics is the time dependence of the rotational diffusion of a solute. In fluorescence spectroscopy, when a solute is excited with polarized light, the emission from the solute is mostly polarized. The extent of polarization is expressed in terms of anisotropy.[155] The anisotropy measurement provides the average angular displacement of the solute that occurs between absorption and emission. The angular displacement of solute is dependent upon the rate and extent of rotational diffusion during its fluorescence lifetime. The rotational

motions depend on the viscosity of the medium and the size and shape of the solute. By following the anisotropy decay profile of solute one can get detailed information about the rotational dynamics of the solute. The structures of some frequently used solutes for rotational dynamics studies are given in Chart 1.8. The method of studying rotational dynamics has been elaborated in Chapter 2.

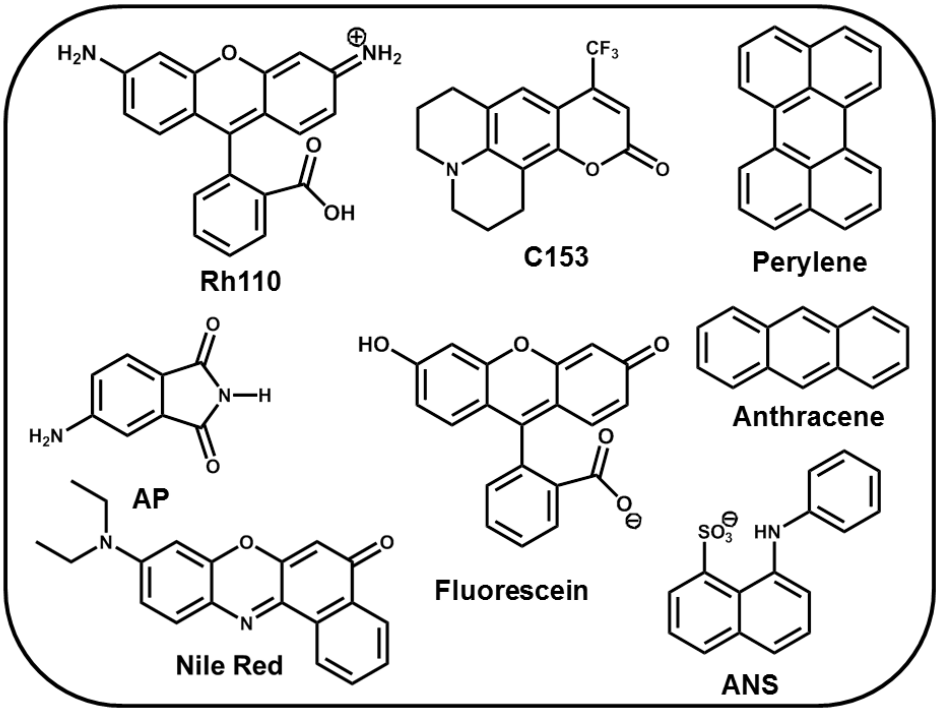

Char 1.8. Some common probes used for rotational dynamics study

1.4.1. Rotational dynamics in conventional solvents

The study of rotational dynamics in solution helps understanding the interaction between a solute and its solvent surroundings.[177-180] The rotational

dynamics of a fluorophore is quite fast compared to its fluorescence lifetime in conventional molecular solvents. In conventional solvents, the rotational dynamics is generally non exponential in nature and is slow in polar solvents compared to the nonpolar solvents of same viscosity. In most of the cases the rotational dynamics of a solute can be understood by the commonly used Stokes-Einstein-Debye (SED) hydrodynamic model.[177-179] However, in a few cases where van der Waals volume of a solute is quite small compared to solvent volume, a quasihydrodynamic theory is introduced to explain the dynamic behaviour of the solute.[177,178,180]

1.4.2. Rotational dynamics in confined environment

Rotational dynamics has also been studied in organized molecular assemblies such as micelles, reverse micelles, vesicles, proteins, lipid etc. to understand the microscopic physical property like viscosity of the confined medium and electrostatic interaction, etc.[181-186] Most of these studies show that the rotational dynamics is bi-exponential in nature and is associated with a fast and a slow component. These studies also show that the microscopic viscosity of these media is different from the bulk viscosity of the solvent.

1.4.3. Rotational dynamics in RTILs

Ever since the early work of Baker et al,[187] many groups have studied the rotational dynamics in RTILs with a view of obtaining insight into the nature of these media. These studies have shown that the rotational dynamics in RTILs follow the Stokes-Einstein-Debye (SED) hydrodynamic model.[188-200] However, in

a few cases the SED model fails to explain the experimental results.[192,194,198] The SED model in these cases overestimates or underestimates the rotational time constants. The overestimated results are explained due to the specific interaction such as strong hydrogen bonding between the solute and RTILs and the underestimated results are explained by a quasihydrodynamic model considering the small van der Waals volumes of the solute compared to van der Waals volumes of the RTILs. The rotational dynamics of charged solutes in RTILs is studied to probe the electrostatic interaction between the charged moieties of the solute and RTILs. These studies indicate that columbic interaction between charged components of RTILs is much more pronounced than that between the solute and RTILs.[193,194] Generally, the rotational dynamics of a solute in a variety of the RTILs is governed by the viscosity of the media. However, the rotational dynamics of a hydrogen bond donating solute depends on the basicity of the anionic component of the RTILs over the same cationic moiety.[188] The effect of alkyl chain length of the cation/anion on solute rotation depends on the kind of solute being studied.[201]

1.5. Motivation behind the thesis

The photophysical behaviour of some organic solutes are studied in room temperature ionic liquids (RTILs) based on imidazolium and morpholinium cation with a view to understand some of the microscopic physicochemical properties of these media and also to exploit some of the unique properties of these liquids to tune the photophysical processes of some well-studied organic solutes. With these

objectives we have chosen the following imidazolium and morpholinium RTILs (Chart 1.9) and the fluorescent systems (Chart 1.10).

The photophysical processes studied in this thesis are (i) excited state conformational dynamics, (ii) solvation dynamics and (iii) rotational dynamics.

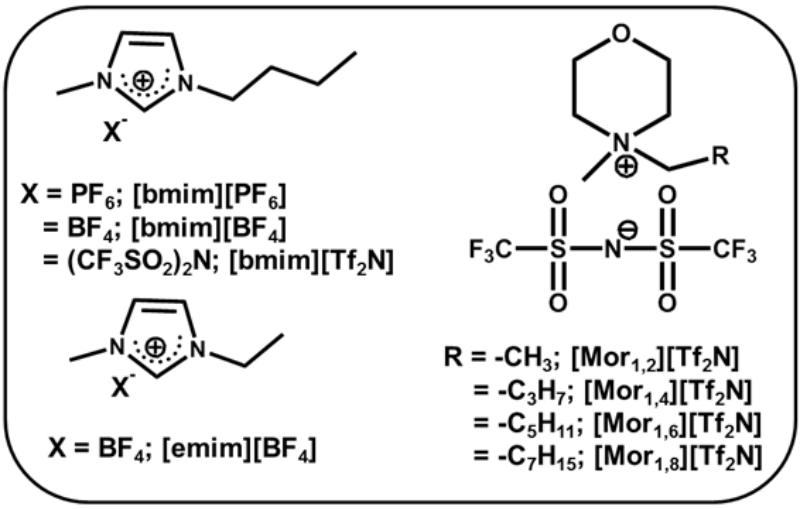

Chart 1.9. Structure and abbreviation of RTILs used in this study

Binanthryl (**BA**) is an interesting system whose excited state behaviour has attracted considerable attention.[157] In conventional solvents, the two anthryl moieties of bianthryl are perpendicular to each other in the ground state. Interestingly, in the electronically excited state, the perpendicular conformer of BA transforms into a relaxed planer form in polar solvents.[157] This conformation dynamics is known to be extremely fast in conventional solvents at room temperature. In the present study, highly polar and viscous nature of the RTILs has been employed to tune the relaxation dynamics of BA in the excited state. The

excited state dynamics of BA has been studied by using time-resolved fluorescence technique in three imidazolium ionic liquids, which is differ in their polarity and viscosity.

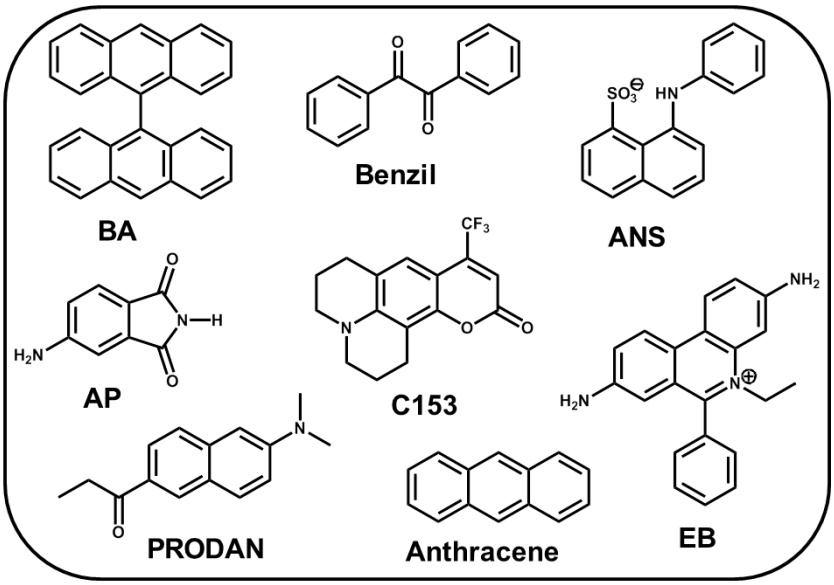

Chart 1.10. Structure and abbreviation of the probes used in this study

Photophysics of simple molecular system, benzil, is quite stimulating as it involves several excited state processes such as conformational dynamics, reverse intersystem crossing, and emission from higher excited singlet state and triplet state at room temperature, the latter is something rarely observed for common organic molecules.[202-208] Photophysics of benzil has been studied by using UV-visible absorption, temperature and excitation wavelength dependent steady-state

and delayed emission measurements in three imidazolium ionic liquids, which differ in their polarity and viscosity.

A large number of photophysical processes involving the neutral solutes have been studied in imidazolium ionic liquids.[80,171,188,189,209-212] Interestingly, very few studies have been made involving the charged species to determine the importance of the electrostatic interaction between the solute and RTILs. Hence, steady-state and time-resolved fluorescence behavior of two charged solutes (both anionic, **ANS** and cationic, **EB**, Chart 1.10.) have been studied in [bmim][BF_4] to investigate the importance of electrostatic interaction between the solutes and ionic constituents of the ionic liquid.

RTILs based on the N, N′-dialkylimidazolium salts have thus far been the most widely studied because of their attractive physical properties. However, considering the high cost of industrial scale synthesis of these salts, the focus seems to be shifting gradually towards other less expensive alternatives such as the morpholinium RTILs, which are not only cheap and easy to develop, but also possess good physicochemical characteristics.[44,213-215] However, the physicochemical properties of the morpholinium RTILs have not been explored yet. Hence, a series of N-alkyl-N-methylmropholinium RTILs have been studied here by monitoring the temperature dependent steady-state and time-resolved fluorescence behavior of C153.

The rotational dynamics of solute provides valuable information on the interaction between the solute and solvent and sheds considerable light on the physicochemical properties of the medium.[155,177,216] Hence, the rotational dynamics of two dipolar solutes (**AP** and **PRODAN**) and a nonpolar solute

(**anthracene**) have been studied by measuring the time-resolved fluorescence anisotropy of the systems in a series of N-alkyl-N-methylmorpholinium ionic liquids to understand the physicochemical properties of RTILs. The results obtained in this study have been analyzed in terms of Stokes-Einstein-Debye (SED) model.

References

(1) Hallett, J. P.; Welton, T. *Chem. Rev.* **2011**, *111*, 3508.

(2) Ferraz, R.; Branco, L. C.; PrudÞncio, C.; Noronha, J. P.; Petrovski, Z. *ChemMedChem* **2011**, *6*, 975

(3) Wang, H.; Gurau, G.; Rogers, R. D. *Chem. Soc. Rev.* **2012**, *41*, 1519.

(4) Zhang, Q.; Zhang, S.; Deng, Y. *Green Chem.* **2011**, *13*, 2619.

(5) Gao, R.; Wang, D.; Heflin, J. R.; Long, T. E. *J. Mater. Chem.* **2012**, *22*, 13473.

(6) Ramdin, M.; Loos, T. W. d.; Vlugt, T. J. H. *Ind. Eng. Chem. Res.* **2012**, *51*, 8149.

(7) Scholten, J. D.; Leal, B. r. C.; Dupont, J. *ACS Catal.* **2012**, *2*, 184.

(8) Pulati, N.; Sobkowiak, M.; Mathews, J. P.; Painter, P. *Energy Fuels* **2012**, *26*, 3548.

(9) Shiddiky, M. J. A.; Torriero, A. A. J. *Biosensors and Bioelectronics* **2011**, *26*, 1775.

(10) Vidala, L.; Riekkolaa, M. L.; Canals, A. *Analy. Chimica Acta* **2012**, *715*, 19.

(11) Seddon, K. R. *Nature Materials* **2003**, *2*, 363.

(12) Rogers, R. D.; Seddon, K. R. *Science* **2003**, *302*, 792.

(13) Wasserscheid, P.; Keim, W. *Angew. Chem. Int. Ed.* **2000**, *39*, 3772.

(14) Gabriel, S.; Weiner, J. *Ueber einige Abkömmlinge des Propylamins* **1888**, *21*, 2669.

(15) Walden, P. *Bull. Acad. Sci. (St. Petersburg)* **1914**, 405.

(16) Boon, J. A.; Levisky, J. A.; Pflug, J. L.; Wilkes, J. S. *J. Org. Chem.* **1986**, *51*, 480.

(17) Wilkes, J. S.; Levisky, J. A.; Wilson, R. A.; Hussey, C. L. *Inorg. Chem.* **1982**, *21*.

(18) Sheldon, R. *Chem. Commun.* **2001**, 2399.

(19) Welton, T. *Chem. Rev.* **1999**, *99*, 2071.

(20) MacFarlane, D. R.; Meakin, P.; Sun, J.; Amini, N.; Forsyth, M. *J. Phys. Chem. B* **1999**, *103*, 4164.

(21) Latała, A.; Nedzia, M.; Stepnowski, P. *Green Chem.* **2010**, *12*, 60.

(22) Freire, M. G.; Neves, C. M. S. S.; Marrucho, I. M.; Coutinho, J. A. P.; Fernandes, A. M. *J. Phys. Chem. A* **2010**, *114*, 3744.

(23) Coleman, D.; Gathergood, N. *Chem. Soc. Rev.* **2010**, *39*, 600.

(24) Wang, X.; Ohlin, C. A.; Lu, Q.; Fei, Z.; Hub, J.; Dyson, P. J. *Green Chem.* **2007**, *9*, 1191.

(25) Docherty, K. M.; Charles F. Kulpa, J. *Green Chem.* **2005**, *7*, 185.

(26) Bica, K.; Rodrıguez, H.; Gurau, G.; Cojocaru, O. A.; Riisager, A.; Fehrmannd, R.; Rogers, R. D. *Chem. Commun.* **2012**, *48*, 5422.

(27) Pernak, J.; Syguda, A.; Janiszewska, D.; Materna, K.; Praczyk, T. *Tetrahedron* **2011**, *67*, 4838

(28) Kumar, V.; Malhotra, S. V. *In Ionic Liquid Applications: Pharmaceuticals, Therapeutics, and Biotechnology; Malhotra, S.; ACS Symposium Series; American Chemical Society: Washington, DC* **2010**.

(29) Bica, K.; Rijksen, C.; Nieuwenhuyzena, M.; Rogers, R. D. *Phys. Chem. Chem. Phys.* **2010**, *12*, 2011.

(30) Hough, W. L.; Smiglak, M.; Rodrıguez, H.; Swatloski, R. P.; Spear, S. K.; Daly, D. T.; Pernak, J.; Grisel, J. E.; Carliss, R. D.; Soutullo, M. D.; James H. Davis, J.; Rogers, R. D. *New J. Chem.* **2007**, *31*, 1429.

(31) Hough, W. L.; Rogers, R. D. *Bull. Chem. Soc. Jpn.* **2007**, *80*, 2262.

(32) Chiappe, C.; Pieraccini, D. *J. Phys. Org. Chem.* **2005**, *18*, 275.

(33) Reichardt, C. *Green chem.* **2005**, *7*, 339.

(34) Aki, S. N. V. K.; Brennecke, J. F.; Samanta, A. *Chem. Commun.* **2001**, 413.

(35) Crowhurst, L.; Mawdsley, P. R.; Perez-Arlandis, J. M.; Salter, P. A.; Welton, T. *Phys. Chem. Chem. Phys* **2003**, *5*, 2790.

(36) Anderson, J. L.; Ding, J.; Welton, T.; Armstrong, D. W. *J. Am. Chem. Soc.* **2002**, *124*, 14247.

(37) Daguenet, C.; Dyson, P. J.; Krossing, I.; Oleinikova, A.; Slattery, J.; Wakai, C.; Weingartner, H. *J. Phys. Chem. B* **2006**, *110*, 12682.

(38) Wakai, C.; Oleinikova, A.; Ott, M.; Weingartner, H. *J. Phys. Chem. B* **2005**, *109*, 17028.

(39) Earle, M. J.; Esperanc, J. M. S. S.; Gilea, M. A.; Lopes, J. N. C.; Rebelo, L. S. P. N.; Magee, J. W.; Seddon, K. R.; Widegren, J. A. *Nature* **2006**, *439*, 831.

(40) Hapiot, P.; Lagrost, C. *Chem. Rev.* **2008**, *108*, 2238.

(41) Lewandowski, A.; Swiderska-Mocek, A. *J. Power Sources* **2009**, *194*, 601.
(42) Wilkes, J. S.; Zaworotko, M. J. *Chem. Commun.* **1992**, 965.
(43) Kolle, P.; Dronskowski, R. *Inorg. Chem.* **2004**, *43*, 2803.
(44) Lava, K.; Binnemans, K.; Cardinaels, T. *J. Phys. Chem. B* **2009**, *113*, 9506.
(45) Tokuda, H.; Hayamizu, K.; Ishii, K.; Susan, M. A. B. H.; Watanabe, M. *J. Phys. Chem. B* **2004**, *108*, 16593.
(46) Mandal, P. K.; Sarkar, M.; Samanta, A. *J. Phys. Chem. A* **2004**, *108*, 9048.
(47) Turton, D. A.; Sonnleitner, T.; Ortner, A.; Walther, M.; Hefter, G.; Seddon, K. R.; Stana, S.; Plechkova, N. V.; Buchner, R.; Wynne, K. *Faraday Discuss.* **2012**, *154*, 145.
(48) Russina, O.; Triolo, A.; Gontrani, L.; Caminiti, R. *J. Phys. Chem. Lett.* **2012**, *3*, 27.
(49) Patra, S.; Samanta, A. *J. Phys. Chem. B* **2012**, *116*, 12275.
(50) Kashyap, H. K.; Hettige, J. J.; Annapureddy, H. V. R.; Margulis, C. J. *Chem. Commun.* **2012**, *48*, 5103.
(51) Guo, J.; Baker, G. A.; Hillesheim, P. C.; Dai, S.; Shaw, R. W.; Mahurin, S. M. *Phys. Chem. Chem. Phys.* **2011**, *113*, 12395.
(52) Dou, Q.; Sha, M. L.; Fu, H. Y.; Wu, G. Z. *J. Phys.: Condens. Matter* **2011**, *23*, 175001.
(53) Aoun, B.; Goldbach, A.; González, M. A.; Kohara, S.; Price, D. L.; Saboungi, M. L. *J. Chem. Phys.* **2011**, *134*, 104509.
(54) Urahata, S. M.; Ribeiro, M. C. C. *J. Phys. Chem. Lett.* **2010**, *1*, 1738.
(55) Shimomura, T.; Fujii, K.; Takamuku, T. *Phys. Chem. Chem. Phys.* **2010**, *12*, 12316.
(56) Russina, O.; Gontrani, L.; Fazio, B.; Lombardo, D.; Triolo, A.; Caminiti, R. *Chem. Phys. Lett.* **2010**, *493*, 259.
(57) Karimi-Varzaneh, H. A.; Muller-Plathe, F.; Balasubramanian, S.; Carbone, P. *Phys. Chem. Chem. Phys.* **2010**, *12*, 4714.
(58) Hardacre, C.; Holbrey, J. D.; Mullan, C. L.; Youngs, T. G. A.; Bowron, D. T. *J. Chem. Phys.* **2010**, *133*, 074510.
(59) Bodo, E.; Gontrani, L.; Caminiti, R.; Plechkova, N. V.; Seddon, K. R.; Triolo, A. *J. Phys. Chem. B* **2010**, *114*, 16398.

(60) Annapureddy, H. V. R.; Kashyap, H. K.; Biase, P. M. D.; Margulis, C. J. *J. Phys. Chem. B* **2010**, *114*, 16838.
(61) Xiao, D.; Jr., L. G. H.; Li, S.; Bartsch, R. A.; Quitevis, E. L.; Russina, O.; Triolo, A. *J. Phys. Chem. B* **2009**, *113*, 6426.
(62) Habasaki, J.; Ngai, K. L. *J. Chem. Phys.* **2008**, *129*, 194501.
(63) Triolo, A.; Russina, O.; Bleif, H. J.; Bleif, H. J.; Cola, E. D. *J. Phys. Chem. B* **2007**, *111*, 4641.
(64) Iwata, K.; Okajima, H.; Saha, S.; Hamaguchi, H.-O. *Acc. Chem. Res.* **2007**, *40*, 1174.
(65) Xiao, D.; Rajian, J. R.; Li, S.; Bartsch, R. A.; Quitevis, E. L. *J. Phys. Chem. B* **2006**, *110*, 16174.
(66) Wang, Y.; Voth, G. A. *J. Phys. Chem. B* **2006**, *110*, 18601.
(67) Shigeto, S.; Hamaguchi, H.-o. *Chem. Phys. Lett.* **2006**, *427*, 329.
(68) Lopes, J. C.; Gomes, M. F. C.; Padua, A. A. H. *J. Phys. Chem. B* **2006**, *110*, 16816.
(69) Lopes, J. A. C.; Padua, A. A. H. *J. Phys. Chem. B* **2006**, *110*, 3330.
(70) Hu, Z.; Margulis, C. J. *Proc. Natl. Acad. Sci. U. S. A.* **2006**, *103*, 831.
(71) Wang, Y.; Voth, G. A. *J. Am. Chem. Soc.* **2005**, *127*, 12192.
(72) Fletcher, K. A.; Pandey, S. *J. Phys. Chem. B* **2003**, *107*, 13532.
(73) Fletcher, K. A.; Baker, S. N.; Baker, G. A.; Pandey, S. *New J. Chem.* **2003**, *27*, 1706.
(74) Baker, S. N.; Baker, G. A.; Bright, F. V. *Green Chem.* **2002**, *4*, 165.
(75) Seth, D.; Chakraborty, A.; Setua, P.; Sarkar, N. *J. Phys. Chem. B* **2007**, *111*, 4781.
(76) Li, W.; Zhang, Z.; Han, B.; Hu, S.; Xie, Y.; Yang, G. *J. Phys. Chem. B* **2007**, *111*, 6452.
(77) Seth, D.; Chakraborty, A.; Setua, P.; Sarkar, N. *Langmuir* **2006**, *22*, 7768.
(78) Harifi-Mood, A. R.; Habibi-Yangjeh, A.; Gholami, M. R. *J. Phys. Chem. B* **2006**, *110*, 7073.
(79) Chakrabarty, D.; Chakraborty, A.; Seth, D.; Sarkar, N. *J. Phys. Chem. A* **2005**, *109*, 1764.
(80) Samanta, A. *J. Phys. Chem. B* **2006**, *110*, 13704.

(81) Zhang, Q.; Vigier, K. D. O.; Royer, S.; Jerome, F. *Chem. Soc. Rev.* **2012**, *41*, 7108.
(82) Payagala, T.; Armstrong, D. W. *Chirality* **2012**, *24*, 17.
(83) Suresh; Sandhu, J. S. *Green Chem. Lett. Rev.* **2011**, *4*, 289.
(84) Suresh; Sandhu, J. S. *Green Chem. Lett. Rev.* **2011**, *4*, 311.
(85) Isambert, N.; Duque, M. d. M. S.; Plaquevent, J. C.; nisson, Y. G.; Rodriguez, J.; Constantieux, T. *Chem. Soc. Rev.* **2011**, *40*, 1347.
(86) Freudenmann, D.; Wolf, S.; Wolff, M.; Feldmann, C. *Angew. Chem. Int. Ed.* **2011**, *50*, 11050
(87) Betza, D.; Altmann, P.; Cokoja, M.; Herrmann, W. A.; Kühn, F. E. *Coordination Chem. Rev.* **2011**, *255*, 1518.
(88) Ahmed, E.; Ruck, M. *Coordination Chem. Rev.* **2011**, *255*, 2892.
(89) Giernoth, R. *Angew. Chem. Int. Ed.* **2010**, *49*, 2834
(90) Bellina, F.; Chiappe, C. *Molecules* **2010**, *15*, 2211.
(91) Sledz, P.; Mauduit, M.; Grela, K. *Chem. Soc. Rev.* **2008**, *37*, 2433.
(92) Martins, M. A. P.; Frizzo, C. P.; Moreira, D. N.; Zanatta, N.; Bonacorso, H. G. *Chem. Rev.* **2008**, *108*, 2015.
(93) Haumann, M.; Riisager, A. *Chem. Rev.* **2008**, *108*, 1474.
(94) Lane, G. H. *Electrochimica Acta* **2012**, *83*, 513.
(95) Kunchornsup, W.; Sirivat, A. *Sensors and Actuators A* **2012**, *175*, 155.
(96) Doherty, A. P.; Diaconu, L.; Marley, E.; Spedding, P. L.; Barhdadi, R.; Troupel, M. *Asia-Pac. J. Chem. Eng.* **2012**, *7*, 14.
(97) Pringle, J. M.; Armel, V. *Intern. Rev. Phys. Chem.* **2011**, *30*, 371.
(98) Hofft, O.; Endres, F. *Phys. Chem. Chem. Phys.* **2011**, *13*, 13472.
(99) Ueki, T.; Watanabe, M. *Macromolecules* **2008**, *41*, 3739.
(100) Vancov, T.; Alston, A. S.; Brownb, T.; McIntosh, S. *Renewable Energy* **2012**, *45*, 1.
(101) Muhammad, N.; Man, Z.; Khalil, M. A. B. *Eur. J. Wood Prod.* **2012**, *70*, 125.
(102) Liu, C. Z.; Wang, F.; Stiles, A. R.; Guo, C. *Applied Energy* **2012**, *92*, 406.
(103) JinXing, L.; XueHui, L.; LeFu, W.; Ning, Z. *Sci. China Chem.* **2012**, *55*, 1500.
(104) Gericke, M.; Fardim, P.; Heinze, T. *Molecules* **2012**, *17*, 7458.
(105) Andreani, L.; Rocha, J. D. *Brazil. J. Chem. Eng.* **2012**, *29*, 1.

(106) Zhang, Y.; Gao, H.; Joo, Y.-H.; Shreeve, J. M. *Angew. Chem. Int. Ed.* **2011**, *50*, 9554.

(107) Wilpiszewska, K.; Spychaj, T. *Carbohydrate Poly.* **2011**, *86*, 424.

(108) Mora-Pale, M.; Meli, L.; Doherty, T. V.; Linhardt, R. J.; Dordick, J. S. *Biotechnology and Bioengineering* **2011**, *108*, 1229.

(109) Marıa, P. D. d.; Maugeri, Z. *Current Opinion Chem. Bio.* **2011**, *15*, 220.

(110) Wu, C.; Senftle, T. P.; Schneider, W. F. *Phys. Chem. Chem. Phys.* **2012**, *14*, 13163.

(111) Shannon, M. S.; Bara, J. E. *Separation Sci. and Techn.* **2012**, *47*, 178.

(112) Lovelock, K. R. J. *Phys. Chem. Chem. Phys.* **2012**, *14*, 5071.

(113) Chen, X.; Sun, J.; Wanga, J.; Cheng, W. *Tetrahedron Lett.* **2012**, *53*, 2684.

(114) Yang, Z. Z.; Zhao, Y.-N.; He, L.-N. *RSC Advances* **2011**, *1*, 545.

(115) Hu, Y. F.; Liu, Z. C.; Xu, C. M.; Zhang, X. M. *Chem. Soc. Rev.* **2011**, *40*, 3802.

(116) Lodge, T. P. *Science* **2008**, *321*, 50.

(117) Chemat, F.; Vian, M. A.; Cravotto, G. *Int. J. Mol. Sci.* **2012**, *13*, 8615.

(118) Wytze, M. G.; B., D. H. A. *Sci. China Chem.* **2012**, *55*, 1488.

(119) Vičkačkaitė, V.; Padarauskas, A. *Cent. Eur. J. Chem.* **2012**, *10*, 652.

(120) Tonova, K. *Separation and Purif. Techn.* **2012**, *89*, 57.

(121) Tang, B.; Bi, W.; Tian, M.; Row, K. H. *J Chromatography B* **2012**, *904*, 1.

(122) Sun, X.; Luo, H.; Dai, S. *Chem. Rev.* **2012**, *112*, 2100.

(123) Stojanovic, A.; Keppler, B. K. *Separation Sci. and Techn.* **2012**, *47*, 189.

(124) Rao, P. R. V.; Venkatesan, K. A.; Rout, A.; Srinivasan, T. G.; Nagarajan, K. *Separation Sci. and Techn.* **2012**, *47*, 204.

(125) Pino, V.; German-Hernandez, M.; Martı´n-Pe´rez, A.; Anderson, J. L. *Separation Sci. and Techn.* **2012**, *47*, 264.

(126) Pereiro, A. B.; Araújo, J. M. M.; Esperança, J. M. S. S.; Marrucho, I. M.; Rebelo, L. P. N. *J. Chem. Thermodynamics* **2012**, *46*, 2.

(127) Liu, Y.; Chen, J.; Li, D. *Separation Sci. Techn.* **2012**, *47*, 223.

(128) LiLi, Z.; Lin, G.; ZhenJiang, Z.; Ji, C.; ShaoMin, Z. *Sci. China Chem.* **2012**, *55*, 1479.

(129) Joshi, M. D.; Anderson, J. L. *RSC Advances* **2012**, *2*, 5470.

(130) Poole, C. F.; Poole, S. K. *J. Sep. Sci.* **2011**, *34*, 888.

(131) Lozanoa, L. J.; Godíneza, C.; Ríosa, A. P. d. l.; F.J. Hernández-Fernándeza; Sánchez-Segadoa, S.; Alguacil, F. J. *J. Membrane Sci.* **2011**, *376*, 1.

(132) Billard, I.; Ouadi, A.; Gaillard, C. *Anal. Bioanal. Chem.* **2011**, *400*, 1555.

(133) Baba, Y.; Kubota, F.; Kamiya, N.; Goto, M. *J. Chem. Eng. Japan* **2011**, *44*, 679.

(134) Martinis, E. a. M.; Berton, P.; Monasterio, R. P.; Wuilloud, R. G. *Trends Analy. Chem.* **2010**, *29*, 1184.

(135) Li, Z.; Pei, Y.; Wang, H.; Fan, J.; Wang, J. *Trends Analy. Chem.* **2010**, *29*, 1336.

(136) Han, D.; Row, K. H. *Molecules* **2010**, *15*, 2405.

(137) Blasuccia, V. M.; Harta, R.; Pollet, P.; Liotta, C. L.; Eckert, C. A. *Fluid Phase Equilibria* **2010**, *294*, 1.

(138) Ueki, T.; Watanabe, M. *Bull. Chem. Soc. Jpn.* **2012**, *85*, 33.

(139) Tunckol, M.; Durand, J.; Serp, P. *CARBON* **2012**, *50*, 4303

(140) Perkin, S. *Phys. Chem. Chem. Phys.* **2012**, *14*, 5052.

(141) Jiao, J.; Zhang, H.; Yua, L.; Wanga, X.; Wang, R. *Colloids and Surfaces A: Physicochem. Eng. Aspects* **2012**, *408*, 1.

(142) Vollmer, C.; Janiak, C. *Coordination Chem. Rev.* **2011**, *255*, 2039.

(143) Patil, R. S.; Kokate, M. R.; Salvi, P. P.; Kolekar, S. S. *C. R. Chimie* **2011**, *14*, 1122.

(144) Torimoto, T.; Tsuda, T.; Okazaki, K. I.; Kuwabata, S. *Adv. Mater.* **2010**, *22*, 1196.

(145) Kuwabata, S.; Tsuda, T.; Torimoto, T. *J. Phys. Chem. Lett.* **2010**, *1*, 3177.

(146) Dupont, J.; Scholten, J. D. *Chem. Soc. Rev.* **2010**, *39*, 1780.

(147) Yang, Z.; Huang, Z. L. *Catal. Sci. Technol.* **2012**, *2*, 1767.

(148) Tietze, A. A.; Heimer, P.; Stark, A.; Imhof, D. *Molecules* **2012**, *17*, 4158.

(149) Naushada, M.; ALOthman, Z. A.; Khan, A. B.; Ali, M. *Intern. J. Bio. Macromolecules* **2012**, *51*, 555

(150) Ha, S. H.; Koo, Y. M. *Korean J. Chem. Eng.* **2011**, *28*, 2095.

(151) Fischer, F.; Mutschler, J.; Zufferey, D. *J. Ind. Microbiol Biotechnol* **2011**, *38*, 477.
(152) Moniruzzaman, M.; Nakashima, K.; Kamiya, N.; Goto, M. *Biochem. Eng. J.* **2010**, *48*, 295.
(153) Page, T. A.; Kraut, N. D.; Page, P. M.; Baker, G. A.; Bright, F. V. *J. Phys. Chem. B* **2009**, *113*, 12825.
(154) McCarty, T. A.; Page, P. M.; Baker, G. A.; Bright, F. V. *Ind. Eng. Chem. Res.* **2008**, *47*, 560.
(155) Lakowicz, J. R. *Principles of Fluorescence Spectroscopy*, Third Edition ed.; Springer Science Business Media: New York, 2006.
(156) Valeur, B. *Molecular Fluorescence Principles and Applications*; WILEY-VCH Verlag GmbH, 69469: Weinheim, 2002.
(157) Grabowski, Z. R.; Rotkiewicz, K. *Chem. Rev.* **2003**, *103*, 3899.
(158) Maroncelli, M.; Macinnis, J.; Fleming, G. R. *Scince* **1989**, *243*, 1674.
(159) Maroncelli, M.; Fleming, G. R. *J. Chem. Phys.* **1987**, *86*, 6221.
(160) Kometani, N.; Kajimoto, O.; Hara, K. *J. Phys. Chem. A* **1997**, *101*, 4916.
(161) Hara, K.; Kuwabara, H.; Kajimoto, O. *J. Phys. Chem. A* **2001**, *105*, 7174.
(162) Sarkar, N.; Datta, A.; Das, S.; Bhattacharyya, K. *J. Phys. Chem.* **1996**, *100*, 15483.
(163) Mandal, D.; Datta, A.; Pal, S. K.; Bhattacharyya, K. *J. Phys. Chem. B* **1998**, *102*, 9070.
(164) Datta, A.; Mandal, D.; Pal, S. K.; Bhattacharyya, K. *J. Phys. Chem. B* **1997**, *101*, 10221.
(165) Bagchi, B. *Chem. Rev.* **2005**, *21*, 3197.
(166) Bhattacharyya, K. *Acc. Chem. Res.* **2003**, *36*, 95.
(167) Nandi, N.; Bhattacharyya, K.; Bagchi, B. *Chem. Rev.* **2000**, *100*, 2013.
(168) Jimenez, R.; Fleming, G. R.; Kumar, P. V.; Maroncelli, M. *Nature* **1994**, *369*, 471.
(169) Karmakar, R.; Samanta, A. *J. Phys. Chem. A* **2002**, *106*, 4447.
(170) Karmakar, R.; Samanta, A. *J. Phys. Chem. A* **2002**, *106*, 6670.
(171) Samanta, A. *J. Phys. Chem. Lett.* **2010**, *1*, 1557.

(172) Mandal, P. K.; Saha, S.; Karmakar, R.; Samanta, A. *Current Science* **2006**, *90*, 301.

(173) Muramatsu, M.; Nagasawa, Y.; Miyasaka, H. *J. Phys. Chem. A* **2011**, *115*, 3886.

(174) Turton, D. A.; Hunger, J.; Stoppa, A.; Hefter, G.; Thoman, A.; Walther, M.; Buchner, R.; Wynne, K. *J. Am. Chem. Soc.* **2009**, *131*, 11140.

(175) Hunt, N. T.; Jaye, A. A.; Meech, S. R. *Phys. Chem. Chem. Phys.* **2007**, *9*, 2167.

(176) Zhang, X. X.; Liang, M.; Ernsting, N. P.; Maroncelli, M. *J. Phys. Chem. B* **2012**, *113*, ASAP.

(177) Horng, M. L.; Gardecki, J. A.; Maroncelli, M. *J. Phys. Chem. A* **1997**, *101*, 1030.

(178) Dutt, G. B.; Sachdeva, A. *J. Chem. Phys.* **2003**, *118*, 8307.

(179) Dutt, G. B.; Ghanty, T. K.; Singh, M. K. *J. Chem. Phys.* **2001**, *115*, 10845.

(180) Nagachandra, K. H.; J.R.Mannekutla; M.A.Shivkumar; S.R.Inamdar. *J. Luminescence* **2012**, *132*, 570.

(181) Maiti, N. C.; Krishna, M. M. G.; Britto, P. J.; Periasamy, N. *J. Phys. Chem. B* **1997**, *101*, 11051.

(182) Singh, P. K.; Kumbhakar, M.; Pal, H.; Nath, S. *J. Phys. Chem. B* **2009**, *113*, 1353.

(183) Saito, H.; Minamida, T.; Arimoto, I.; Handa, T.; Miyajima, K. *J. Biophy. Chem.* **1996**, *127*, 15515.

(184) Mali, K. S.; Dutt, G. B.; Mukherjee, T. *J. Chem. Phys.* **2007**, *127*, 154904.

(185) Mali, K. S.; Dutt, G. B.; Mukherjee, T. *J. Phys. Chem. B* **2007**, *111*, 5878.

(186) Ruiz, C. C. *Photochem. Photobiol. Sci.* **2012**, *11*, 1331.

(187) Baker, S. N.; Baker, G. A.; Kane, M. A.; Bright, F. V. *J. Phys. Chem. B* **2001**, *105*, 9663.

(188) Karve, L.; Dutt, G. B. *J. Phys. Chem. B* **2012**, *116*, 1824.

(189) Karve, L.; Dutt, G. B. *J. Phys. Chem. B* **2012**, *116*, 9107.

(190) Gangamallaiah, V.; Dutt, G. B. *J. Phys. Chem. B* **2012**, *116*, 12819.

(191) Fruchey, K.; Lawler, C. M.; Fayer, M. D. *J. Phys. Chem. B* **2012**, *116*, 3054.

(192) Das, S. K.; Sarkar, M. *J. Phys. Chem. B* **2012**, *116*, 194.
(193) Karve, L.; Dutt, G. B. *J. Phys. Chem. B* **2011**, *115*, 725.
(194) Khara, D. C.; Samanta, A. *Phys. Chem. Chem. Phys.* **2010**, *12*, 7671.
(195) Dutt, G. B. *Ind. J. Chem.* **2010**, *49A*, 705.
(196) Dutt, G. B. *J. Phys. Chem. B* **2010**, *114*, 8971.
(197) Mali, K. S.; Dutt, G. B.; Mukherjee, T. *J. Chem. Phys.* **2008**, *128*, 054504.
(198) Mali, K. S.; Dutt, G. B.; Mukherjee, T. *J. Chem. Phys.* **2005**, *123*, 174504.
(199) Ito, N.; Arzhantsev, S.; Heitz, M.; Maroncelli, M. *J. Phys. Chem. B* **2004**, *108*, 5771.
(200) Ingram, J. A.; Moog, R. S.; Ito, N.; Biswas, R.; Maroncelli, M. *J. Phys. Chem. B* **2003**, *107*, 5926.
(201) Fruchey, K.; Fayer, M. D. *J. Phys. Chem. B* **2010**, *114*, 2840.
(202) Bhattacharya, B.; Jana, B.; Bose, D.; Chattopadhyay, N. *J. Chem. Phys.* **2011**, *134*, 044535 .
(203) Bhattacharyya, K.; Chowdhury, M. *J. Photochemistry.* **1986**, *33*, 61.
(204) Roy, D.; Bhattacharyya, K.; Bera, S. C.; Chowdhury, M. *Chem. Phys. Lett.* **1980**, *69*, 134.
(205) Bhattacharyya, K.; Roy, D.; Chowdhury, M. *J. Luminescence* **1980**, *22*, 95.
(206) Fang, T. S.; Brown, R. E.; Kwan, C. L.; Singer, L. A. *J. Phys. Chem.* **1978**, *82*, 2489.
(207) Morantz, D. J.; Wright, A. J. C. *J. Chem. Phys.* **1971**, *54*, 692.
(208) Bera, S. C.; Mukherjee, R.; Chowdhury, M. *J. Chem. Phys.* **1969**, *51*, 754.
(209) Maroncelli, M.; Zhang, X. X.; Liang, M.; Roy, D.; Ernsting, N. P. *Faraday Discuss.* **2012**, *154*, 409.
(210) Liang, M.; Kaintz, A.; Baker, G. A.; Maroncelli, M. *J. Phys. Chem. B* **2012**, *116*, 1370.
(211) Koch, M.; Rosspeintner, A.; Angulo, G.; Vauthey, E. *J. Am. Chem. Soc.* **2012**, *134*, 3729.
(212) Bhattacharya, B.; Samanta, A. *J. Phys. Chem. B* **2008**, *112*, 10101.

(213) Brigouleix, C.; Anouti, M.; Jacquemin, J.; Caillon-Caravanier, M.; Galiano, H.; Lemordant, D. *J. Phys. Chem. B* **2010**, *114*, 1757.

(214) Galinski, M.; Stepniak, I. *J Appl Electrochem* **2009**, *39*, 1949.

(215) Kim, K. S.; Choi, S.; Demberelnyamba, D.; Lee, H.; Oh, J.; Lee, B.-B.; Mun, S. J. *Chem. Comm.* **2004**, 828

(216) Fleming, G. R. *Chemical Applications of Ultrafast Spectroscopy*; Oxford University Press, 1986.

Chapter 2

Materials, Instrumentation and Methods

This chapter lists the materials used in this study procured from various commercial sources followed by description of the methods of purification of reagents and solvents. Synthesis and purification of the RTILs employed in the present study have also been described. The instrumental details of the time-correlated single-photon counting technique (TCSPC) based picosecond setup have been outlined. Various methodologies employed in the present investigation, such as the analysis of TCSPC data and estimation of $E_T(30)$ values of RTILs have been discussed. A detailed procedure to get an anisotropy decay profile from the lifetime decay carves has discussed. The method of analysis of data for spectral reconstruction of the time-resolved emission spectra from the decay curves has also been discussed.

2.1. Materials

Bianthryl was synthesized by dimerization of anthraquinone following a reported procedure.[1] The compound was characterized by spectroscopic techniques and purity was checked by chromatography. Benzil was bought from Loba Chemicals and recrystallized twice from methanol. ANS was procured from Molecular Probes and was recrystallized from ethanol. EB was obtained from Aldrich and recrystallized from methanol. It showed a single spot on the thin layer chromatography (TLC) plate (4:1:1 butanol:acetic acid:water). Laser grade C153

and PRODAN were procured from Eastman Kodak and Molecular probes, respectively and used without further purification. AP and anthracene were obtained from TCI (Japan) and Sigma Aldrich, respectively and recrystallized twice from ethanol prior to photophysical experiments. The purity of all the probe molecules was checked by single spot in thin layer chromatography (TLC), as well as by matching the absorption and emission spectra with literature.

The various drying agents such as phosphorous pentoxide (P_2O_5), potassium hydroxide (KOH), calcium sulphate ($CaSO_4$), sodium metal, magnesium turning and iodine used at different stages of the purification procedure, were purchased from local companies (India). Calcium hydride was obtained from Spectrochem (India). GR grade solvents were obtained from Merck (India) for spectroscopic and synthetic purposes and their purification procedures are given in the following section. Deuteriated solvents, chloroform-d, and DMSO-d_6 used for NMR spectral measurements were obtained either from Aldrich or from Merck (India).

Advanced Material Research grade imidazolium ionic liquids, [bmim][PF_6], [bmim][BF_4], [bmim][Tf_2N] and [emim][BF_4] used in this work, were obtained from Kanto Chemicals (Japan) and this liquid was rigorously dried under high vacuum before use.

The reagents required for synthesis of morpholinium RTILs employed in different studies embodied in this thesis were obtained from various sources and carefully purified following standard procedures. The materials like N-methylmorpholine and lithilum bis(trifluoromethanesulfonyl)imide ($LiTf_2N$) were

obtained from Sigma Aldrich. 1-bromoethane, 1-bromobutane, 1-bromohexane, 1-bromooctane were procured from Merck (India).

2.2. Purification of conventional solvents

The solvents used at various stages of the study were purified using standard procedures.[2] Briefly, we adopted the following procedures for the purification of various solvents.

Cyclohexane: The solvent was refluxed over metallic sodium for 3 - 4 h and then benzophenone was added after cooling. The dark blue solution was refluxed for another hour and distilled under dry condition. The purified solvents were found optically transparent in the spectral region of interest.

Ethanol and Methanol: Initially the solvent was dried over CaH_2 by keeping overnight. Then 50 - 75 mL of the dried solvent was added to clean dry magnesium turnings (5 g) and iodine (0.5 g) and warmed until all magnesium was converted into magnesium alkoxide. About 1 L of alcohol was added to this, refluxed for 2-3 h and distilled out.

Dichloromethane (DCM): The solvent was stirred with calcium hydride for 5-6 h and then distilled. The distilled solvent was collected and stored under dry condition.

Ethyl acetate: After stirring with P_2O_5 for some hours, the solvent was distilled out.

Acetone: The solvent was refluxed for some hours with anhydrous $CaSO_4$ and then distilled out.

Water: Water was initially distilled using potassium permanganate and potassium hydroxide. This was subsequently distilled twice before taken to study.

2.3. Synthesis and purification of RTILs

The morpholinium RTILs were synthesized by following a two-step procedure[3] depicted in Scheme 2.1.

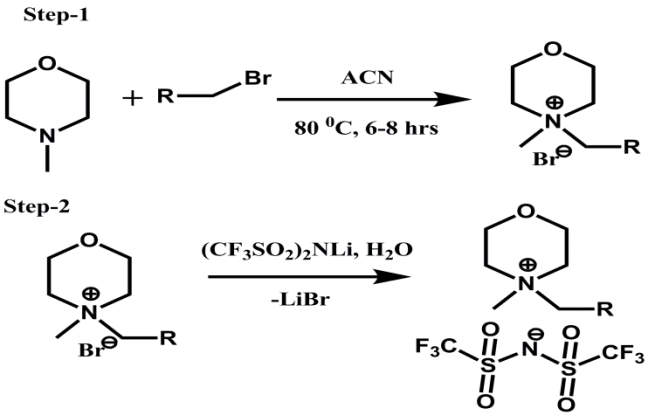

Scheme 2.1. Synthetic steps of RTILs employed in the present study

The first step involved preparation of the bromide salt of N-alkyl-N-methylmorpholinium ion, [$Mor_{1,n}$][Br] and the second step consisted of exchange of the bromide ion by the bis(trifluoromethanesulfonyl)imide ion. Specifically, the procedure followed for the synthesis of the RTILs is outlined below. The alkyl bromide was slowly added to an acetonitrile solution of N-methylmorpholine and then the solution was refluxed at 80 ^{0}C for 6 - 8 h. Subsequently, acetonitrile was removed from the reaction mixture in a rotary evaporator. The bromide salt, [$Mor_{1,n}$][Br], was washed with acetone several times to remove the unreacted

materials from the reaction mixture. The salt was dried under vacuum and weighed for the next step. In the second step, an aqueous solution of the bromide salt was first treated with activated charcoal under reflux condition for overnight and then the filtrate was used for a metathesis reaction by adding lithium bis(trifluoromethanesulfonyl)imide and stirring for nearly 24 h. Then DCM was added to the solution and the organic layer was separated out from the reaction mixture. Subsequently, the organic layer was washed several times with water until it was free from any halide (checked with a $AgNO_3$ solution). Finally, DCM was removed from the mixture and the RTIL was dried for several hours under high vacuum prior to use.

2.4. Instrumentation

The NMR spectra were measured using Bruker AVANCE 400 MHz NMR spectrometer. Steady-state absorption and fluorescence spectra were recorded on a UV-vis spectrophotometer (Cary100, Varian) and a spectrofluorimeter (FluoroLog-3, Jobin Yvon), respectively. The delayed component of the emission spectra were recorded in the same spectrofluorimeter employing a pulsed xenon lamp (FWHM = 3 μs). The temperature dependent study was performed using a peltier controller (Wavelength electronics) and the low temperature (77 K) study was performed by directly immersing the solution taken in quartz tube into a dewar flask containing liquid nitrogen. The emission spectra were corrected for the instrumental response. The viscosity of the RTILs and other viscous solvents was measured by a LVDV-III Ultra Brookfield Cone and Plate viscometer (1%

accuracy and 0.2% repeatability). For variable temperature viscosity measurement, a Julabo water circulator bath was used.

2.4.1. Picosecond time-correlated single-photon counting setup

Time-resolved fluorescence measurements were carried out using a time-correlated single-photon counting (TCSPC) spectrometer (5000, IBH).[4] Diode lasers were used as excitation sources and a micro-channel plate (MCP) photomultiplier tube was used as the detector. Three diode lasers, namely, the one having output at 375 nm with FWHM = 50 ps, 405 nm with FWHM = 50 ps and the other 439 nm with FWHM = 90 ps were used in the present study. The maximum repetition rate of the diode lasers were 10 MHz (375 and 405 nm) and 1 MHz (439 nm) respectively. A Hamamatsu R3809U-50 MCP-PMT (160-850 nm range) was used as a detector.

The lamp profile was recorded by placing a scatterer (dilute solution of Ludox in water) in place of the sample. Decay curves were analyzed by nonlinear least-squares iteration procedure using IBH DAS6 (Version 2.2) decay analysis software.

The same setup, with attached polarizers, was used for time-resolved anisotropy measurements and the same software was used to analyze the anisotropy data.

2.5. Sample preparation for spectral measurements

For measurements in conventional solvents, the solutions were prepared such that the absorbance of the solution (1 cm path length) at the excitation

wavelength was around 0.1 - 0.3. The concentration of the probe molecules corresponding to an absorbance value of around 0.3 was found to be in the range of 10^{-6} - 10^{-4} M.

In case of experiments in RTILs, the sample preparation was not so straightforward. Prior to the sample preparation, these liquids were dried under high vacuum at room temperature for 10 - 12 h in order to ensure the removal of the trapped moisture, if any. Generally 2.5 mL of RTIL was used to prepare sample solution in 1 cm quartz cuvette. After addition of sample solute, the cuvettes were tightly sealed with septum and parafilm. Since the dissolution of the solid probes in RTILs is slow, the absorption spectra were measured from time to time to ensure complete dissolution. The concentration of the solute was optimized to have 0.2 - 0.3 absorbance at the excitation wavelength. For probe with long lifetime and oxygen sensitivity, cf. benzil, the solutions were deoxygenated by purging argon gas.

2.6. Measurement of emission quantum yields and rate constant for reverse intersystem crossing

For fluorescence quantum yield measurements, optically matched solutions (or solutions with very similar absorbance) of the sample and the standard at a given absorbing wavelength (the excitation wavelength) were prepared. The quantum yield was calculated by measuring the integrated area under the emission curves and by using the following equation,[5]

$$\Phi_{sample} = \frac{A_{sample} \times OD_{std} \times n^2_{sample}}{A_{std} \times OD_{sample} \times n^2_{std}} \times \Phi_{std} \qquad (2.1)$$

where, Φ is the quantum yield, A is the integrated area of emission, OD is the optical density at the excitation wavelength, and n is the refractive index. The subscripts 'sample' and 'std' refer to the fluorophore of unknown quantum yield and the reference fluorophore of known quantum yield, respectively.

The room temperature phosphorescence quantum yield of benzil was calculated by using the following formula.[6]

$$\phi_p = \frac{I_p}{I_f}\phi_T\phi_f \quad \text{.....(2.2)}$$

Where I_f and I_p are the integrated areas under the fluorescence spectrum (oxygenated solution) and phosphorescence spectrum (degassed solution) respectively. ϕ_f is fluorescence quantum yield for oxygenated solution and ϕ_T is the quantum yield of the triplet state.

The phosphorescence and delayed fluorescence quantum yield can be expressed as follows.

$$\phi_P = \phi_T \frac{k_{RP}}{k_{RP} + k_n^T + k_{risc}} \quad \text{.....(2.3)}$$

$$\phi_{DF} = \phi_T\phi_f \frac{k_{risc}}{k_{RP} + k_n^T + k_{risc}} \quad \text{.....(2.4)}$$

where ϕ_P and ϕ_{DF} represent the phosphorescence and delayed fluorescence quantum yield respectively. k_{RP}, k_n^T and k_{risc} are the radiative rate constant from triplet state, non-radiative rate constant from the triplet state and the rate constant of $T_1 \rightsquigarrow S_1$ process, respectively.

Combination of equations (2.3) and (2.4) give

$$\frac{\phi_{DF}}{\phi_P} = \phi_f \frac{k_{risc}}{k_{RP}} \quad \text{……(2.5)}$$

At any given time t (t>> k_f), this equation can be represented as

$$\frac{i_{DF}(t)}{i_p(t)} = \phi_f \frac{k_{risc}}{k_{RP}} \quad \text{…….(2.6)}$$

k_{risc} is estimated from this equation by substituting the values of i_{DF}, i_p, ϕ_f and k_{RP}. The last quantity, k_{RP}, is obtained from the measured ϕ_P and τ_P values in the following equation at 20 ^{0}C.

$$k_{RP} = \frac{\phi_P}{\tau_P} \quad \text{……..…..(2.7)}$$

2.7. Data analysis

The lifetimes of the samples were estimated from the measured fluorescence decay curves and instrumental profiles using a nonlinear least-squares iterative fitting procedure (using decay analysis software IBH DAS6, Version 2.2). This program uses a reconvolution method for the analysis of the experimental data.[7] When the decay time is long compared to the pulse width of the excitation pulse, the excitation may be described as a δ-function. However, when the lifetime is short, distortion of the experimental data occurs by the finite decay time of the lamp pulse and response time of the photomultiplier and associated electronics. Since the measured decay function is convolution of the true fluorescence decay and the instrumental pulse, it is necessary to analyze the

data by deconvolution in order to get the actual fluorescence lifetime. The mathematical statement of the problem is given by the following equation:

$$D(t) = \int_0^t P(t')G(t-t')dt' \qquad (2.8)$$

where, D(t) is the fluorescence intensity at any given time t, P(t') is the intensity of the exciting light at time t' and G(t–t') is the response function of the experimental system. The experimental data D(t) and P(t') from the MCA were fed into a personal computer (PC) to determine the lifetime. We used the IBH program to analyze the multi-exponential decays. An excitation pulse profile was recorded and then deconvolution started with mixing of the excitation pulse and a projected decay to form a new reconvoluted set. The data was compared with the experimental set and the difference between the data points was summed, generating χ^2 function for fitting. The deconvolution proceeded through a series of such iterations until an insignificant change of χ^2 occurred between iterations. The inspection of reduced χ^2, a plot of weighted residuals and autocorrelation function of the residuals allowed assessment of the quality of the fit.

2.8. Construction of time-resolved emission spectra (TRES)

The time-resolved emission spectra (TRES) were constructed by an indirect method described here.[8] A series of time-resolved emission decay profiles were measured at every 5/10 nm interval across the entire steady-state emission spectra. The total number of measurements was 22-25 in each case. Each decay curve was then fitted to multi-exponentially a (usually, bi- or tri-exponential)

decay function with an iterative reconvolution program (IBH) to obtain the best fits with χ^2 around 1.0 - 1.2. This procedure deconvoluted the measured decay from the instrumental response and increased the effective time resolution of the experiment to ~40 ps. The *impulse response function*, I(λ,t) was then calculated from the best-fitted curve for each wavelength. To make the time-integrated intensity at each wavelength equivalent to the steady-state intensity at that particular wavelength, a normalization factor of the following form

$$H(\lambda) = \frac{I_{ss}(\lambda)}{\sum_i \alpha_i(\lambda)\tau_i(\lambda)} \qquad (2.9)$$

was constructed, where, $I_{ss}(\lambda)$ is the steady-state intensity, $\alpha_i(\lambda)$ and $\tau_i(\lambda)$ are the preexponential factor and decay time, respectively, at a particular wavelength with $\sum\alpha_i(\lambda) = 1$. The time-resolved emission spectra (TRES) were calculated from the appropriately normalized intensity decay (impulse response) function, I′(λ,t) for the given set of wavelengths at different times, where I′(λ,t) = H(λ) × I(λ,t). The peak emission frequencies (in cm^{-1}), $\bar{\nu}(t)$ at various times were obtained by fitting each TRES to the following log-normal function,

$$I = h\exp[-\ln 2\{\ln(1+\alpha)/\gamma\}^2] \quad \text{for, } \alpha > -1 \qquad (2.10)$$
$$= 0 \quad \text{for, } \alpha \le -1$$

Where, $\alpha = \frac{2\gamma(\bar{\nu}-\bar{\nu}_{peak})}{\Delta}$, $\bar{\nu}_{peak}$ is the wavenumber corresponding to the peak, h is the peak height, Δ is the FWHM and γ is the asymmetry of the band-shape. The

best fitted curve was obtained by optimizing these four parameters by nonlinear least-squares iteration technique.

2.9. Time-resolved Anisotropy decay profiles

The anisotropy measurements were performed using two polarizers by placing one of them in the excitation beam path and the other in front of the detector.[8] An alternate collection of the fluorescence intensity in parallel (I_{II}) and perpendicular ($I_{\perp}$) polarization (with respect to the vertically polarized excitation laser beam) for equal interval of time was made until the count difference between the two polarizations (at t = 0) was ~5000. For G-factor calculation, the same procedure was followed, but with only 4 cycles and horizontal polarization of the exciting laser beam. The anisotropy measurements were performed at the respective fluorescence maxima of the probe using a monochromator with a bandpass of 2 nm. Time-resolved fluorescence anisotropy, r(t), is calculated using the following equation,

$$r(t) = \frac{I_{II}(t) - GI_{\perp}(t)}{I_{II}(t) + 2GI_{\perp}(t)} \qquad (2.11)$$

where, G is the correction factor for the detector sensitivity to the polarization direction of the emission and $I_{II}(t)$ and $I_{\perp}(t)$ are the fluorescence decays polarized parallel and perpendicular to the polarization of the excitation light, respectively. The rotational time constants were estimated by fitting the anisotropy decay profiles to a single and/or a bi-exponential function depending on the situation.

2.10. Estimation of polarity

The solvatochromic visible absorption of the betaine dye has been used as a solvent dependent reference probe to define empirically a solvent polarity scale, namely $E_T(30)$ scale.[9] These $E_T(30)$ values are defined as the molar transition energies of the pyridinium-N-phenoxide betaine dye (shown in Chart 1.3), measured in solvents of different polarity at room temperature (25°C) and normal pressure (1 bar). Thus,

$$E_T(30)/\text{kcal mol}^{-1} = hc\bar{\nu}_{max} N_A = (2.8591 \times 10^{-3})\ \bar{\nu}_{max}\ /\text{cm}^{-1}$$

$$= 28591/\lambda_{max}\ (\text{nm}) \qquad (2.12)$$

where, $\bar{\nu}_{max}$ is the wavenumber and λ_{max} is the wavelength corresponding to the maximum of the long-wavelength, solvatochromic, intramolecular charge transfer absorption band of the standard betaine dye; and h, c, and N_A are the Planck's constant, speed of light, and Avogadro number, respectively. This is the direct way of solvent polarity measurement.

As mentioned in Chapter 6, the $E_T(30)$ values of the RTILs can also be measured using probe other than the standard betaine dye, by an indirect method. Here, the wavenumber corresponding to the fluorescence maximum, $\bar{\nu}_{max}^{fluo}$ of probe molecule in various conventional solvents was measured at room temperature. A calibration line was drawn by plotting measured $\bar{\nu}_{max}^{fluo}$ values (in cm^{-1}) against the known $E_T(30)$ values of the solvents, from which the $E_T(30)$ value of a RTIL was obtained using the measured $\bar{\nu}_{max}^{fluo}$ value of the probe in the given RTIL.

2.11. Standard error limits

Standard error limits involved in the measurements are:

λ_{max} (abs./fluo.)	± 1 nm
Φ_f	± 10%
τ_f (> 1 ns)	± 5%
τ_f (< 1 ns)	± 5-8% (depending on the excitation source)
Polarity of RTILs in $E_T(30)$ scale	± 5%
Relaxation time	± 5%
Viscosity	± 2%

References

(1) Bell, F.; Waring, D. H. *J. Chem. Soc.* **1949**, *149*, 267.

(2) Perrin, D. D.; Armarego, W. L. F.; Perrin, D. D. *Purification of Laboratory Chemicals*; Pergamon Press Ltd. Oxford, England, 1980.

(3) Kim, K. S.; Choi, S.; Demberelnyamba, D.; Lee, H.; Oh, J.; Lee, B. B.; Mun, S. J. *Chem. Comm.* **2004**, 828

(4) O'Connor, D. V.; Philips, D. *Time-Correlated Single Photon Counting*; Academic Press: New York, 1984.

(5) Austin, E.; Gouterman, M. *Bioinorg. Chem.* **1978**, *9*, 281.

(6) Duchowicz, R.; Ferrer, M. L.; Acuna, A. U. *Photochem. Photobiol.* **1998**, *68*, 494.

(7) Bevington, P. R. *Data Reduction and Analysis for the Physical Sciences*; McGraw-Hill: New York, 1969.

(8) Lakowicz, J. R. *Principles of Fluorescence Spectroscopy*, Third Edition ed.; Springer Science Business Media: New York, 2006.

(9) Reichardt, C. *Solvents and Solvent Effects in Organic Chemistry*, Second ed.; VCH Verlagsgesellschaft, 1988.

Chapter 3

Excited State Process of Bianthryl in Imidazolium Ionic Liquids

In this chapter, the excited state dynamic process of 9,9′-bianthryl (BA) has been studied in three different imidazolium ionic liquids of different viscosity to understand the conformational dynamics of BA. Steady-state emission spectra of BA in RTILs reveal that the emission mostly occurs from the charge transfer (CT, two anthryl units are planer to each other) state which is originated from the locally excited (LE, two anthryl units are perpendicular to each other) state due to excited state conformational dynamics process. However, in time-resolved measurements we could observe the early part of the formation of the CT state. It is found that these two processes occur in different time scales in RTILs unlike that in the conventional solvents.

3.1. Introduction

The photoprocesses investigated in RTILs are mostly the studies on dynamic Stokes shift and solvation dynamics of dipolar probes, intramolecular excimer formation, photoinduced electron and proton transfer reactions, photoisomerization reaction, etc.[1-18] Recently, Nagasawa et al have studied the excited state dynamics of 9,9´-Bianthryl (**BA**, Chart 3.1) in imidazolium ionic liquids using femtosecond time-resolved absorption and picosecond time-resolved fluorescence spectroscopic techniques.[19] BA is a well-known system whose excited state behavior and dynamical processes have been studied extensively in a

range of conventional solvents.[20-29] The interest in BA is mainly due to the fact that this pre-twisted molecule with mutually perpendicular anthracene rings in the ground state undergoes symmetry breaking upon photoexcitation and its fluorescence spectra show distinct charge transfer (CT) character, especially in polar solvents.[21,25,28,29] In nonpolar solvents the first excited state (S_1) is predominantly a locally excited (LE) state with very little or no CT character,[22,25,28,29] whereas, in highly polar solvents a CT state, which is formed rapidly from the LE state, is the emitting state.[23,24,27] The transient absorption study on BA in the picosecond and sub-picosecond regime has revealed the ultrafast time-scale (20 - 50 ps) of the formation of the CT state in conventional solvents of low viscosity.[23] However, in more viscous media this time is much longer, indicating the effect of viscosity on the symmetry-breaking process.[26]

The femtosecond transient absorption measurements in RTILs by Nagasawa et al suggest that charge transfer in BA is multi-exponential with the time scale ranging from sub-picosecond to several hundreds of picoseconds, the latter being dependent on the viscosity of the media.[19] The fluorescence study on the other hand reveals dynamic Stokes shift of the CT emission in the nanosecond time domain, reflecting the stabilization of the CT state through solvent reorganization.[19]

However, one aspect of the relaxation dynamics of BA in RTILs that is not clear from the results presented in this interesting study is the following. Since the LE and CT emission bands of BA overlap significantly in the 21000 – 25000 cm^{-1} region, and the LE state, which is the precursor of the CT state, survives for several hundreds of picoseconds,[19] one expects its signature on the fluorescence

spectra as well, particularly in the early time domain. However, this is surprisingly not the case. The lack of any signature of the LE state in the time-resolved fluorescence spectra, even in the early time domain, appears inconsistent and it implies that the LE state may be much short-lived than what is indicated by the time-resolved absorption measurements. In order to resolve this important issue concerning the excited state dynamics of BA in RTILs we have taken up this work in which we have investigated the time-resolved fluorescence behavior of BA in three different RTILs (Chart 3.1) based on 1-butyl-3-methylimidazolium cation.

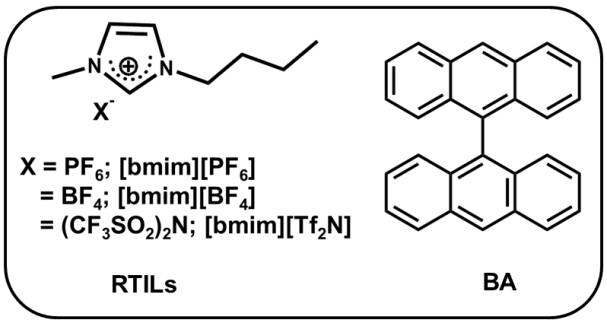

Chart 3.1. Chemical formula and abbreviation of RTILs and 9,9´-bianthryl (BA).

3.2. Steady-state behavior

Steady-state absorption and fluorescence spectra of BA in RTILs are shown in Figure 3.1. Very little difference in the spectral behavior of BA can be observed in different RTILs. The 0-0 transition is estimated to be around 25400 cm^{-1} from the structured absorption spectrum, which is not very different from that observed in polar conventional solvents such as acetonitrile 25650 cm^{-1}.[22] The steady-state fluorescence spectra of BA in RTILs are characterized by a broad emission,

which is indicative of the charge transfer nature of the band, as is the case with the ordinary polar solvents.[21,25,28,29] One can also observe some structure near the onset of the broad emission (~ 410 nm), where the LE emission (as evident from the emission spectrum of BA in hexane, shown in Fig. 3.1) is expected. We note in this context that the fluorescence spectral behavior of BA in RTILs, including even the structured portion of the emission, is very similar to that observed by Nagasawa et al.[19] The emission maxima (λ_{max}^{fluo}) of BA in RTILs are found centered around 480 nm, which is nearly 10 nm red-shifted compared to acetonitrile (λ_{max}^{fluo} = 470.6 nm).[25] This observation is consistent with the measured polarity parameters of RTILs, which suggest that the RTILs are more polar than acetonitrile.

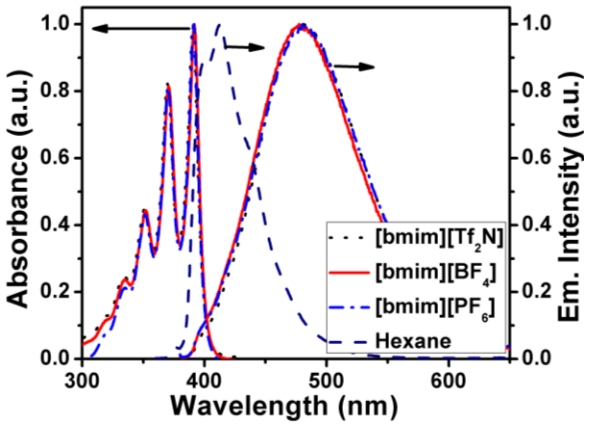

Fig. 3.1. Steady-state absorption and emission spectra of BA in RTILs and hexane. Excitation wavelength 375 nm. All spectra were normalized at the corresponding peak maximum.

3.3. Time-resolved behavior

In each RTIL, we have measured the emission decay profiles of BA at 5/10 nm interval across the entire steady-state emission spectra by selecting the wavelength using a monochromator with a bandpass of 2 nm. The total number of measurements was around 26-28 in each RTIL. Wavelength-dependent decay profiles, which are a typical signature of slow solvation dynamics, have been observed. One representative wavelength dependent decay behavior is illustrated in Figure 3.2. When monitored at the shorter wavelength region, only monotonous decay is observed, and at the longer wavelengths, the time profiles consist of a slow rise followed by the decay.

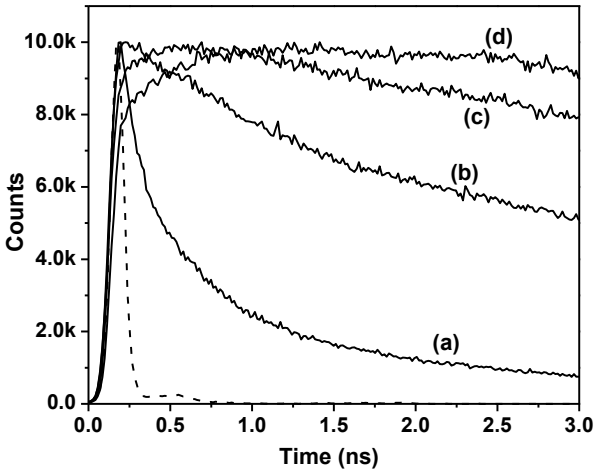

Figure 3.2. Wavelength-dependent decay profiles of BA in [bmim][PF_6] at (a) 410 nm, (b) 480 nm, (c) 520 nm, (d) 580 nm. The lamp profile is shown as dashed line.

The time-resolved emission spectra (TRES) have been constructed by fitting the individual decay curves to a multiexponential function followed by normalization of the decay traces by steady-state spectra, a procedure described Chapter 2. The TRES for BA in [bmim][PF_6] is shown in Figure 3.3 for a wide range of time-scale (in ps-ns regime). It can be seen clearly that in the short time-scale (0 - 150 ps), the TRES are a combination of two distinct bands; a structured high energy band with peak at around 23800 cm^{-1} and a broad band extending over several thousands of wavenumbers in the low energy region. A closer look at this figure reveals that while the sharp structure on the broad emission envelope decays rather rapidly (with no shift in its position) and vanishes almost completely in about 200 ps, the broad band displays a time-dependent Stokes shift of the maximum that continues for a much longer time (up to several nanoseconds). A similar observation has been made in [bmim][BF_4] and [bmim][Tf_2N], which is shown in Figure 3.4 & 3.5, respectively.

It is thus evident that the time-dependent emission behavior of BA reveals two relaxation processes, not just one, as found recently by Nagasawa et al.[19] In the short time scale, the decay of the sharp peak at around 23800 cm^{-1} is the most prominent feature of relaxation and at longer time, when the sharp peak has decayed completely, the relaxation process consists of dynamic Stokes shift of the CT emission maxima. As the sharp peak position matches closely with the peak position of the LE state as observed in nonpolar solvents like hexane or cyclohexane,[25,28,29] it is evident that the decay of the LE state is what is observed in the early time scale. On the other hand, monotonic red shift of the CT band is the typical signature of the solvent relaxation dynamics.

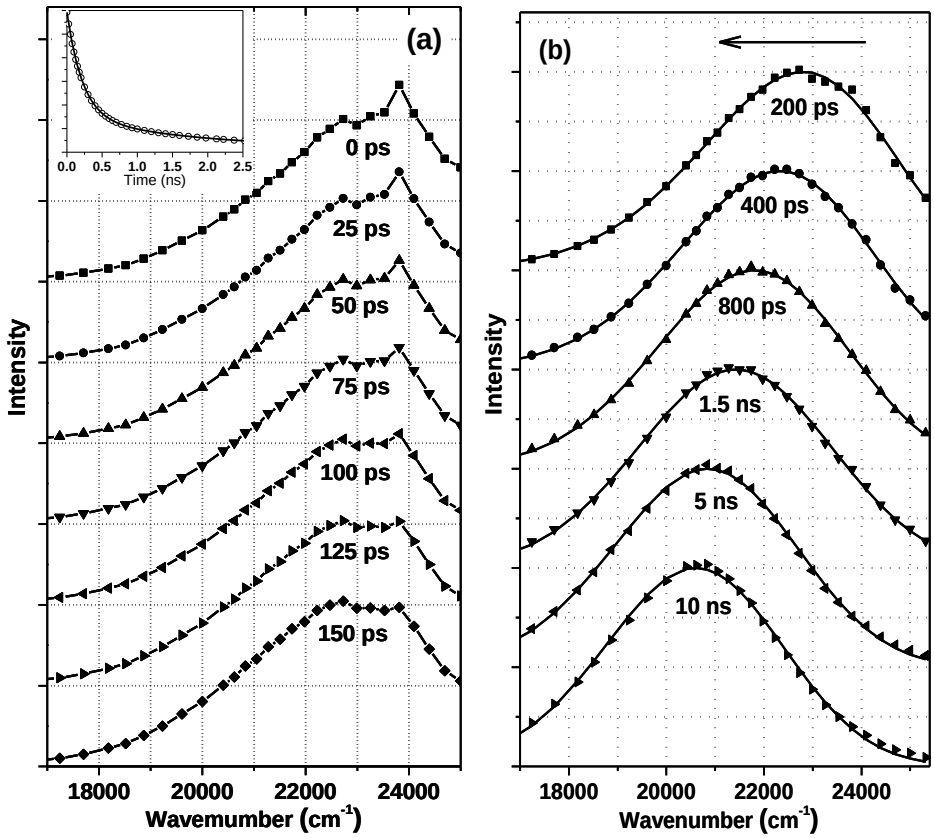

Figure 3.3. (a) Time-resolved emission spectra (TRES) of BA in [bmim][PF_6] at the early stage of dynamics. The inset shows the decay of the emission intensity at 23800 cm^{-1}, which corresponds to the peak position of the LE emission. The maximum of the CT bands are normalized in each case. (b) TRES for BA in [bmim][PF_6] in the long time-scale. All spectra are normalized at the corresponding peak maximum. (λ_{exc} = 375 nm). The spectral data points are fitted to lognormal function.

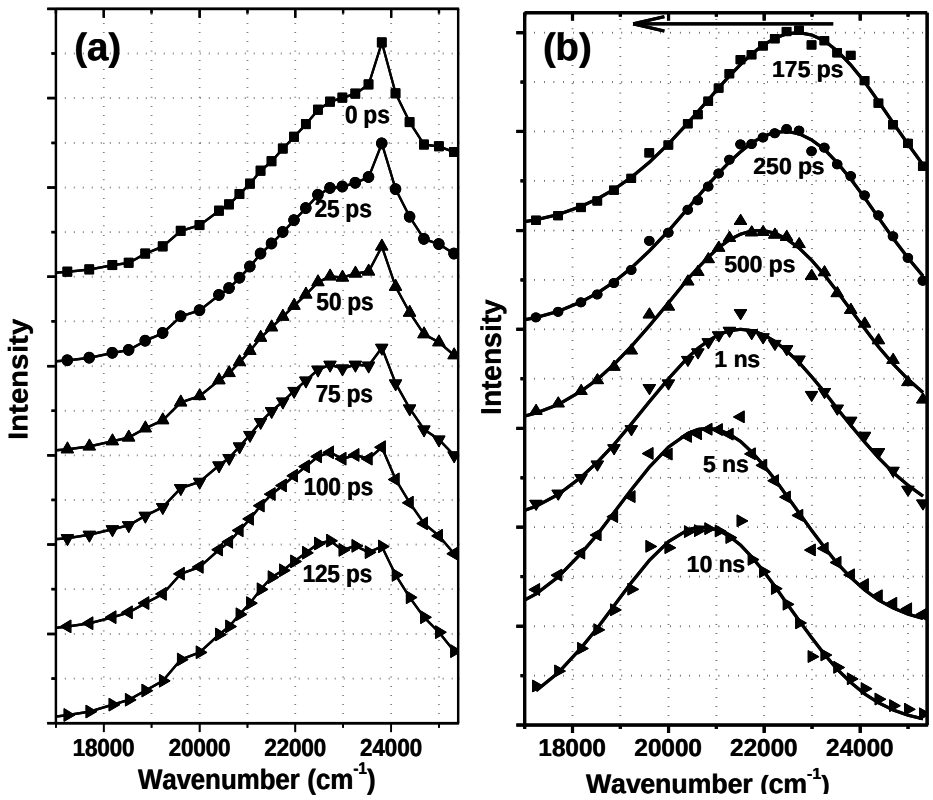

Figure 3.4. (a) Time-resolved emission spectra (TRES) of BA in [bmim][BF_4] at the early stage of dynamics. The sharp high-energy band is ascribed to the LE emission (centering around 23800 cm^{-1}), whereas the broad shoulder to the low-energy side is the CT emission. The maximum of CT bands are normalized in each case. (b) TRES for BA in [bmim][BF_4] in the long time-scale.

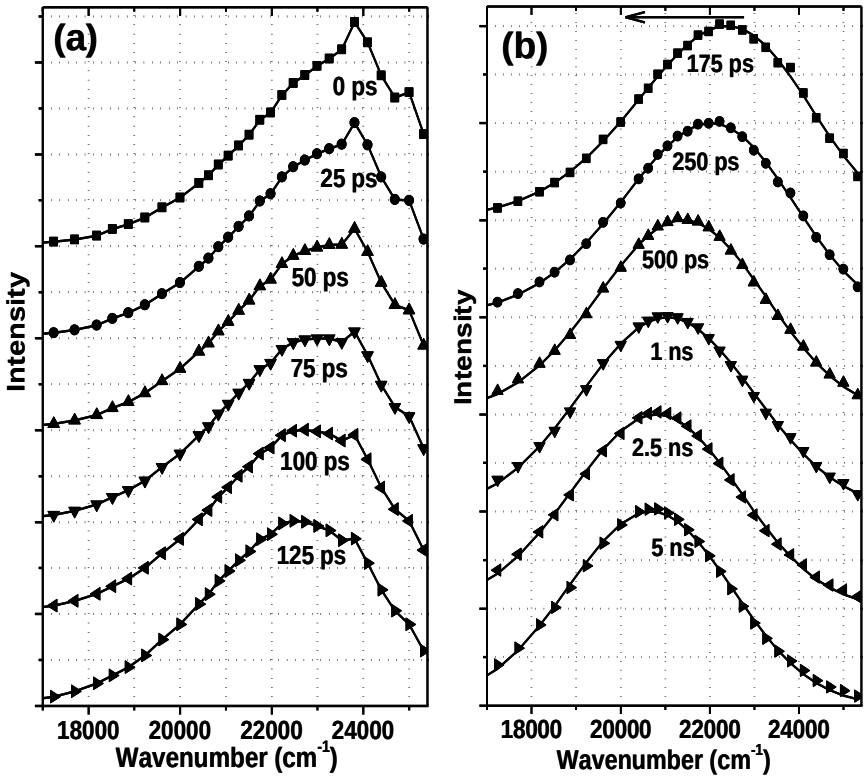

Figure 3.5. (a) Time-resolved emission spectra (TRES) of BA in [bmim][Tf_2N] at the early stage of dynamics. The sharp high-energy band is ascribed to the LE emission (centering around 23800 cm^{-1}), whereas the broad shoulder to the low-energy side is the CT emission. The maximum of CT bands are normalized in each case. (b) TRES for BA in [bmim][Tf_2N] in the long time-scale.

Since evolution of the CT state from the LE state is commonly an ultrafast process, we can expect to miss a large part of this dynamics due to limited time-resolution (~50 ps) of our setup. What we have captured in our measurements is essentially the slow component of this dynamics. A quantitative estimate of the slow component of the dynamics is obtained from the decay of the emission intensity at 23800 cm^{-1} in the early time scale, say 0 – 3 ns. The best fit is found to be biexponential with the short time component contributing to nearly 80-90% of the decay. This time is ascribed to the time constant (τ_{CT}) of the formation of the CT state. The τ_{CT} values obtained in different RTILs are collected in Table 3.1. In this context we note that for reasons not clear to us Nagasawa et al did not observe any sign of the decaying LE state in their TRES even though their time resolution (30 ps) was better than ours. It is possible that they have missed the 23800 cm^{-1} sharp peak as the decay curves were sampled at intervals of 5 - 10 nm. In their transient absorption measurements, Nagasawa et al.[19] found the formation of the CT state to be multiexponential with an appreciable contribution (almost $1/3^{rd}$) from a substantially long time-component of 140 - 330 ps, the exact magnitude of which is dependent on the viscosity of the media, whereas the associated sub-picosecond component (typically 0.5 ps) was found to be independent of viscosity.[19] These values are also collected in Table 3.1. As can be seen, these values are very similar to those obtained by us. The viscosity dependence of the lifetime of the LE state, as indicated in the two studies, is also quite similar. Therefore, we can conclude that LE $\rightarrow$ CT relaxation dynamics, at least the latter stage of it, is possible to observe in picosecond time-resolved fluorescence study.

Table 3.1. Relaxation parameters of the dynamical processes of BA in the three ILs of different viscosity

RTILs	η^a (cP)	Short component of the decay at 23800 cm^{-1} $(\tau_{CT})^b$/ns	Decay parameters of the spectral shift correlation function[c]		Average solvation time $\tau_{av}{}^d$ (ns)	Literature value of longest time-constant/ns for CT formation[e]	Observed shift $(\Delta\bar{\nu})$ (cm^{-1})
			τ_1/ns (a_1)	τ_2/ns (a_2)			
[bmim][PF_6]	260	0.22 (0.75)	0.39 (0.6)	4.0 (0.4)	1.84	0.33 (0.3)	2940
[bmim][BF_4]	98	0.14 (0.8)	0.25 (0.6)	2.67 (0.4)	1.22	0.22 (0.3)	2820
[bmim][Tf_2N]	50	0.12 (0.9)	0.23 (0.8)	2.17 (0.2)	0.62	0.14 (0.36)	3020

[a]Measured at 25°C. [b]Short component of the biexponential fit in a short time-scale (0-4 ns), the numbers in the parenthesis indicate the weighted amplitude. [c]Obtained from the biexponential fit to the data. [d]Average solvation time $\tau_{av} = a_1\tau_1 + a_2\tau_2$, where $a_1 + a_2 = 1$, experimental error is ±5%. [e]From Ref. 12. The numbers in the parenthesis indicates the weighted amplitude.

The time constant of the solvent relaxation of the CT state can be calculated from the time dependence of the spectral shift correlation function, C(t), which is defined in terms of the peak frequencies at various times as,

$$C(t) = [\bar{\nu}(t) - \bar{\nu}(\infty)]/[\bar{\nu}(0) - \bar{\nu}(\infty)].$$

The determination of the peak frequencies (in cm^{-1}) of the measured spectra at zero time $\bar{\nu}(0)$ and at early times is found to be not so straightforward in the present case because of considerable overlap of the LE and CT emission. We considered an average of the peak wavenumbers of the two components of emission as a fair approximation of the value of $\bar{\nu}(0)$ and $\bar{\nu}(t)$ values at the early

stage of the dynamics. This was achieved by fitting the TRES to the log-normal function, just like it is done for the later stages dynamics, when CT emission is the only component observed (Figure 3.3-3.5(b)). Following this procedure, the total time dependent shifts of the emission, $\Delta\bar{\nu} = \bar{\nu}(0) - \bar{\nu}(\infty)$, are found to be 2940, 2820 and 3025 cm^{-1} in [bmim][PF_6], [bmim][BF_4] and [bmim][Tf_2N], respectively (Table 3.1).

In the present situation, it is difficult to estimate the exact amount of ultrafast component of the dynamics that is missed in our measurements because of the ambiguity associated with the determination of the precise values of $\bar{\nu}(0)$ and also due to the involvement of more than one excited state in the emission process.[30] Nonetheless, an approximate estimate of the missed component of the dynamics can be calculated from the following consideration. The Stokes shift observed in the steady-state spectra in RTILs is around 4700 cm^{-1}. The reported Stokes shift of the steady state fluorescence spectra of BA in nonpolar solvents like hexane, cyclohexane, perfluoro-n-hexane, etc. varies between 900 and 1500 cm^{-1}.[25] Since, in these solvents the emitting state is almost purely an LE state, whose solvent stabilization is negligible, we can assume that in RTILs the total expected time-dependent shift due to solvation will amount to ~3200 - 3800 cm^{-1}, whereas the observed shift is 2800 - 3000 cm^{-1} depending on the RTIL. Hence, the extent of the missing component is in the range of only 200 - 1000 cm^{-1}. This implies that the missing component is quite less and is not more than 25%. Considering the fact that charge transfer occurs mostly in an ultrafast time scale, we can surmise that the formation of CT state is almost completed in the early

stage of dynamic solvation and so at a longer time-scale (ps-ns regime), the excited-state dynamics entirely involves the solvation process.

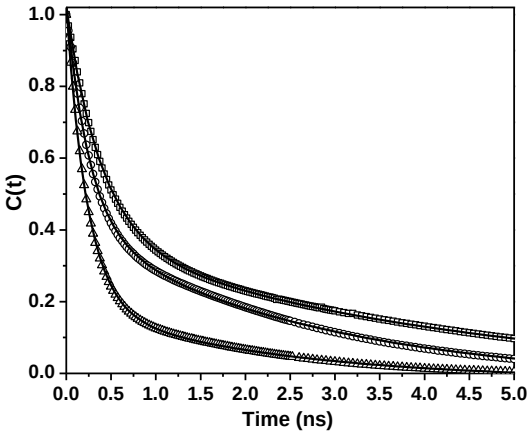

Figure 3.6. Decay of the spectral shift correlation function, C(t), of BA in [bmim][PF_6] (□), [bmim][BF_4] (○) and [bmim][Tf_2N] (△). In each case the solid line denotes the biexponentioal fit to the data.

Biexponential fits to the C(t) vs t plots (Figure 3.6) yielded the time constants for the solvation of the CT state of BA. The time constant of the short component of this dynamics is measured to be 390 ps, 250 ps and 230 ps for BA in [bmim][PF_6], [bmim][BF_4] and [bmim][Tf_2N], respectively and the corresponding long component is 4.0 ns, 2.67 ns and 2.17 ns. The average solvation time, τ_{av}, estimated in these three RTILs is 1.84 ns, 1.22 ns and 0.62 ns, respectively (Table 3.1). The average solvation time (τ_{av}) increases with increasing viscosity of the media. These values are in good agreement with those estimated by Nagasawa et al[19] and other studies.[1] If we compare the τ_{CT} values (150 - 300 ps) with these τ_{av} values, we can see that even though the CT formation kinetics depends on the viscosity of the RTILs (at least in part), the influence of

viscosity is much more dominant on the solvation process. Therefore, while in ordinary polar solvents the CT formation kinetics occurs simultaneously with the solvation dynamics, the two processes proceed in different time-scale in RTILs.

3.4. Conclusion

The time-resolved fluorescence spectra of bianthryl in imidazolium ionic liquids reveal overlapping dual emission arising from the locally excited (LE) and charge transfer (CT) states. This observation allowed us to capture the dynamics of both LE $\rightarrow$ CT relaxation and solvent relaxation from fluorescence measurements. The results show that the charge transfer dynamics, a part of which is viscosity dependent, is faster than the solvation dynamics in ionic liquids. As such these two relaxation processes occur in two different time scales and hence, in this respect the excited state dynamics of bianthryl in ionic liquids is different from that in conventional solvents, where both the dynamics occur in similar time scale.

References

(1) Samanta, A. *J. Phys. Chem. B* **2006**, *110*, 13704.
(2) Mandal, P. K.; Saha, S.; Karmakar, R.; Samanta, A. *Current Science* **2006**, *90*, 301.
(3) Kashyap, H. K.; Biswas, R. *J. Phys. Chem. B* **2008**, *112*, 12431.
(4) Paul, A.; Samanta, A. *J. Phys. Chem. B* **2007**, *111*, 4724.
(5) Jin, H.; Baker, G. A.; Arzhantsev, S.; Dong, J.; Maroncelli, M. *J. Phys. Chem. B* **2007**, *111*, 7291.
(6) Adhikari, A.; Sahu, K.; Dey, S.; Ghosh, S.; Mandal, U.; Bhattacharyya, K. *J. Phys. Chem. B* **2007**, *111*, 12809.
(7) Halder, M.; Headley, L. S.; Mukherjee, P.; Song, X.; Petrich, J. W. *J. Phys. Chem. A* **2006**, *110*, 8623.
(8) Arzhantsev, S.; Jin, H.; Ito, N.; Maroncelli, M. *Chem. Phys. Lett.* **2006**, *417*, 524.
(9) Chowdhury, P. K.; Halder, M.; Sanders, L.; Calhoun, T.; Anderson, J. L.; Armstrong, D. W.; Song, X.; Petrich, J. W. *J. Phys. Chem. B* **2004**, *108*, 10245.
(10) Karmakar, R.; Samanta, A. *J. Phys. Chem. A* **2003**, *107*, 7340.
(11) Chakrabarty, D.; Hazra, P.; Chakraborty, A.; Seth, D.; Sarkar, N. *Chem. Phys. Lett.* **2003**, *381*, 697.
(12) Arzhantsev, S.; Ito, N.; Heitz, M.; Maroncelli, M. *Chem. Phys. Lett.* **2003**, *381*, 278.
(13) Karmakar, R.; Samanta, A. *J. Phys. Chem. A* **2002**, *106*, 4447.
(14) Paul, A.; Samanta, A. *J. Phys. Chem. B* **2007**, *111*, 1957.
(15) Bhattacharya, B.; Samanta, A. *J. Phys. Chem. B* **2008**, *112*, 10101.
(16) Mali, K. S.; Dutt, G. B.; Mukherjee, T. *J. Chem. Phys.* **2008**, *128*, 124515.
(17) Chakrabarty, D.; Chakraborty, A.; Hazra, P.; Seth, D.; Sarkar, N. *Chem. Phys. Lett.* **2004**, *397*, 216.
(18) Karmakar, R.; Samanta, A. *Chem. Phys. Lett.* **2003**, *376*, 638.
(19) Nagasawa, Y.; Itoh, T.; Yasuda, M.; Ishibashi, Y.; Ito, S.; Miyasaka, H. *J. Phys. Chem. B* **2008**, *112*, 15758.
(20) Takaya, T.; Saha, S.; Hamaguchi, H.-o.; Sarkar, M.; Samanta, A.; Iwata, K. *J. Phys. Chem. A* **2006**, *110*, 4291.
(21) Grabowski, Z. R.; Rotkiewicz, K. *Chem. Rev.* **2003**, *103*, 3899.
(22) Piet, J. J.; Schuddeboom, W.; Wegewijs, B. R.; Grozema, F. C.; Warman, J. M. *J. Am. Chem. Soc.* **2001**, *123*, 5337.

(23) Jurczok, M.; Plaza, P.; Rettig, W.; Martin, M. M. *Chem. Phys.* **2000**, *256*, 137
(24) Mataga, N.; Nishikawa, S.; Okada, T. *Chem. Phys. Lett.* **1996**, *257*, 327.
(25) Catalan, J.; Dıaz, C.; Lopez, V.; Perez, P.; Claramunt, R. M. *J. Phys. Chem.* **1996**, *100*, 18392.
(26) Lueck, H.; Windsor, M. W.; Rettig, W. *J. Luminescence* **1991**, *48 & 49*, 425 429.
(27) Mataga, N.; Yao, H.; Okada, T.; Rettig, W. *J. Phys. Chem.* **1989**, *89*, 3383.
(28) Schneider, F.; Lippert, E. *Ber. Bunsenges. Phys. Chem.* **1970**, *74*, 624.
(29) Schneider, F.; Lippert, E. *Ber. Bunsenges. Phys. Chem.* **1968**, *72*, 1155.
(30) Fee, R. S.; Maroncelli, M. *Chem. Phys.* **1994**, *183*, 235.

Chapter 4

Photophysical Processes of Benzil in Imidazolium Ionic Liquids

The photophysical behavior of benzil is studied in three room temperature ionic liquids differing in their polarity and viscosity. The influence of high viscosity, low solubility of the dissolved gases and microheterogeneous nature of the ionic liquids as a function of temperature and excitation wavelength is investigated here.

4.1. Introduction.

The primary interest of studying the photophysical processes of well-known molecular systems in RTILs is to obtain information on some of the physicochemical properties of these novel medium. The second objective is to exploit some of these properties to tune/regulate the photophysical responses of some molecules of interest. Several photophysical processes have already been studied in these media by several groups both experimentally and theoretically.[1-19] We have also used the high viscosity and polarity of the ionic liquids to regulate the photophysical process of some interesting molecular systems in these medium.[6,19-21] The present study explores the effect of the ionic liquids on the emission behavior of a well-studied α-dicarbonyl, benzil (Chart 4.1).

The photophysical behavior of α-dicarbonyls is an interesting topic of research because these molecules display a huge stokes shift in the emission

spectra in solution. Among the aromatic α-dicarbonyls, the photophysics of benzil has received the largest attention.[22-43] It is believed that in the ground state benzil exists as a skew conformer, where the dihedral angle between the two adjacent carbonyl groups is ~ 72^0.[28,37,40] On photoexcitation it is believed to undergo an excited state conformational relaxation process forming the trans-planar form of the molecule, where the dihedral angle between the two adjacent carbonyl groups is 180^0. Though Roy et al could able to see the slow relaxation process of triplet state in melted frozen matrices, but the excited state relaxation process (both in the singlet and triplet state) is believed to be very fast, occurring in the sub-picoseconds time scale at room temperature.[32,43] Benzil shows room temperature phosphorescence in conventional solvents, which is a property that is rarely displayed by the organic molecules.[44] Literature also suggests that the singlet-triplet energy gap in benzil is quite low compared to the thermal energy available at room temperature.[36] Hence, it undergoes reverse intersystem process from the $T_1 \rightsquigarrow S_1$ state by either the triplet-triplet annihilation (P-type) process or a thermally activated (E-type) process depending on the concentration of benzil in the solution.[36] This is why the photophysics of benzil is so interesting. Recently, a relaxed skew conformer and emission from a higher excited state (S_2) of benzil were observed by Bhattacharya et al at room temperature and in frozen condition.[22]

In this work, we have studied the photophysical behavior of benzil in three different room temperature ionic liquids (Chart 4.1) to investigate the influence of the high viscosity, low solubility of the dissolved gases and microheterogeneous nature of the ionic liquids as a function of temperature and excitation wavelength.

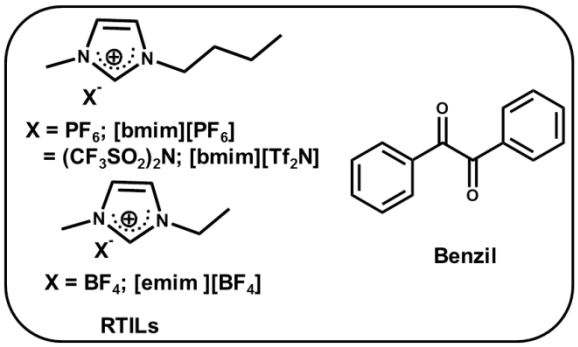

Chart 4.1. Structure and abbreviation of RTILs and probe molecule.

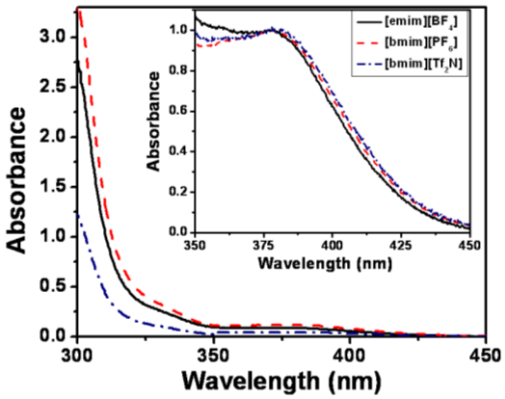

Fig. 4.1. Absorption spectra of benzil in different ionic liquids. Inset shows an expanded view of the n→π* transition region**.**

4.2. Steady-state absorption

Steady-state absorption spectra of benzil in ionic liquids are shown in Fig. 4.1. These are quite similar to those in conventional polar solvents. The first absorption band due to the n-π* transition appears at around 375-380 nm region. This band is slightly red-shifted compared to the absorption spectrum of the benzaldehyde,[38] indicating that the two benzoyl units of benzil are not completely

decoupled in these media. The first absorption band of benzil in ionic liquids is blue-shifted by ca. 10 nm compared to molecular solvents having similar polarity, like ethanol (abs max = 387 nm),[28] which indicates that the two benzoyl units are more decoupled/twisted in ionic liquids when compared with that in molecular solvents. A blue-shift (~ 5 nm) of the first absorption band maximum of benzil with increase in the polarity of the ionic liquids is consistent with the n-π* nature of the transition.

4.3. Steady-state emission

Considering the fact that benzil is weakly fluorescent (ϕ_f = 0.94 x 10^{-3} in benzene)[30] and the ionic liquids also contribute to some emission,[45] the excitation wavelength for the emission measurements is chosen (310 nm) such that the emission contribution due to the ionic liquids is minimum. Room temperature emission spectra of benzil in three ionic liquids, shown in Fig. 4.2, consist of two bands; one is centered ca. 505 nm and the second one around 560 nm. Degassing of the solution leads to intensification of the 560 nm band without affecting the intensity of the 505 nm band. Purging of oxygen leads to complete disappearance of the 560 nm band without affecting the 505 nm band intensity. These observations suggest that the 560 nm band is due to phosphorescence and the 505 nm band due to fluorescence. It is interesting to note in this context that the dual emission of benzil is reported only in degassed condition in conventional organic solvents at room temperature.[30,36] The observation of the 560 nm band even without degassing implies a low solubility of oxygen in the ionic liquids or its poor quenching ability in these media due to slow diffusional process. The

literatures suggest that the solubility of most of the gases in ionic liquids is lower compared to conventional solvents.[46,47] The Henry's constant for oxygen in [bmim][PF_6] and [bmim][Tf_2N] (7190 and 1730 respectively at 25 ^{0}C)[47] when compared with (811.9 and 1734.7 in cyclohexane and ethanol, respectively)[47], implies a lower solubility of oxygen in ionic liquids, and it explains why phosphorescence of benzil is observed in ionic liquids even in non-degassed condition at room temperature. In this context though ethanol and [bmim][Tf_2N] has similar Henry's constant the relative phosphorescence intensity in ethanol is less compared to [bmim][Tf_2N], shown in Figure 4.2b. However, these values do not explain why the phosphorescence intensity of benzil is higher in [bmim][Tf_2N] compared to [bmim][PF_6] in degassed condition. The trend should have been the opposite based on the solubility of oxygen in these two media. Hence it is evident that, additional factors influence the phosphorescence intensity of benzil in ionic liquids.

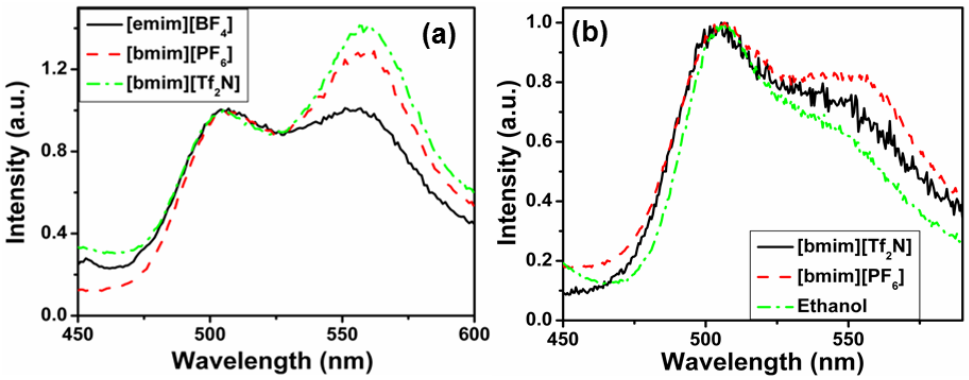

Fig. 4.2. Normalized emission spectra of degassed (a) and non-degassed (b) solution of benzil in ionic liquids (λ_{ex}=310 nm) at room temperature**.**

It is also reported that the cis-skew form of benzil undergoes conformational relaxation upon photo-excitation and emits from the relaxed trans-planar conformer.[32,43] This excited state conformational dynamics is very fast in conventional solvents. In ionic liquids, it is however possible for the unrelaxed state of benzil to contribute to the emission process if the high viscosity of the medium slows down the conformational relaxation process. Interestingly, even at low temperature (273 K), when the ionic liquids are in semi solid form, no emission due to the unrelaxed state is observable. Thus we conclude that the excited state conformational dynamics of benzil is also very fast in ionic liquids.

A study of the temperature dependence of the emission behavior, shown in Fig. 4.3, reveals a drastic reduction of the intensity of the long wavelength emission band with increase in temperature (with very little or no change of the intensity of the short wavelength band). This observation seems to be a reflection of the faster depopulation of the triplet state at higher temperature due to increased collisional deactivation process. However, as the T_1-S_1 energy gap of benzil is quite low (~6 kcal/mol),[36] depopulation of the triplet state can also be due the reverse intersystem process ($T_1 \rightsquigarrow S_1$) resulting from either triplet-triplet annihilation or a thermally activated process, as the thermal energy available even at 273 K is much higher (~40 kcal/mol) than the singlet-triplet energy gap. In the case of a thermally activated $T_1 \rightsquigarrow S_1$ intersystem crossing process, one expects enhancement of the emission intensity of the fluorescence band with increasing temperature. As Fig. 4.3 shows very little change in intensity of the fluorescence band, it may appear that the latter process does not contribute to the photophysics

of benzil in ionic liquids. However, temperature dependence measurements, as described below, suggest otherwise.

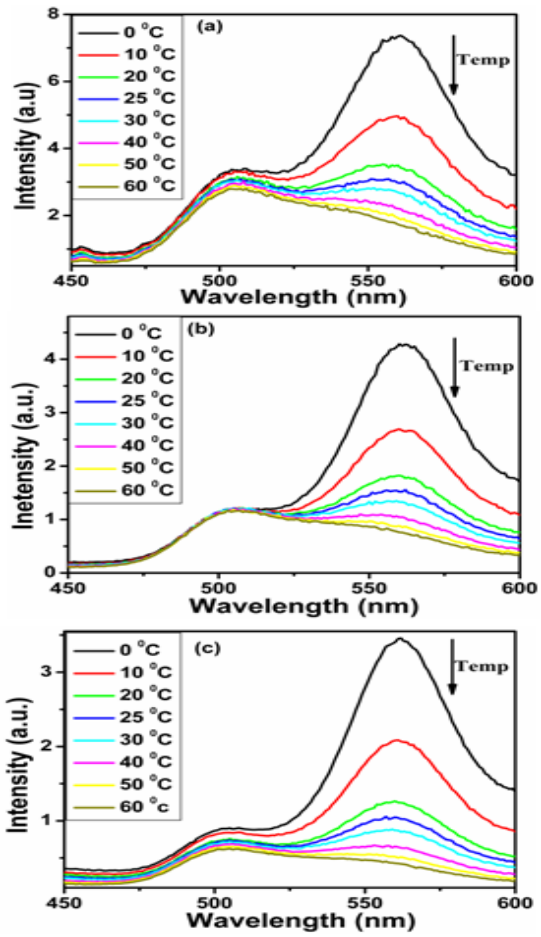

Fig. 4.3. Temperature dependent variation of the steady-state emission spectra of benzil in ionic liquids, (a) [emim][BF_4], (b) [bmim][PF_6] and (c) [bmim][Tf_2N], (λ_{ex}=310 nm).

4.4. Temperature dependence of the delayed emission

In order to further probe the reasons for drastic change of intensity of the long wavelength band with temperature, we have recorded the delayed component of the emission alone as a function of temperature by collecting the emission signal only after a certain delay time (10 μs) following the excitation pulse. The delay time was chosen such that the contribution of the prompt fluorescence is eliminated completely and only the delayed fluorescence and phosphorescence are observed. Temperature dependence of the normalized delayed emission spectra is shown in Fig. 4.4. At 273 K we could observe the intense phosphorescence at around 560 nm with a shoulder around the 505 nm region. This weak 505 nm band which is similar to steady-state fluorescence is clearly the delayed fluorescence. With increasing temperature, the relative intensity of the 505 nm increases in all the ionic liquids. This change of intensity of the delayed fluorescence is most pronounced in the most polar ionic liquids, [emim][BF_4]. It is to be noted that the phosphorescence lifetime, measured by monitoring the decay profile 560 nm, decreases drastically with increasing temperature (Table 4.1).

Triplet lifetimes of the aromatic compounds are expected to be independent of temperature in the absence of any bimolecular quenching mechanism or photoreaction.[48] In our case, as benzil does not undergo any permanent photoreaction and a dilute (7-18 X 10^{-4} M) degassed solution is used in the measurements, we can ignore this possibility, as it is reported that triplet-triplet annihilation quenching of benzil is observable for >0.01 M solution.[36] It is thus evident that the bimolecular quenching processes are absent in our

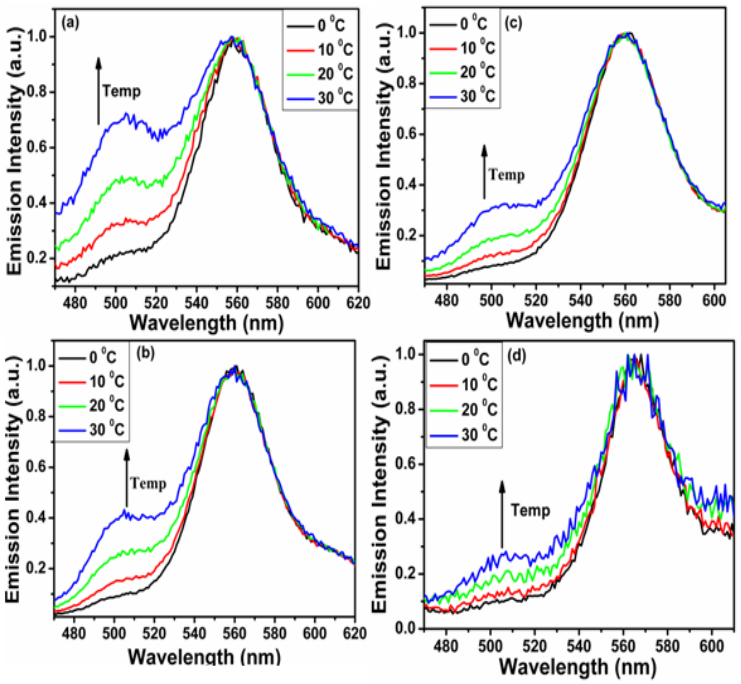

Fig. 4.4. Temperature dependent delayed emission spectra of benzil in ionic liquids, (a) [emim][BF_4], (b) [bmim][PF_6], (c) [bmim][Tf_2N] and (d) ethanol, (λ_{ex}=310 nm). A delay time of 10 μs was used for recording the spectra.

Table 4.1. Phosphorescence lifetime of benzil at different temperatures in ionic liquids

IL	Polarity[a] $E_T(30)$	Viscosity[a] (cP)	τ (μs)			
			0 ^{0}C	10 ^{0}C	20 ^{0}C	30 ^{0}C
[emim][BF_4]	53.7	34	22 ± 0.12	14 ± 0.1	9 ± 0.1	7 ± 0.14
[bmim][PF_6]	52.3	285	43 ± 0.22	24 ± 0.14	15 ± 0.54	9 ± 0.08
[bmim][Tf_2N]	50	50	67 ± 0.13	36 ± 0.18	22 ± 0.17	13 ± 0.11
Ethanol	51.9	1.2	38 ± 0.08	31 ± 0.08	23 ± 0.09	13 ± 0.08

[a] from reference 19. Triplet lifetimes were obtained from single-exponential fit to the decay profiles.

experimental condition. Benzil can form ketyl radical in presence of an amine which acts as electron donor to photo-excited benzil.[24] However, in ionic liquids the free amines are not available for donation of its electron pair to the triplet of benzil. Moreover, a recent laser flash photolysis study on benzil suggests that benzil does not form ketyl radical in [bmim][PF_6].[49] As neither bimolecular quenching nor any photoreaction is responsible for the reduction of phosphorescence lifetime of benzil at higher temperature, it is evident that an enhanced reverse intersystem crossing process is responsible for the observation at higher temperature. We have calculated the rate constant of the $T_1 \rightsquigarrow S_1$ process (k_{risc}) in all ionic liquids at different temperatures, interestingly we found that with increasing temperature the rate of $T_1 \rightsquigarrow S_1$ increases. The plots of $\ln k_{risc}$ vs 1/T are shown in Fig. 4.5 and the slopes of these plots have been used to calculate the singlet-triplet splitting energy gap according to equation (2.7). The estimated values are 6.8, 9.3 and 7.4 kcal/mol in [emim][BF_4], [bmim][PF_6] and [bmim][Tf_2N] respectively. These values are comparable to those obtained from the steady-state spectra (~6 kcal/mol)[36]. It is also evident that the rate constant (k_{risc}) is dependent on the polarity of ionic liquids, the values are given in Table 4.2. In more polar ionic liquid, [emim][BF_4], k_{risc} value is ~5 times higher than in least polar ionic liquid [bmim][Tf_2N]. However, in iso-polar organic solvent, ethanol, $T_1 \rightsquigarrow S_1$ rate constant is found to be lower by a factor of ~10 compared to ionic liquids. The singlet-triplet splitting energy (6.6 kcal/mole) in ethanol, obtained from the plot of $\ln k_{risc}$ vs 1/T, is similar to the values estimated in the

ionic liquids. Since the phosphorescence life-time and phosphorescence quantum yields are similar in ethanol and ionic liquids, the lower value of the $T_1 \rightsquigarrow S_1$ rate constant indicates the occurrance some additional competitive process is going on in ethanol other than the $T_1 \rightsquigarrow S_1$ process.

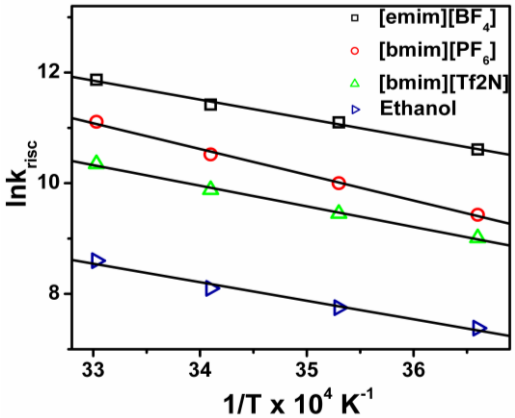

Fig. 4.5. Plots of ln(k_{risc}) vs 1/T in different ionic liquids and ethanol. Solid lines represent the best linear fits to the data points**.**

Table 4.2: Photophysical parameters of benzil at 20 ^{0}C in different ionic liquids

RTILs	Polarity[a] $E_T(30)$	Viscos.[a] (cP)	ϕ_f x 10^3	ϕ_P x 10^3	k_{RP} (s^{-1})	k_P (s^{-1}) x 10^3	k_{risc} (s^{-1}) x 10^4
[emim][BF_4]	53.7	34	0.34	0.58	64	111	9.10
[bmim][PF_6]	52.3	285	0.32	0.64	42	67	3.70
[bmim][Tf_2N]	50	50	0.37	0.83	36	45	1.96
Ethanol	51.9	1.2	1.5	0.60	26	43	0.330

[a] from reference 19.

4.5. Emission at 77 K

Unlike in the fluid media, the phosphorescence spectra of benzil in frozen condition (77 K) are found to be dependent on the excitation wavelength. The excitation wavelength dependence of the phosphorescence maximum of benzil is depicted in Fig. 4.6. The phosphorescence maximum is observed at ca. 532 nm for an excitation wavelength of 430 nm. However, as the excitation wavelength is lowered the emission maximum shifts towards blue. Interestingly, a further decrease of the excitation wavelength beyond 350 nm, leads to a red-shift. As can be seen from the Fig. 4.6 the excitation wavelength dependent variation is observed in all the ionic liquids. In order to find out whether benzil exhibits a similar behavior in frozen media comprising the conventional solvents as well, we have carried out the experiments in ethanol and cyclohexane matrices, the results of which are also presented in Fig. 4.6. In frozen cyclohexane, no excitation wavelength dependence could be observed. However, in ethanol we could observe an excitation wavelength dependent spectral behavior, though this dependency is not as pronounced as in ionic liquids.

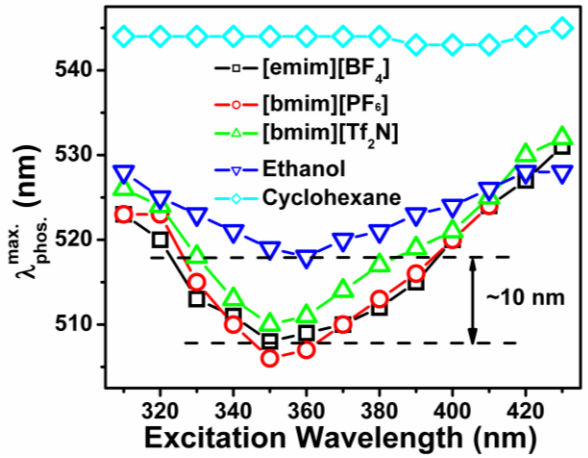

Fig. 4.6. Plots of phosphorescence maximum vs excitation wavelength at 77 K**.**

As all quickly frozen matrices are generally heterogeneous at the microscopic level, this excitation wavelength dependency can arise from the microheterogeneous nature of the glassy environment. However, the very fact that not all frozen matrices give rise to the excitation wavelength dependency implies that the effect is not just due to the heterogeneous nature of the frozen matrices. For flexible molecular systems such as benzil, when frozen rapidly in any glassy matrix, one can expect a large number of conformers differing in their twist angle and energy level. It is reported that a change of the dihedral angle between the two adjacent carbonyl group in 1,2-diketones results in considerable shift of the spectral maximum.[50] We attribute the excitation wavelength-dependent phosphorescence spectra of benzil in frozen conditions to the presence of a distribution of energetically different benzil molecules, which can be distinguished based on their dihedral angles between the two adjacent carbonyl groups. Additional factors such as molecular location in different domains of the

frozen media (a highly likely scenario in ionic liquids) can also contribute to a wider distribution of energetically different molecules.

The n-π* state of benzil is reported to be the lowest excited state of benzil irrespective of the polarity of the medium.[22,25,28] For higher excitation wavelengths, the n-π* state of the most planar form of benzil is excited. As the excitation wavelength is lowered, the n-π* state of more and more twisted forms of the molecule are excited. As these molecules emit at a higher energy, a blue shift is observed. This explains the variation of phosphorescence maximum for the excitation wavelength range of 430 – 350 region. When the excitation wavelength is further lowered (i.e. below 350 nm), the π-π* state of benzil starts getting excited.[22] The emission, however, originates from the n-π* state, the lowest excited state of the molecule. As the conformer having the highest n-π* energy has the lowest π-π* energy, one observes a red-shift of the phosphorescence maximum for excitation wavelengths lower than 350 nm. We note, however, in this context that the present interpretation, which accounts for the experimental results qualitatively, requires further studies to address the problem, in particular, the solvent effect, in a quantitative manner.

4.6. Conclusion

The emission behavior of a well-studied α-dicarbonyl, benzil, has been studied in three imidazolium ionic liquids differing in their polarity and viscosity. It is shown that at room temperature the molecule mainly exists as a skew conformer, but the two halves of the molecule are more decoupled in ionic liquids compared to polar molecular solvents. It is shown that due to low solubility of oxygen in

ionic liquids one can observe room temperature phosphorescence of benzil even in non-degassed condition. It is also shown that E-type delayed fluorescence intensity and the rate of reverse intersystem crossing process is dependent on the polarity of the ionic liquids. The excitation wavelength dependence phosphorescence of benzil at liquid nitrogen temperature reflects the presence of multiple conformers of the molecule.

References

(1) Samanta, A. *J. Phys. Chem. Lett.* **2010**, *1*, 1557.
(2) Samanta, A. *J. Phys. Chem. B* **2006**, *110*, 13704.
(3) Khara, D. C.; Samanta, A. *Ind. J. Chem.* **2010**, *49A*, 714.
(4) Khara, D. C.; Samanta, A. *Phys. Chem. Chem. Phys.* **2010**, *12*, 7671.
(5) Paul, A.; Samanta, A. *J. Phys. Chem. B* **2008**, *112*, 16626.
(6) Paul, A.; Samanta, A. *J. Phys. Chem. B* **2007**, *111*, 1957.
(7) Paul, A.; Samanta, A. *J. Phys. Chem. B* **2007**, *111*, 4724.
(8) Mandal, P. K.; Saha, S.; Karmakar, R.; Samanta, A. *Current Science* **2006**, *90*, 301.
(9) Mandal, P. K.; Samanta, A. *J. Phys. Chem. B* **2005**, *109*, 15172.
(10) Weingrtner, H. *Angew. Chem. Int. Ed.* **2008**, *47*, 654.
(11) Kobrak, M. N.; Li, H. *Phys. Chem. Chem. Phys.* **2010**, *12*, 1922.
(12) Kashyap, H. K.; Biswas, R. *J. Phys. Chem. B* **2010**, *114*, 254.
(13) Kashyap, H. K.; Biswas, R. *J. Phys. Chem. B* **2010**, *114*, 16811.
(14) Kashyap, H. K.; Biswas, R. *Ind. J. Chem.* **2010**, *49A*, 685.
(15) Kobrak, M. N. The Chemical Environment of Ionic Liquids: Links Between Liquid Structure, Dynamics, and Solvation In *Advances in Chemical Physics*; Rice, S. A., Ed.; John Wiley & Sons, Inc., 2008; Vol. 139; pp 83.
(16) Kashyap, H. K.; Biswas, R. *J. Phys. Chem. B* **2008**, *112*, 12431.
(17) Shim, Y.; Jeong, D.; Choi, M. Y.; Kim, H. J. *J. Chem. Phys.* **2006**, *125*, 061102.
(18) Shim, Y.; Duan, J.; Choi, M. Y.; Kim, H. J. *J. Chem. Phys.* **2003**, *119*, 6411.
(19) Santhosh, K.; Samanta, A. *J. Phys. Chem. B* **2010**, *114*, 9195.
(20) Khara, D. C.; Paul, A.; Santhosh, K.; Samanta, A. *J. Chem. Sci.* **2009**, *121*, 309.
(21) Bhattacharya, B.; Samanta, A. *J. Phys. Chem. B* **2008**, *112*, 10101.
(22) Bhattacharya, B.; Jana, B.; Bose, D.; Chattopadhyay, N. *J. Chem. Phys.* **2011**, *134*, 044535.
(23) Chattopadhyay, N.; Serpa, C.; Silva, M. I.; Arnaut, L. G.; Formosinho, A. J. *Chem. Phys. Lett.* **2001**, *347*, 361.
(24) Okutsu, T.; Ooyama, M.; Hiratsuka, H.; Tsuchiya, J.; Obi, K. *J. Phys. Chem. A* **2000**, *104*, 288.

(25) Aindrila Sarkar; Chakravorti, S. *J. Luminescence* **1996**, *69*, 161.
(26) Santhosh, C.; Mishra, P. C. *J. Photochem. Photobio A: Chemistry* **1990**, *51*, 245.
(27) Inoue, H.; Sakurai, T.; Hoshi, T.; Okubo, J.; Kawashima, T. *J. Chem. Soc. Faraday Trans 2* **1986**, *82*, 523.
(28) Bhattacharyya, K.; Chowdhury, M. *J. Photochemistry.* **1986**, *33*, 61.
(29) Scypinski, S.; Love, L. J. C. *Anal. Chem.* **1984**, *56*, 322.
(30) Flamigni, L.; Barigelletti, F.; Dellonte, S.; Orlandi, G. *J. Photochemistry.* **1983**, *21*, 237.
(31) Debnath, R.; Bera, S. C. *Chem. Phys. Lett.* **1983**, *95*, 339.
(32) Roy, D.; Bhattacharyya, K.; Bera, S. C.; Chowdhury, M. *Chem. Phys. Lett.* **1980**, *69*, 134.
(33) Bhattacharyya, K.; Roy, D.; Chowdhury, M. *J. Luminescence* **1980**, *22*, 95.
(34) Fang, T. S.; Singer, L. A. *Chem. Phys. Lett.* **1978**, *60*, 117.
(35) Fang, T. S.; Brown, R. E.; Singer, L. A. *J. C.S. Chem. Comm.* **1978**, 116.
(36) Fang, T. S.; Brown, R. E.; Kwan, C. L.; Singer, L. A. *J. Phys. Chem.* **1978**, *82*, 2489.
(37) Arnett, J. F.; McGlynn, S. P. *J. Phys. Chem.* **1975**, *79*, 626.
(38) Morantz, D. J.; Wwright, A. J. C. *J. Chem. Phys.* **1971**, *54*, 692.
(39) Morantz, D. J.; Wright, A. J. C. *J. Chem. Phys.* **1970**, *53*, 1622.
(40) Bera, S. C.; Mukherjee, R.; Chowdhury, M. *J. Chem. Phys.* **1969**, *51*, 754.
(41) Parker, C. A.; Joyce, T. *Chem. Commun.* **1968**, 1421.
(42) Brown, C. J.; Sadanaga, R. *Acta Cryst.* **1965**, *18*, 158.
(43) Singh, A. K.; Palit, D. K.; Mittal, J. P. *Chem. Phys. Lett.* **2002**, *360*, 443.
(44) Lower, S. K.; El-Sayed, M. A. *Chem. Rev.* **1966**, *66*, 199.
(45) Paul, A.; Mandal, P. K.; Samanta, A. *J. Phys. Chem. B* **2005**, *109*, 9148.
(46) Kumełan, J.; Kamps, A. P. S.; Urukova, I.; Tuma, D.; Maurer, G. *J. Chem. Thermodynamics* **2005**, *37*, 595.
(47) Anthony, J. L.; Anderson, J. L.; Maginn, E. J.; Brennecke, J. F. *J. Phys. Chem. B* **2005**, *109*, 6366.

(48) Park, S.; Kwon, O. H.; Lee, Y.-S.; Jang, D. J.; Park, S. Y. *J. Phys. Chem. A* **2007**, *111*, 9649.
(49) Ruth, A.; Netto-Ferreira, J. B. C. *Quim. Nova* **2009**, *32*, 1934.
(50) Leonard, N. J.; Mader, P. M. *J. Am. Chem. Soc.* **1950**, *72*, 5388.

Chapter 5

Solute Rotation and Solvation Dynamics of Charged Solutes in Imidazolium Ionic Liquids

Rotational and solvation dynamics of two, negatively and positively charged solutes have been studied in an ionic liquid to understand the electrostatic interaction between the charged solutes and imidazolium ionic liquid by using steady-state and time-resolved fluorescence spectroscopy. This study did not does not reveal any influence of the electrostatic interaction between the charged solutes and ionic liquid.

5.1. Introduction

Several photophysical processes have been studied in RTILs to explore the physicochemical properties of the RTILs. However, the physicochemical properties of these liquids are yet to be understood fully.[1,2] As the solvent properties of a medium can be understood by studying the interaction of a solute with the medium, one of the common approaches has been the study of dynamics of solvation and rotational relaxation of the solute molecules in the medium.[1,3-10] Even though a wealth of information is available on the solvation dynamics and rotational dynamics of various solutes in conventional solvents, similar information is rather limited in RTILs.

Early studies of rotational dynamics in RTILs revealed that the solute rotation in RTILs were similar like rotational dynamics in conventional molecular solvents and the results were explained with the most common Stokes-Einestien-

Debye (SED) hydrodynamic model.[3,4,6,11-13] Even though these studies did not reveal any influence of specific solute-solvent interaction on the rotational motion of the solutes, a few examples do exist where rotational motion of the solute is shown to be influenced by its specific interaction with the RTILs.[14] Mali et al,[12] while studying the rotational dynamics of two structurally similar nonpolar solutes, 2,5-dimethyl-1,4-dioxo-3,6-diphenylpyrrolo[3,4-*c*]pyrrole (DMDPP) and 1,4-dioxo-3,6-diphenylpyrrolo[3,4-*c*]pyrrole (DPP) in [bmim][PF_6], with only the latter having hydrogen bond donating ability, as a function of temperature, found that rotational diffusion of DPP in [bmim][PF_6] was slower compared to DMDPP due to specific hydrogen bonding interaction between N-H hydrogen and anionic moiety of the RTIL. We also observed that the rotational motion of AP was slower compared to coumarin 153 (C153) in alcohol-functionalized ionic liquid, 1-(hydroxy-ethyl)-3-methylimidazilium bis(trifluoromethanesulphonyl)imide ([HO-emim][Tf_2N]), even though the van der Waals volume of C153 is higher than that of AP.[14] This observation is a reflection of the hydrogen bonding interaction between the carbonyl groups of AP and the hydroxyl moiety of the substituted imidazolium cation of the RTIL. Mali et al.[11] studied the rotational diffusion of two solutes, nonpolar 9-phenylanthracene (9-PA) and dipolar rhodamine 110 (R110), of comparable size in [bmim][PF_6] and glycerol and observed that in isoviscous condition, PA rotates faster in RTIL than in glycerol, whereas the dipolar solute R110 displayed an opposite behavior. The rotational behavior of PA was explained considering the sizes of glycerol and [bmim][PF_6] using the quashihydrodynamic theories of Gierer and Wirtz and Dote-Kivelson-Schwartz model. On the other hand, strong hydrogen bonding interaction between

R110 and [bmim][PF_6] was attributed to the slower rotation of this solute in RTIL compared to glycerol. Recently, Fruchey and Fayer[15] have studied the orientational dynamics with charged sodium 8-methoxypyrene-1,3,6-sulfonate (MPTS) and uncharged perylene probe in RTILs. It is found that the charged anionic MPTS molecule shows superstick behavior which is due to strong association with the imidazolium cation of the RTILs. However, neutral perylene molecule rotates in the slip to subslip regime depending upon the alkyl chain length of the imidazolium moiety and its rotational behavior is comparable to that in paraffine oil comprising an n-octyl chain. In this context, we note that rotational dynamics of molecular system have also been studied in RTILs and binary mixture of RTILs and water/organic solvent mainly by Chakrabarty et al.[16-18] They found that addition of water/organic solvent in RTILs usually decreases the rotational time due to a reduction of the viscosity of the media. We have also observed recently that addition of a nonpolar molecular solvent to RTILs makes the rotational motion of the probe molecules faster owing to a lowering of the viscosity of the medium.

On the other hand, solvation dynamics studies based on the time dependent dynamic Stokes shift of dipolar solutes have shown that the time-resolvable component of the dynamics is slow and biphasic (or non-exponential) in nature and is dependent on the viscosity of the medium.[1,2] Of the two components, the fast component has a lifetime of a few hundreds of picoseconds, and the slow component has a lifetime of a few nanoseconds. The first component was attributed to the translational motion of the anion and the slower component to the collective motion of both the cation and anion. These interpretations are

based primarily on the literature available on high temperature solvation dynamics data on molten salts.[19,20] In order to obtain insight into the solvation process in RTILs simulation studies have been performed by several groups.[21,22] Shim et al[22] attributed the fast component of the dynamics to the translational motion of the anion and the slow component to the overall diffusional motion of the cation and anion. On the other hand, Kobark and Znamenskiy[21] assigned the ultrafast component of the dynamics is due to the collective cation-anion motion.

While some of these studies involving the dipolar probe molecules revealed a probe dependence of the dynamics, the origin of such dependence was not clear.[1,2] In one of their studies on solvation and rotational dynamics in RTIL, Ito et al[3] used an ionic solute, namely, 10-methyl-9-phenylacridinium ion, along with a few other neutral dipolar probes. The ionic probe molecule in this study appears to have been chosen without the specific intent of finding out whether solvation dynamics is dependent of the charge on the probe molecule. While a significant variation of the solvation time with the probe molecule was noted in this study, no particular significance was however attached to the data obtained with the ionic probe molecule. Sarkar and coworkers[16,23] have studied the solvation dynamics in mixed solvents comprising RTIL and conventional solvents. Recently, femtosecond Kerr-gate spectroscopy and upconversion techniques have also been employed to elucidate the nature of various ultrafast relaxation processes and their exact time-scales in imidazolium and other RTILs.[24-28]

It is therefore evident that the nature of various forces in operation between the solvent and solute in RTILs is still unclear. As further studies can

only unravel this issue, we have undertaken the present study in which the dynamics of rotational diffusion and solvation dynamics of two charged probes (Chart 5.1), anionic 1-anilinonaphthalene-8-sulfonate (ANS) and cationic ethidium bromide (EB), has been investigated in a RTIL, 1-butyl-3-methylimidazolium tetrafluoroborate, [bmim][BF_4] and conventional viscous solvent, glycerol, to find out the importance of the electrostatic and other forces operative in RTILs. Since the viscosities of the [bmim][BF_4] and glycerol at any given temperature are very different, the measured rotational times under isoviscous conditions, maintained by appropriately adjusting the temperature of the systems, have been compared to arrive at any conclusion.

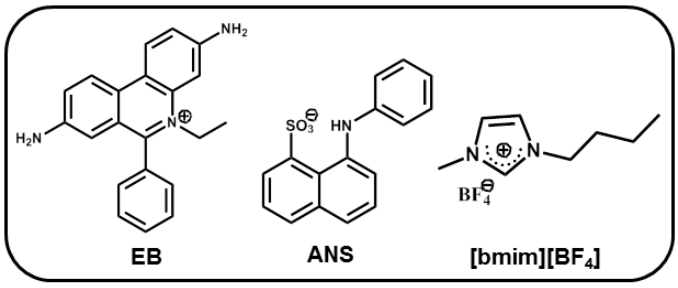

Chart 5.1. Structure/abbreviation of the solutes and ionic liquid

5.2. Steady-State Behavior

Steady state fluorescence and fluorescence excitation spectra of ANS and EB in [bmim][BF_4] are shown in Fig. 5.1. The spectral behavior of the systems is consistent with that observed in conventional polar solvents.[29,30]

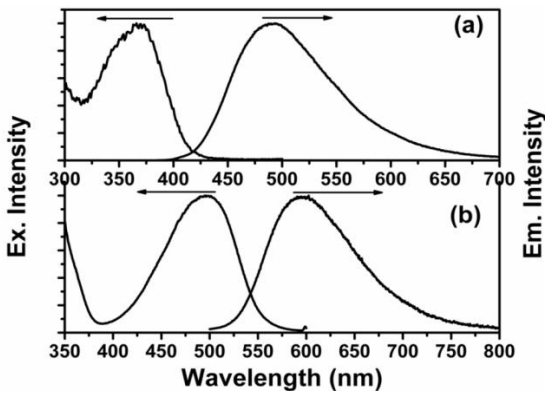

Fig. 5.1 Fluorescence excitation and emission spectra of (a) ANS, (b) EB in [bmim][BF_4]. Spectra are recorded at isoviscous condition (81 cP). The excitation wavelengths are 405 and 439 nm for ANS and EB, respectively.

5.3. Time-Resolved Measurements.

5.3.1. Rotational Dynamics.

Representative anisotropy decay profiles for ANS and EB are shown in Fig. 5.2. The initial anisotropies, r_0, are found to be within the limiting value of 0.4 for both the probe molecules. The time dependence of the anisotropy profiles is described by a single exponential decay function. A bi-exponential fit to the anisotropy data did not improve the quality of the fitting and also, the average relaxation time estimated from the biexponential fit is found to be almost identical with that obtained from the single exponential fit. Interestingly, while our observation is similar to that of Ingram et al.,[6] non-exponential anisotropy decay, which could be fit to the stretched exponential function, is also reported by Ito et al.[3] The rotational orientation times of the two probe molecules estimated from the single exponential fit to our anisotropy decay profiles in [bmim][BF_4] and glycerol at different temperatures are collected in Tables 5.1. and 5.2. It is evident

from the anisotropy decay profiles shown in Fig. 5.2. and the data presented in Tables 5.1. and 2 that with increase in temperature as the viscosity of the media decreases, the rotational diffusion of the solutes becomes faster. It is interesting to note that under isoviscous conditions (maintained by adjusting the temperatures of the solvents), the reorientation times of the probe molecules in RTIL and glycerol are very similar. This implies that electrostatic component of the rotational friction is negligible. This conclusion is in agreement with the recent studies.[3,12] Under isoviscous conditions, that the reorientation time of ANS is less than that of EB is consistent with the sizes of the two molecular systems (estimated van der Waals volume of ANS and EB are 251 and 294 $Å^3$, respectively. See later for details). A careful scrutiny of the anisotropy decay profiles also reveals that in highly viscous conditions the rotational anisotropy at infinite time (r_∞) of EB is nonzero suggesting strong interaction or attachment with the solvent. This kind of behavior is often observed for ionic probes bound to the surfaces.[31,32]

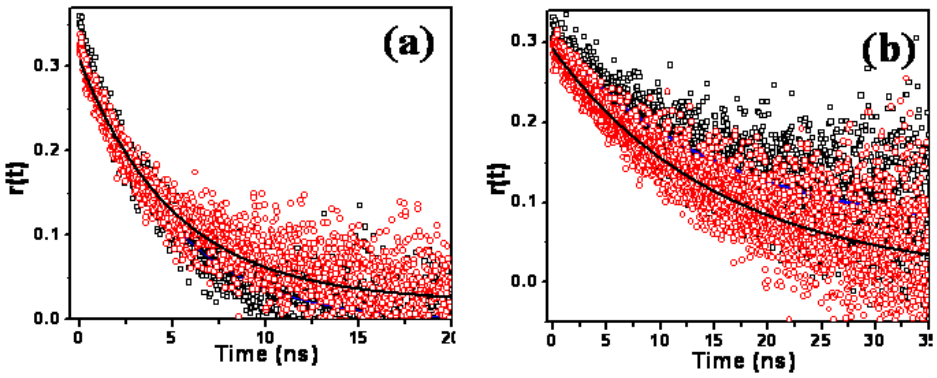

Fig. 5.2. Anisotropy decay profiles of (a) ANS and (b) EB in [bmim][BF_4] (□) and glycerol (○) under isoviscous condition (81 cP). Solid lines are the single exponential fit to data.

Table 5.1. Summary of the rotational data of ANS in [bmim][BF_4] and glycerol

Medium	Temperature (K)	Viscosity[a] (cP)	r_0[b]	τ_{rot} (ns)[c]	C_{rot}[d]
[bmim][BF_4]	288	131	0.34	7.51±0.13	0.64
glycerol	318		0.31	7.60±0.15	0.72
[bmim][BF_4]	298	81	0.35	4.66±0.07	0.67
glycerol	328		0.32	5.14±0.08	0.81
[bmim][BF_4]	308	48	0.35	2.72±0.04	0.68
glycerol	338		0.33	3.42±0.06	0.94
[bmim][BF_4]	318	31	0.33	1.75±0.03	0.70
glycerol	348		0.33	2.42±0.04	1.06

[a] ±2%, [b]initial anisotropy, [c]rotational time, [d]rotational coupling constant.

Table 5.2. Summary of the rotational data of EB in [bmim][BF_4] and glycerol

Medium	Temperature (K)	Viscosity[a] (cP)	r_0[b]	τ_{rot} (ns)[c]	C_{rot}[d]
[bmim][BF_4]	288	131	0.37	25.64±1.14	1.89
glycerol	318		0.30	22.74±1.01	1.85
[bmim][BF_4]	298	81	0.32	15.49±0.35	1.91
glycerol	328		0.26	15.67±0.35	2.13
[bmim][BF_4]	308	48	0.31	9.0±0.18	1.93
glycerol	338		0.31	9.51±0.14	2.25
[bmim][BF_4]	318	31	0.32	6.10±0.09	2.10
glycerol	348		0.26	6.78±0.11	2.56

[a] ±2%, [b]initial anisotropy, [c]rotational time, [d]rotational coupling constant.

Table 5.3. Properties of the solutes

Probe	van der Waals Volume[a] (Å^3)	Axial radii[a] (Å)	Shape factor[a]*(f)*	Boundary conditions[a] (C_{slip})
ANS	251	5.72 x 3.39 x 3.09	1.41	0.17
EB	294	5.72 x 4.67 x 2.62	1.40	0.083

[a]See text for details.

In an attempt to understand the rotational dynamics of the cationic and anionic probe molecules, EB, and ANS, respectively, we analyze our experimental data in terms of the most commonly used model of rotational diffusion, the Stokes–Einstein–Debye (SED) hydrodynamic theory. According to this theory, the reorientation time (τ_r^{SED}) of a non-interacting solute in a solvent continuum of viscosity η is given by

$$\tau_r^{SED} = \frac{V_h \eta}{k_B T} \qquad (5.1)$$

In this equation, V_h is the hydrodynamic volume of the solute molecule, which is a product of the van der Waals volume V of the molecule, its shape factor f and boundary condition parameter C. k_B is the Boltzmann constant and T is the absolute temperature of the system. The shape factor f, introduced by Perrin to take into account the nonspherical shape of the solute molecule, is a function of the axial ratio of the semi axes and is greater than 1 for an asymmetric ellipsoid. For a spherical solute, f is unity. The boundary conditions parameter, C is unity when the size of the rotating solute is much bigger than the solvent molecule. This represents the stick boundary condition. However, in the case of a solute of

comparable size or smaller than the solvent molecule, C is less than unity and is commonly 0 < C < 1. It is to be noted that the τ_r^{SED} given by eqn (5.1), represents only the mechanical or hydrodynamic friction experienced by the solute molecule. In order to calculate the τ_r^{SED} values of the solutes, one requires the knowledge of van der Waals volumes of the solutes. Using the Edward's volume increment method,[33] the volumes are estimated as 251 $Å^3$ and 294 $Å^3$ for ANS and EB, respectively. For modeling the solutes as ellipsoids, the largest dimension, i.e. the distance between the two furthest atoms of the solute molecule was taken as the long axis (2a), the largest dimension perpendicular to it was considered short-in-plane axis (2b), and the thickness of the aromatic ring was considered as out of plane axis (2c). While a and b were estimated from the optimized geometries of the molecules, c was evaluated using the known values of V, a and b from the relation,

$$V = \frac{4}{3}\pi abc \qquad (5.2)$$

The evaluated values for the probe molecules are collected in Table 5.3. Since all three axial radii are different, each solute has been treated as an asymmetric ellipsoid. The friction coefficients (ξ_i) along the three principal axes of rotation for the stick and slip boundary conditions were obtained from the literature available numerical tabulations.[34,35] The diffusion coefficients along the three axes (D_i) were then obtained using the Einstein relation,

$$D_i = \frac{k_B T}{\xi_i} \qquad (5.3)$$

Assuming that the transition dipole is along the long axis of the molecule, the rotational times were estimated from the diffusion coefficients by the following relation:[36]

$$\tau_r = \frac{1}{12}\left(\frac{4D_a + D_b + D_c}{D_aD_b + D_bD_c + D_cD_a}\right) \qquad (5.4)$$

Where, D_a, D_b and D_c are the diffusion coefficients along a, b and c axis, respectively. The shape factor (f) and boundary condition for slip (C_{slip}) were obtained from the calculated rotational times for the stick and slip boundary conditions. Fig. 5.3 shows the plots of experimentally measured reorientation times of ANS in [bmim][BF_4] and glycerol versus η/T along with the calculated stick (upper) and slip (lower) lines obtained from the SED theory treating the molecule as an asymmetric ellipsoid. Similar plots for EB are shown in Fig. 5.4. According to SED theory, τ_r bears a linear relationship with η/T. The linear fits to the data are shown in Fig. 5.3 and 5.4 and the quality of the fits is evident from the correlation coefficients given in the captions to the Figures. That the degree of nonlinearity in these plots, particularly in RTIL, is small is also evident from the fitting parameters (indicated below) when the data was fit to the following function, $\tau_r = A(\eta/T)^p$, a procedure followed by Mali et al.[11,12]

ANS in [bmim][BF_4],

$$\tau_r = (15.81 \pm 0.13)\left(\frac{\eta}{T}\right)^{0.94\pm0.007} \qquad (N=4, R=0.999)$$

ANS in glycerol,

$$\tau_r = (14.75 \pm 0.1)\left(\frac{\eta}{T}\right)^{0.75\pm0.005} \qquad \text{(N=4, R=0.999)}$$

EB in [bmim][BF_4],

$$\tau_r = (54.46 \pm 1.07)\left(\frac{\eta}{T}\right)^{0.96\pm0.017} \qquad \text{(N=4, R=0.999)}$$

EB in glycerol,

$$\tau_r = (46.28 \pm 1.72)\left(\frac{\eta}{T}\right)^{0.79\pm0.028} \qquad \text{(N=4, R=0.998)}$$

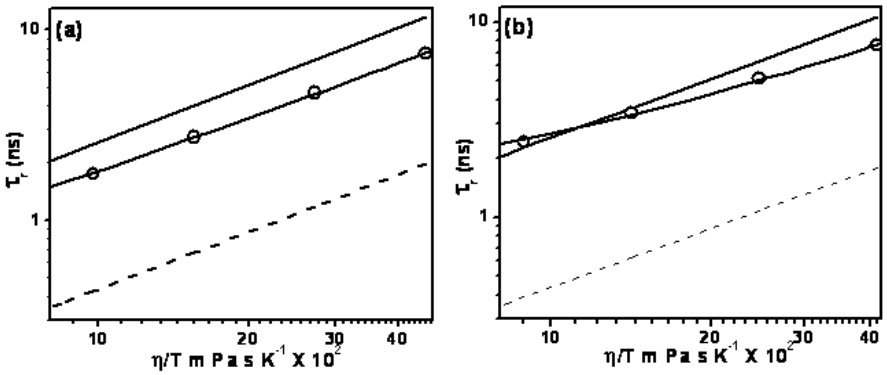

Fig. 5.3. Plots of τ_{rot} vs η/T for ANS in (a) [bmim][BF_4] and (b) glycerol. Computed data are with stick (▬), slip (- - - - -) boundary conditions, and experimentally measured data (O). The linear fits [R=0.9998 (a) and 0.9991(b)] to the data points are also shown.

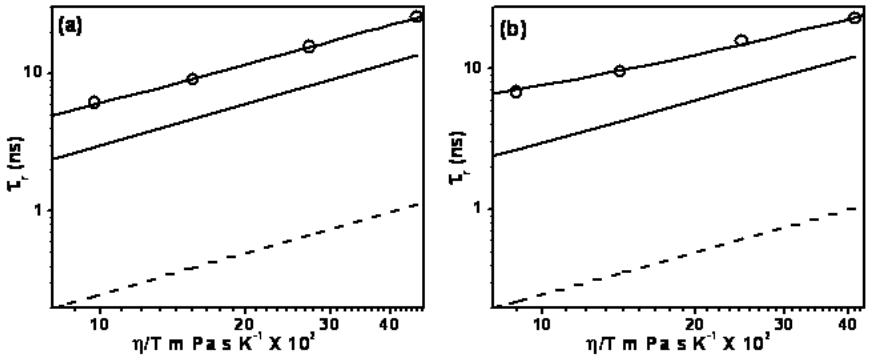

Fig. 5.4. Plots of τ_{rot} vs η/T for EB in (a) [bmim][BF_4] and (b) glycerol. Computed data with stick (▬), slip (▬ ▬ ▬) boundary conditions, and experimentally measured data (O). The linear fits [R=0.9999 (a) and 0.9972(b)] to the data points are also shown.

For both the probes, the departure from linear behavior is more pronounced in glycerol. It is evident that rotational dynamics of the anionic probe, ANS, is in between that of the stick and slip boundary conditions (with the behavior closer to the stick condition). The rotational times of the cationic probe, EB, however, is higher than that predicted by the stick boundary condition both in [bmim][BF_4] and glycerol. Behavior of this kind, known as ‘‘superstick’’ behavior,[6] is indicative of association of the probe molecule with the solvent. Strong hydrogen bonding interaction of AP with alcohols is well known to give rise to this kind of behavior in alcoholic solvents.[6] As EB displays superstick behavior both in RTIL and glycerol, the strong solute–solvent association is not driven by charge–charge interaction.

Even though a recent work[15] shows that negatively charged, MPTS follows superstick behavior, in our case only positively charged EB shows the

superstick behavior; the negatively charged molecule, ANS, does not. This difference in behavior can be explained considering the hydrogen bonding interaction between the solute and solvent molecules, which is most often responsible for strong association of the solute with the solvent and its superstick behavior. In case of MPTS, it can enter into hydrogen bonding interaction through its three sulfonate groups, whereas ANS can only get hydrogen bonded through one sulfonate group, that too if the –NH moiety is not intramolecularly hydrogen bonded to the former. Clearly, ANS will experience less friction compared to MPTS. The work of Mali et al.[11] on a neutral solute, 9-phenylanthracene (9PA), which has molecular dimensions similar to our systems, in [bmim][PF_6] and glycerol, has indicated that 9-PA follows slip behavior in [bmim][PF_6], but in glycerol its rotational time is two-fold higher than that predicted by the slip behavior, even though hydrogen bonding interaction is absent in this solvent. Under viscosity normalized conditions, the rotational time of 9PA is 40 to 60% longer in glycerol than [bmim][PF_6]. This has been explained taking into consideration the difference of the volume of the solvent molecules in two cases. A larger volume of the ionic constituents of the RTILs offers less friction for the solute rotation compared to glycerol. Further insight into the nature of association of EB with glycerol and [bmim][BF_4] can be obtained from the hydrogen bond donating ability of the solute and the hydrogen bond basicity (b) of the solvents. Literature suggests that EB is indeed a hydrogen bond donor to solvent molecules that can act as hydrogen bond acceptor, such as water, ethanol, acetone, etc.[37] This hydrogen bonding interaction of EB is mediated through the four acidic hydrogens of the amino functionality.[37] As EB is known to form hydrogen-

bonded complex with water, which has a 'b' value of 0.47,[38] it is understandable why it would be associated with another hydroxylated solvent glycerol or ionic liquid, [bmim][BF_4], which is characterized by 'b' value of 0.38,[39] through hydrogen bonding interaction. In this context, we take into account the findings of Kurnikova et al.[40] who studied the rotational diffusion of cationic (thionine), anionic (resorufin) and neutral (resorufamine) probes of similar size in dimethylsulfoxide (DMSO) and found that resorufin follows slip boundary condition, resorufamine shows in-between slip and stick boundary conditions, whereas the positively charged molecule, thionine shows superstick behavior. This observation was rationalized by molecular dynamics studies that indicated the importance of solute-solvent hydrogen bonding interactions over the electrostatic interaction in determining the structure and dynamics of the system. Thionine was found to be associated with the solvent through hydrogen bonding interaction much more strongly compared to the other systems and this association was reflected in the rotational time. We have also calculated the rotational coupling constant (C_{rot}) defined as, $C_{rot} = \tau_{rot} / \tau_{stick}$, where, t_{rot} is experimentally measured time and t_{stick} obtained from the following relation.

$$\tau_{stick} = \frac{Vf\,\eta}{k_B T} \qquad (5.5)$$

C_{rot} values are gathered in Tables 5.1 and 5.2. For both the molecules, the rotational coupling constant is slightly higher in glycerol compared to RTIL. Under isoviscous condition, the C_{rot} value of EB is almost 3 times higher than that of ANS, indicating that EB is far more associated than ANS in both RTIL and

glycerol. As the C_{rot} value essentially represents the ratio of the hydrodynamic volume and van der Waals volume of a solute, it is apparent from the C_{rot} values that the hydrodynamic volume of EB is nearly twice its van der Waals volume. As far as the extent of association is concerned, the behavior of EB is similar to that exhibited by AP in protic media.

5.3.2. Solvation Dynamics

Wavelength-dependent decay profiles, which are a typical signature of slow solvation dynamics, have been observed for both the systems. Representative wavelength-dependent decay behavior is illustrated in Fig. 5.5. When monitored at the shorter wavelength region, only monotonous decay is observed, while at the longer wavelengths, the time profiles consist of a slow rise followed by the decay. The time-resolved emission spectra (TRES) have been constructed by fitting the individual decay curves to a multi-exponential function followed by normalization of the decay traces by steady-state spectra, by a procedure described in Chapter 2. The TRES for EB and ANS at different time intervals are shown in Fig. 5.6. In both cases, a time-dependent solvent mediated relaxation of the excited state is observable.

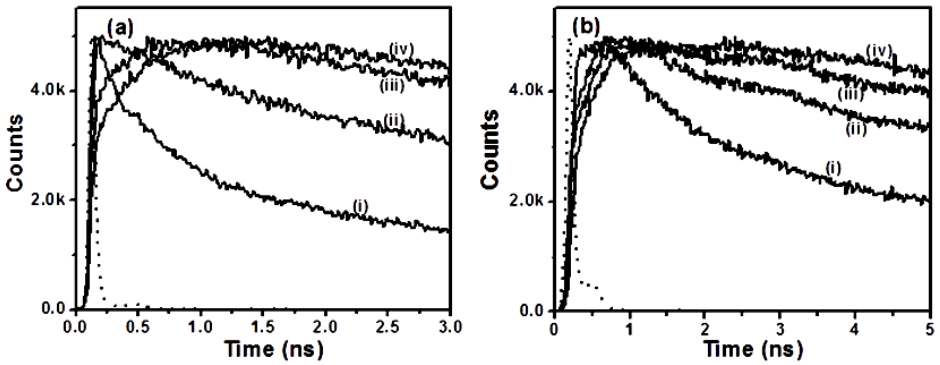

Figure 5.5. Wavelength-dependent decay profiles of (a) ANS at (i) 450 nm, (ii) 490 nm, (iii) 550 nm, (iv) 610 nm and, (b) EB at (i) 550 nm, (ii) 590 nm (iii) 630 nm, (iv) 670 nm in [bmim][BF_4]. The lamp profiles are shown as dashed line.

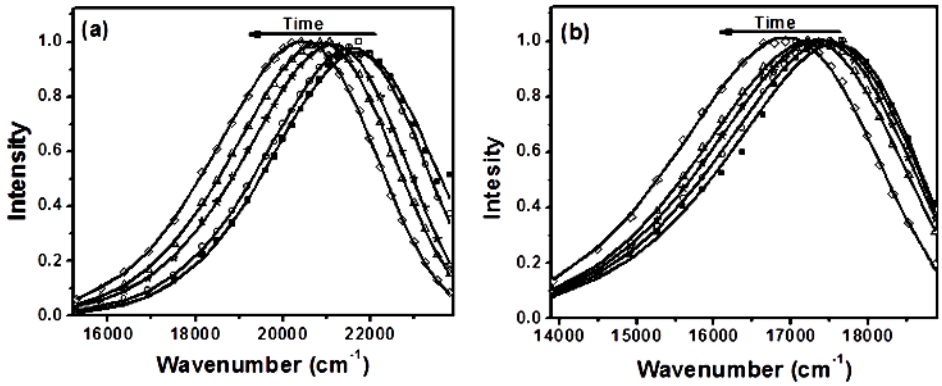

Fig. 5.6. TRES of (a) ANS at (■) 0 ps, (○) 50 ps, (★) 250ps, (△) 500ps, (◇) 2.0 ns and, (b) EB at (■) 0 ps, (○) 100 ps, (★) 250 ps, (△) 500 ps, (◇) 2.0 ns in [bmim][BF_4]. All spectra are normalized at the corresponding peak maxima.

The total observed shift of the time-dependent emission peak calculated from the difference between the frequencies of the measured spectra at zero time, $t(0)$, and

infinite time, $t(\infty)$, is found to 1397 and 864 cm^{-1} for ANS and EB, respectively. It is evident that due to the finite time resolution of our experimental setup (40-50 ps), we might have missed the ultrafast portion of the dynamics, if any, in our measurements. An estimate of this missed component of the dynamics is obtained following the procedure of Fee and Maroncelli.[41] In this procedure, the exact time zero frequency, $\bar{\nu}_{cal}(0)$, is calculated from the steady-state absorption, $\bar{\nu}(abs)$, and fluorescence, $\bar{\nu}(em)$, using Eq. (5.6),

$$\bar{\nu}_{cal}(0) \approx \bar{\nu}_{p}(abs) - \left[\bar{\nu}_{np}(abs) - \bar{\nu}_{np}(em)\right] \qquad (5.6)$$

where the subscripts, p and np, refer to the peak frequencies (in cm^{-1}) in polar and nonpolar solvent, respectively. The extent of the missing component is then determined by the value of $(\bar{\nu}_{cal}(0) - \bar{\nu}(0))/(\bar{\nu}_{cal}(0) - \bar{\nu}(\infty))$. We have calculated the missing component for ANS using cyclohexane as the nonpolar solvent, and the literature data on the steady-state absorption and emission.[42] In the present case, the estimated value of the missing component of the dynamics with ANS is found to be as high as ~60 %. As EB is highly insoluble in nonpolar solvents such as hexane and cyclohexane, the spectral data of the system could not be collected in these solvents and hence, the missing component for this system could not be estimated. The time constant for the observable part of the solvation dynamics has been calculated from the peak frequencies at various times obtained from the lognormal fits to the TRES. A spectral shift correlation function, C(t), is defined in terms of the peak frequencies at various times as Eq. (5.7),

$$C(t) = [\bar{\nu}(t) - \bar{\nu}(\infty)]/[\bar{\nu}(0) - \bar{\nu}(\infty)] \qquad (5.7)$$

where $\bar{\nu}(t)$, $\bar{\nu}(0)$, and $\bar{\nu}(\infty)$ are the peak frequencies (in cm^{-1}) at times, *t*, 0, and ∞ following laser excitation of the probe molecule. The calculated C(t) values at different times are then plotted against time and fitted to a biexponential function of the form, $C(t) = \alpha_1 \exp(-t/\tau_1) + \alpha_2 \exp(-t/\tau_2)$, where τ_1 and τ_2 are the solvent relaxation time and α_1 and α_2 are the normalized pre-exponential factors. The C(t) versus time plots for both the probe molecules are shown in Fig. 5.7(a) along with the best biexponential fits to the data. The fitting parameters suggest the fits to be quite good. The average salvation time for ANS is estimated to be 0.78 ns with the short and long time constant as 0.28 ns and 1.45 ns, respectively. On the other hand, the average salvation time for EB is 1.63 ns with the short and long time constant of 0.51 ns and 2.55 ns respectively. In this context, we have also examined the correlation of the Stokes shift data with time according to the stretched exponential function given below, as often followed by Maroncelli and his co-workers[6] to obtain the average solvation time,

$$\bar{\nu}(t) = \bar{\nu}(\infty) + \Delta\bar{\nu}\exp(-(t/\tau_0)^{\beta})$$

$$C(t) = \exp(-(t/\tau_0)^{\beta}) \qquad (5.8)$$

where $\Delta\bar{\nu} = \bar{\nu}(0) - \bar{\nu}(\infty)$, and $0 < \beta \leq 1$, and the average time of solvation is given by

$$\langle \tau_{solv} \rangle = \frac{1}{\Delta\bar{\nu}} \int_0^{\infty} [\bar{\nu}(t) - \bar{\nu}(\infty)]\, dt = \frac{\tau_0}{\beta}\Gamma(\beta^{-1}) \qquad (5.9)$$

where, Γ is the gamma function. Representative stretched exponential fits to our data according to this equation are shown in Fig. 5.7(b) and the average solvation times obtained from this analysis are given in Table 5.4. It is clearly evident that

the stretched exponential fits to the data are not satisfactory for both the probes. Hence, it can be concluded that the time-resolvable part of the solvation dynamics of both ANS and EB in [bmim][BF4] is biphasic in nature.

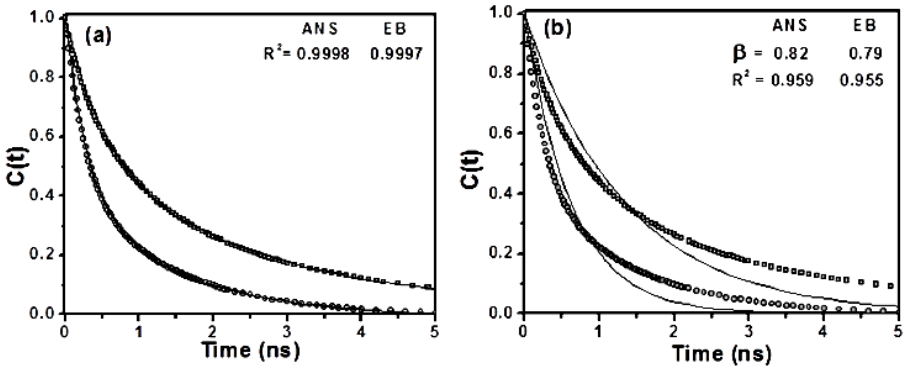

Fig. 5.7. Decay of the spectral shift correlation function, C(t), of ANS (○) and EB(□) in [bmim][BF_4]. In (a) the solid lines represent the biexponentioal fit to the data and, (b) the solid lines represent the stretched-exponential fit to the data. R^2 denotes the correlation coefficient.

Table 5.4. Solvent relaxation parameters of the two probes in [bmim][BF_4]

probe	Decay parameters from biexponential fit[a]			Decay parameters from stretched exponential fit[c]		Observed shit $[\bar{\nu}(0)-\bar{\nu}(\infty)]$
	τ_1/ns (a_1)	τ_2/ns (a_2)	τ_{av}[b]/ ns	β	τ_{solv}[d] /ns	cm^{-1}
ANS	0.28 (0.57)	1.45 (0.43)	0.78	0.82	0.56	1397
EB	0.51 (0.45)	2.54 (0.55)	1.63	0.79	1.21	864

[a]using, $C(t) = a_1\exp(-t/\tau_1) + a_2\exp(-t/\tau_2)$. [b]Average solvation time, $\tau_{av} = a_1\tau_1 + a_2\tau_2$, where, $a_1 + a_2 = 1$, experimental error ±5%. The numbers in the parenthesis indicate the weighted amplitude. [c]Using equn. (5.8). [d]Using equn (5.9).

While some variation of the average solvation time depending on the probe molecule is not uncommon, nearly 2-fold variation of the average solvation time, as observed in this case, with the two probes, is somewhat unexpected and perhaps deserves some attention. In a similar study, Paul and Samanta[14] have observed probe dependence of the solvation time due to specific hydrogen bonding interaction of the probe with one of the constituting ions of the ionic liquid. Since EB is well known for its hydrogen bonding interaction and we have speculated that this interaction is possibly responsible for the large difference of the solvation times obtained with the two probe molecules is perhaps due to the influence of the hydrogen bonding interaction.

5.4. Conclusion

Time-resolved fluorescence anisotropy measurements on the cationic and anionic solutes, EB and ANS, respectively, do not reveal any electrostatic interaction between these ionic solutes and the ionic constituents of the ionic liquid that influences the rotational dynamics of these molecular systems. Instead, the rotational behavior of these ionic solutes is found very similar in ionic liquid and glycerol under isoviscous condition. Interestingly, an analysis of the rotational times using the Stokes-Einstein-Debye theory reveals that EB is strongly associated with both glycerol and [bmim][BF_4]. Hydrogen bonding interaction between the EB and the solvent appears to be the mechanism of solute-solvent association. Solvation dynamics studies also did not reveal any influence of the electrostatic interaction between the charged solutes and ionic liquid.

References

(1) Samanta, A. *J. Phys. Chem. B* **2006**, *110*, 13704.
(2) Mandal, P. K.; Saha, S.; Karmakar, R.; Samanta, A. *Current Science* **2006**, *90*, 301.
(3) Ito, N.; Arzhantsev, S.; Maroncelli, M. *Chem. Phys. Lett.* **2004**, *396*, 83.
(4) Ito, N.; Arzhantsev, S.; Heitz, M.; Maroncelli, M. *J. Phys. Chem. B* **2004**, *108*, 5771.
(5) Karmakar, R.; Samanta, A. *J. Phys. Chem. A* **2003**, *107*, 7340.
(6) Ingram, J. A.; Moog, R. S.; Ito, N.; Biswas, R.; Maroncelli, M. *J. Phys. Chem. B* **2003**, *107*, 5926.
(7) Chakrabarty, D.; Hazra, P.; Chakraborty, A.; Seth, D.; Sarkar, N. *Chem. Phys. Lett.* **2003**, *381*, 697.
(8) Arzhantsev, S.; Ito, N.; Heitz, M.; Maroncelli, M. *Chem. Phys. Lett.* **2003**, *381*, 278.
(9) Karmakar, R.; Samanta, A. *J. Phys. Chem. A* **2002**, *106*, 6670.
(10) Karmakar, R.; Samanta, A. *J. Phys. Chem. A* **2002**, *106*, 4447.
(11) Mali, K. S.; Dutt, G. B.; Mukherjee, T. *J. Chem. Phys.* **2008**, *128*, 054504.
(12) Mali, K. S.; Dutt, G. B.; Mukherjee, T. *J. Chem. Phys.* **2005**, *123*, 174504.
(13) Baker, S. N.; Baker, G. A.; Kane, M. A.; Bright, F. V. *J. Phys. Chem. B* **2001**, *105*, 9663.
(14) Paul, A.; Samanta, A. *J. Phys. Chem. B* **2007**, *111*, 4724.
(15) Fruchey, K.; Fayer, M. D. *J. Phys. Chem. B* **2010**, *114*, 2840.
(16) Chakrabarty, D.; Chakraborty, A.; Seth, D.; Sarkar, N. *J. Phys. Chem. A* **2005**, *109*, 1764.
(17) Chakrabarty, D.; Chakraborty, A.; Seth, D.; Hazra, P.; Sarkar, N. *Chem. Phys. Lett.* **2004**, *397*, 469.
(18) Chakrabarty, D.; Chakraborty, A.; Hazra, P.; Seth, D.; Sarkar, N. *Chem. Phys. Lett.* **2004**, *397*, 216.
(19) Bart, E.; Meltsin, A.; Huppert, D. *J. Phys. Chem. B* **1994**, *98*, 3295.
(20) Bart, E.; Meltsin, A.; Huppert, D. *J. Phys. Chem.* **1994**, *98*, 10819.
(21) Znamenskiy, V.; Kobrak, M. N. *J. Phys. Chem. B* **2004**, *108*, 1072.

(22) Shim, Y.; Duan, J.; Choi, M. Y.; Kim, H. J. *J. Chem. Phys.* **2003**, *119*, 6411.

(23) Pramanik, R.; Rao, V. G.; Sarkar, S.; Ghatak, C.; Setua, P.; Sarkar, N. *J. Phys. Chem. B* **2009**, *113*, 8626.

(24) Lang, B.; Angulo, G.; Vauthey, E. *J. Phys. Chem. A* **2006**, *110*, 7028.

(25) Funston, A. M.; Fadeeva, T. A.; Wishart, J. F.; Edward W. Castner, J. *J. Phys. Chem. B* **2007**, *111*, 4963.

(26) Arzhantsev, S.; Jin, H.; Baker, G. A.; Maroncelli, M. *J. Phys. Chem. B* **2007**, *111*, 4978.

(27) Chowdhury, P. K.; Halder, M.; Sanders, L.; Calhoun, T.; Anderson, J. L.; Armstrong, D. W.; Song, X.; Petrich, J. W. *J. Phys. Chem. B* **2004**, *108*, 10245.

(28) Giraud, G.; Gordon, C. M.; Dunkin, I. R.; Wynne, K. *J Chem. Phys.* **2003**, *119*, 464.

(29) Mandal, P. K.; Sarkar, M.; Samanta, A. *J. Phys. Chem. A* **2004**, *108*, 9048.

(30) Pal, S. K.; Mandal, D.; Bhattacharyya, K. *J. Phys. Chem. B* **1998**, *102*, 11017.

(31) Tleugabulova, D.; Sui, J.; Ayers, P. W.; Brennan, J. D. *J. Phys. Chem. B* **2005**, *109*, 7850.

(32) Tleugabulova, D.; Zhang, Z.; Chen, Y.; Brook, M. A.; Brennan, J. D. *Langmuir* **2004**, *20*, 848.

(33) Edward, J. T. *J. Chem. Educ.* **1970**, *47*, 261.

(34) Sension, R. J.; Hochstrasser, R. M. *J. Chem. Phys.* **1993**, *93*, 2490.

(35) Small, E. W.; I. Isenberg. *Biopolymers* **1977**, *16*, 1907.

(36) Hartman, R. S.; Alavi, D. S.; Waldeck, D. H. *J. Phys. Chem.* **1991**, *95*, 7872.

(37) Olmsted, J. III.; Kearns, D. R. *Biochemistry* **1977**, *16*, 3647.

(38) Marcus, Y. *J. Phys. Chem.* **1987**, *91*, 4422.

(39) Crowhurst, L.; Mawdsley, P. R.; Perez-Arlandis, J. M.; Salter, P. A.; Welton, T. *Phys. Chem. Chem. Phys* **2003**, *5*, 2790.

(40) Kurnikova, M. G.; Balabai, N.; Waldeck, D. H.; Coalson, R. D. *J. Am. Chem. Soc.* **1998**, *120*, 6121.

(41) Fee, R. S.; Maroncelli, M. *Chem. Phys.* **1994**, *183*, 235.

(42) H-J, B.; T, W. *J Photochem Photobiol A* **1999**, *121*, 99.

Chapter 6

Solvation and Rotational Dynamics of C153 in N-alkyl-N-methylmorpholinium Ionic Liquids

In the present work, temperature and excitation wavelength dependent steady-state and time-resolved fluorescence response of C153 have been studied in a series of four N-alkyl-N-methylmorpholinium ionic liquids to understand the physicochemical properties of these RTILs. The steady-state spectra have been exploited for the estimation of the polarity of these RTILs. Temperature and excitation wavelength dependent steady-state emission spectra indicate the domain structure of these RTILs. The time-resolved fluorescence anisotropy measurements substantiate the domain structure of these RTILs. Solvation dynamics study at isothermal condition indicates that the solvation process is governed by the bulk viscosity of the medium and size of the ionic constituents of these RTILs.

6.1. Introduction

The room temperature ionic liquids (RTILs) continue to attract a great deal of attention primarily because of the fact that only a very few of the large number of possible RTILs have so far been studied.[1-7] Additional factor contributing to the vigorous activities with these substances is the complex nature of these materials and the findings that the physicochemical properties of even some of the extensively studied RTILs such as those based on imidazolium, ammonium, phosphonium, pyridinium and pyrolidinium cations are not fully understood.[8-12] It

is thus evident that the intensity with which the ILs are being studied currently from different directions will last for quite some time. ILs based on the N, N′-dialkylimidazolium salts have thus far been the most widely studied because of their favorable physical properties. However, considering the high cost of industrial scale synthesis of these salts, the focus seems to be shifting gradually towards other less expensive alternatives such as the morpholinium ILs, which are not only cheap and easy to develop, but also possess good physicochemical characteristics.[13-17]

In this work, we attempt to explore some of the physicochemical properties of largely unfamiliar four different N-alkyl-N-methylmorpholinium ILs, abbreviated as $[Mor_{1,2}][Tf_2N]$, $[Mor_{1,4}][Tf_2N]$, $[Mor_{1,6}][Tf_2N]$ and $[Mor_{1,8}][Tf_2N]$ (Chart 6.1), consisting of N-alkyl-N-methylmorpholinium cation with four different alkyl chain lengths and an identical anionic component, $[Tf_2N]^-$, by probing the steady-state and time-resolved fluorescence behavior of a dipolar solute, C153, whose fluorescence properties in conventional solvents and several RTILs are very well understood.[18-20] The physicochemical properties of a

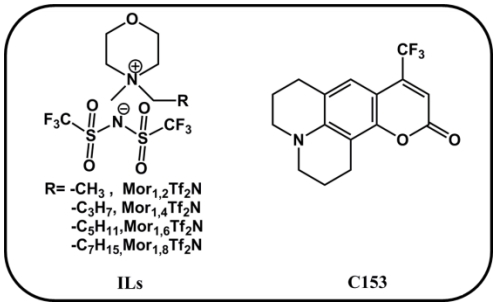

Chart 6.1 Chemical formula and abbreviations of RTILs and probe molecule**.**

RTIL strongly depend on the constituent ions. A gradual variation of the length of the alkyl chain attached to one of the constituent ions is expected to vary systematically the properties of the RTILs that we attempt to capture in this work. While the room temperature measurements reveal the influence of viscosity of these RTILs on the fluorescence response of C153, the experiments performed under an isoviscous condition, maintained by heating the RTILs to different temperatures, help identifying the factor(s), if any, other than the viscosity of the medium that may influence the fluorescence behavior of the probe molecule. In addition to probing the steady-state fluorescence response of C153 in these RTILs, we study its time-resolved behavior, from which we extract information on the dynamics of solvent reorganization and solute rotational diffusion, which is crucial to the understanding of the physicochemical characteristics of the media and their utilization.[21,22] As solvation leads to considerable Stokes shift of the fluorescence spectrum of a dipolar molecule in a polar medium, the solvation dynamics is most commonly studied by measuring the time-dependent Stokes shift of the fluorescence maximum of a dipolar probe molecule following its electronic excitation using a short pulse of light.[23,24] A large number of experimental and theoretical studies on solvation dynamics in various RTILs highlight both the importance of the process and its complex nature.[11,12,20,25-49] The rotational diffusion of a solute molecule, which is commonly investigated by studying the time-resolved fluorescence anisotropy of the solute, is also known to provide important information on the nature of solute-solvent interaction in these media. Hence, several studies dealing with the rotational motion of solutes in

RTILs have been made in recent years employing a variety of probe molecules and RTILs.[29-31,34, 38,39,50-56]

Several experimental and theoretical studies in recent years, have indicated that most of the N-alkyl-N-methylimidazolium RTILs are not homogeneous structureless liquids, but possess an organized domain-like structure formed by the segregation of the alkyl chains on one hand and the charged components on the other.[57-64] An important aspect of this work, which we investigate, is the structural heterogeneity of these RTILs. As the long alkyl chains are known to contribute to the heterogeneity of the RTILs, we have chosen four different alkyl chains to understand the heterogeneity of the N-alkyl-N-methylmorpholinium RTILs.

6.2. Steady-state Measurement

6.2.1. Steady-state absorption and emission. The room temperature (25 ^{0}C) absorption and emission spectra of C153 in four morpholinium RTILs are shown in Figure 6.1. Even though the absorption maximum (λ_{max}^{abs}) of C153 in these RTILs appears at the same wavelength (*ca.* 425 nm), the emission maximum (λ_{max}^{em}) shifts towards the shorter wavelength with increase in the chain length of the cationic component of the RTIL. One can observe ~15 nm blue-shift of the λ_{max}^{em} on changing of the solvent from [$Mor_{1,2}$][Tf_2N] to [$Mor_{1,8}$][Tf_2N]. The shift of the λ_{max}^{em} is most prominent when the solvent is changed from [$Mor_{1,2}$][Tf_2N]

to[$Mor_{1,4}$][Tf_2N]. However, on changing the solvent from [$Mor_{1,4}$][Tf_2N] to [$Mor_{1,8}$][Tf_2N], a small shift of λ_{max}^{em} is observed.

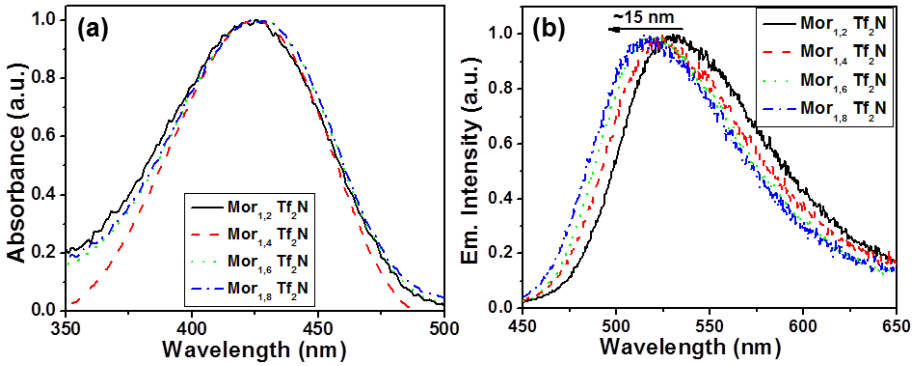

Fig. 6.1 Normalized absorption (a) and fluorescence (b) spectra of C153 in four different morpholinium RTILs at 25 ^{0}C. λ_{exc} for the emission measurements is 405 nm.

That the λ_{max}^{abs} of C153 appears at the same wavelength in four different RTILs but the λ_{max}^{em} is sensitive to the variation of the alkyl chain length of the cation, is consistent with the more polar nature of the emitting state of C153 compared to the ground state.[18] It is evident from the λ_{max}^{em} values that C153 experiences a less polar environment in RTILs comprising a higher alkyl chain length. This is perhaps a reflection of the fact that a longer alkyl chain length of one of the constituent ions implies a larger volume of the nonpolar region.

As C153 is a polarity sensitive probe, one can attempt to estimate the microscopic polarity experienced by the probe in these RTILs from its fluorescence energy ($\bar{\nu}_{max}^{em}$). By measuring the $\bar{\nu}_{max}^{em}$ values of C153 in several

conventional solvents of known polarity ($E_T(30)$) and then using the linear correlation between $\bar{\nu}_{max}^{em}$ and $E_T(30)$ and the measured $\bar{\nu}_{max}^{em}$ values in RTILs, one obtains $E_T(30)$ values (Table 6.1) of 45.1, 45.8, 47.0 and 48.5 for $[Mor_{1,8}][Tf_2N]$, $[Mor_{1,6}][Tf_2N]$, $[Mor_{1,4}][Tf_2N]$ and $[Mor_{1,2}][Tf_2N]$, respectively. It thus appears that the polarity of the long chain containing RTILs, $[Mor_{1,6}][Tf_2N]$ and $[Mor_{1,8}][Tf_2N]$ is comparable to that of acetonitrile [$E_T(30)$ = 45.6], whereas the polarity of the two short chain containing RTILs, $[Mor_{1,2}][Tf_2N]$ and $[Mor_{1,4}][Tf_2N]$ is similar to that of long chain alcohols such as 1-octanol [$E_T(30)$ = 48.1] and cyclopentanol [$E_T(30)$ = 47], respectively.[65] These values are slightly lower than those for the corresponding imidazolium salts.[11,66] However, we show that these values do not correctly represent the true polarity of these RTILs in the following section (Section 6.2.2), where the basis of this statement and the correct polarity estimates of these RTILs are presented.

6.2.2. Temperature dependence of the emission spectra. Temperature dependence of the emission spectrum of C153 in four RTILs has been studied over a range of 50 ^{0}C from 25 to 75 ^{0}C. As can be seen from Figure 6.2 and the data presented in Table 6.1, the λ_{max}^{em} values shift towards a higher wavelength with increase in temperature. The extent of shift is dependent on the RTIL and the effect is more pronounced in RTILs consisting of cation with a higher chain length. For example, for a change of temperature from 25 to 55 ^{0}C, the shifts of the emission maximum observed are 105, 180, 220, and 290 cm^{-1} for $[Mor_{1,2}][Tf_2N]$, $[Mor_{1,4}][Tf_2N]$, $[Mor_{1,6}][Tf_2N]$ and $[Mor_{1,8}][Tf_2N]$, respectively.

No further shift of the emission maximum is observed for increase of temperature beyond 55 ^{0}C.

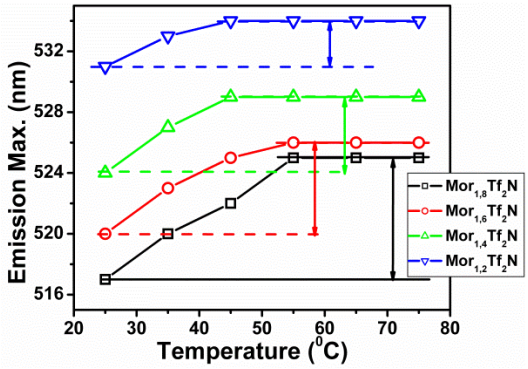

Fig. 6.2 Temperature dependence of the fluorescence maximum (λ_{exc}= 405 nm) of C153 in the RTILs.

Table 6.1. Temperature Dependence of the Steady-state Fluorescence Data of the Probe Molecule (C153) and Estimated Polarity of the RTILs

Temp. (^{0}C)	[Mor$_{1,2}$][Tf$_2$N]		[Mor$_{1,4}$][Tf$_2$N]		[Mor$_{1,6}$][Tf$_2$N]		[Mor$_{1,8}$][Tf$_2$N]	
	$\bar{\nu}_{em}^{max}$	$E_T(30)^a$	$\bar{\nu}_{em}^{max}$	$E_T(30)^a$	$\bar{\nu}_{em}^{max}$	$E_T(30)^a$	$\bar{\nu}_{em}^{max}$	$E_T(30)^a$
25	18830	48.5	19080	47.0	19230	45.8	19340	45.1
35	18760	-	18975	-	19160	-	19230	-
45	18725	-	18900	-	19050	-	19160	-
55	18725	-	18900	-	19010	-	19050	-
65	18725	-	18900	-	19010	-	19050	-
75	18725	49.3	18900	48.1	19010	47.3	19050	47.1

[a]Estimated from the calibration curve obtained by plotting the fluorescence maxima of C153 against known $E_T(30)$ values in conventional solvents.

An increase in temperature commonly results in a blue-shift of the λ_{max}^{em} of dipolar molecules in conventional solvents due to a decrease of the polarity (dielectric constant) of the medium.[67] Hence, the observation of a red shift implies

that the effect of temperature induced small change in polarity of the ILs is masked by other factor, which produces a larger effect of an opposite kind. The viscosity of a medium is lowered at higher temperatures, but such change does not commonly affect the fluorescence peak position of a system in conventional solvents. However, the effect of temperature (T) on the viscosity (η) of the medium is much more pronounced in the case of RTILs. The measured viscosities of the four RTILs at various temperatures are shown in Figure 6.3 along with the curves representing the fits to the Vogel-Fulcher-Tamman equation,[68]

$$\eta = \eta_0 \exp[B/(T - T_c)] \qquad (6.1)$$

where, η_0, B and T_c are fitting parameters that depend on the RTIL. The high viscosity of the RTILs and its strong temperature dependence can account for the temperature dependent shift of λ_{max}^{em} of C153. It is well known that solvent reorganization around a photoexcited dipolar molecule is a slow process in RTILs due to the high viscosity of these media.[11,12,49] As a consequence, the molecules, particularly those having fluorescence lifetime (τ_f) shorter or comparable to the solvation time ($<\tau_{sol}>$), may not be able to emit from the completely solvated excited state at lower temperature. However, at higher temperature, due to a reduction of the viscosity of the medium, the solvation becomes faster thereby allowing the molecules to emit from a more relaxed state. This can account for the observed temperature dependence of the λ_{max}^{em} values of C153 in the present ILs. In this context, we note that a red shift of the kind described here is reported in highly viscous (η = 800 - 900 cP) ammonium RTILs,[39] but we are not aware of any similar report in imidazolium RTILs probably because the imidazolium

RTILs, in which the fluorescence behavior of C153 has been studied so far, are not so viscous that the condition $<\tau_{sol}> \geq \tau_f$ is satisfied.

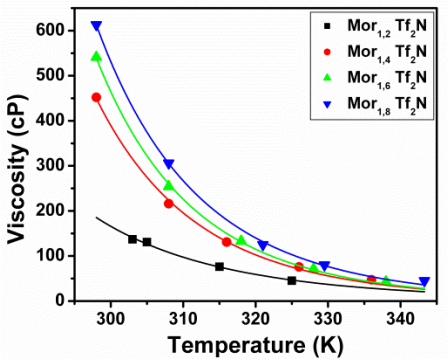

Fig. 6.3. Measured viscosity of the morpholinium ILs at different temperatures. The solid lines represent the fits to the experimental data points according to VFT equation.

The finding that even probes like C153, which has a relatively long fluorescence lifetime (τ_f = 4.8 – 5.2 ns), does not emit from the fully solvated state in morpholinium RTILs implies that the polarities of these RTILs estimated from the measured $\bar{\nu}_{max}^{em}$ values at room temperature in Section 6.2.1. do not represent the correct values. However, as a constant value of $\bar{\nu}_{max}^{em}$ is reached at higher temperatures (Table 6.1), it can be assumed that C153 emits from the fully solvated state under these conditions and one can then use the higher temperature values of $\bar{\nu}_{max}^{em}$ for the polarity estimation. The $E_T(30)$ values estimated from the higher temperature values of $\bar{\nu}_{max}^{em}$ for $[Mor_{1,2}][Tf_2N]$, $[Mor_{1,4}][Tf_2N]$, $[Mor_{1,6}][Tf_2N]$ and $[Mor_{1,8}][Tf_2N]$, which represent the actual polarity of these

media, are 49.3, 48.1, 47.3 and 47.1, respectively. As these numbers are similar to those for the imidazolium RTILs with similar alkyl chain length, we conclude that the polarities of the morpholinium RTILs are comparable to those of the corresponding imidazolium RTILs.[11,66]

6.2.3. Excitation wavelength dependence of the emission spectra. The fluorescence behavior of C153 stated above has been measured for an excitation wavelength of 405 nm. We found that the spectral behavior remains same as long as the excitation wavelength was $\leq \lambda_{max}^{abs}$. However, for excitation wavelength corresponding to the tail part of the first absorption band, a red shift of the λ_{max}^{em} value is observed on increase of the excitation wavelength. This excitation wavelength dependent variation of λ_{max}^{em} is shown in Figure 6.4. As can be seen, the excitation wavelength dependence is most pronounced in ILs having a long alkyl chain length. It is also seen that this excitation wavelength dependence is significantly lowered with increasing temperature (Figure 6.5).

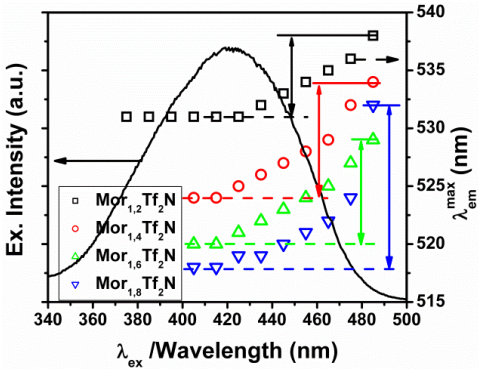

Fig. 6.4. Excitation wavelength dependence of the emission maxima of C153 in the ILs (at 25 ^{0}C). Also shown in the figure, a typical fluorescence excitation spectrum of C153 in these RTILs.

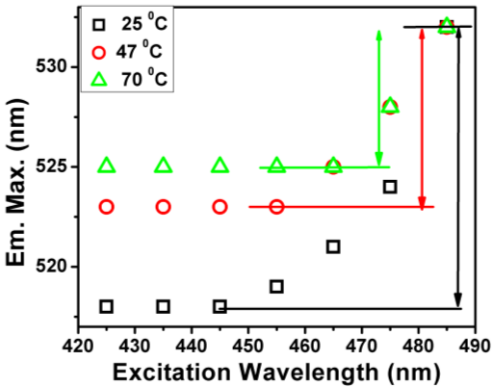

Fig. 6.5. Excitation wavelength dependence of the fluorescence maxima of C153 in $[Mor_{1,8}][Tf_2N]$ at different temperature.

It is documented that some dipolar molecules, when excited in their red edge of the first absorption band, display excitation wavelength dependent fluorescence spectra, which is known as red edge effect (REE).[69] However, unlike a few other molecules C153 does not exhibit REE in imidazolium ILs,[11,70,71] as its fluorescence lifetime (τ_f = 5.6 ns) is considerably higher than the average solvent relaxation time ($<\tau_{sol}>$ = 1.4-2.1 ns) of the ILs.[71] The observation of REE of C153 in morpholinium ILs, which is more pronounced in the case of long alkyl chain containing RTILs, is quite surprising as the fluorescence lifetime of C153 in these liquids (τ_f = 4.8 – 5.2 ns) is still much higher than the estimated solvation time in these solvents.[72] Considering this factor and noting that REE of C153 in a highly heterogeneous medium is recently reported,[73] we think, the excitation wavelength dependent emission of C153 in these morpholinium RTILs is due to the microheterogeneous nature of these media and that is more prominent in case of

long chain containing RTILs. It is obvious that the heterogeneity of these media arises from the segregation of the polar (the ionic constituents) and nonpolar (the alkyl chain) components of the RTILs forming polar and nonpolar domains to which C153 is distributed. The lack of interaction between the molecules from different domains gives rise to emission that is dependent on the kind of molecules excited rather than that by the molecules with the lowest singlet state energy. With increase in temperature as the domain structure is partially destroyed, the excitation wavelength dependence decreases or disappears. Therefore, the excitation wavelength dependent fluorescence behavior of C153 and its temperature dependence suggest that the morpholinium RTILs are more heterogeneous than the imidazolium RTILs of comparable viscosity.

A comparison of the excitation wavelength dependence data of C153 in four RTILs under isoviscous condition also presents a similar picture (Figure 6.6). Under this condition one expects C153 to display similar excitation wavelength dependence in all RTILs. However, Figure 6.6 shows that this is not the case. The fact that the RTILs with a longer alkyl chain length exhibits a more pronounced excitation wavelength dependence compared to the other RTILs with shorter alkyl chain length under an isoviscous condition, can be explained only in terms of domain-like structures for the RTILs.

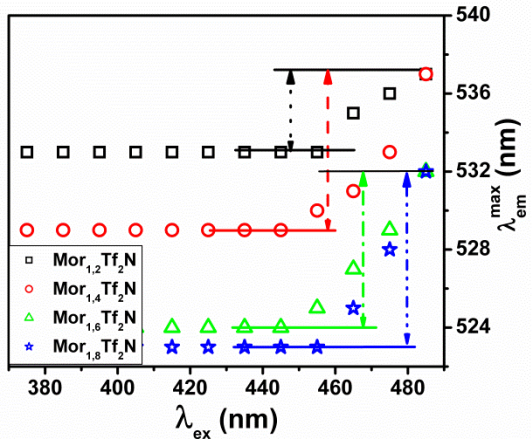

Fig. 6.6. Excitation wavelength dependence of the emission maxima of C153 in the RTILs (under isoviscous condition, η = 130 cP)

6.3. Time-Resolved Measurement

6.3.1. Rotational Dynamics: The time-resolved fluorescence measurements have been performed under both isothermal and isoviscous conditions. The measurements under the isothermal condition is performed at 40 ^{0}C instead of room temperature (25 ^{0}C) as the decay kinetics were found too slow to be estimated accurately at room temperature, particularly in the case of long chain containing RTILs. The rotational diffusion of the probe molecule has been studied by following the time-dependence of the fluorescence anisotropy of the system. Representative fluorescence anisotropy decays of C153 in four RTILs are shown in Figure 6.7. Even though these profiles are better described by a bi-exponential function, the average reorientation time obtained from such analysis was found to be not very different from that obtained from the single-exponential fits to the data. The measured rotational time constants of the molecule in different RTILs

are collected in Table 6.2 together with the solvent viscosity. As can be seen, under isothermal condition, the rotational relaxation time of C153 increases with increasing viscosity (or chain length) of the ionic liquid. However, in highly viscous $[Mor_{1,6}][Tf_2N]$ and $[Mor_{1,8}][Tf_2N]$, the rotational time constants are very similar.

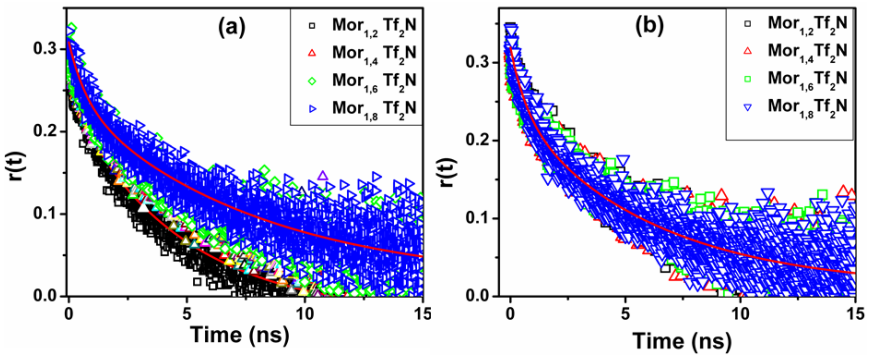

Fig. 6.7. Plots of anisotropy decay profiles of C153 in the RTILs at (a) isothermal (40 ^{0}C) and (b) isoviscous (η = 130 cP) condition. Solid lines represent the fit data to decay profiles.

According to the Stokes-Einstein-Debye (SED) hydrodynamic theory,[22,29] at any given temperature (T), the reorientation time of a solute rotating in a solvent continuum is proportional to (1/η), where, η is the viscosity of the medium. Hence, in the absence of any specific interaction between the solvent and probe molecule, the observations of a very similar reorientation time of C153 in two highly viscous RTILs, $[Mor_{1,6}][Tf_2N]$ and $[Mor_{1,8}][Tf_2N]$, whose bulk viscosities differ by 34 cP, and also, a faster rotation of the probe in these media compared to that in two less viscous RTILs, $[Mor_{1,2}][Tf_2N]$ and $[Mor_{1,4}][Tf_2N]$, are contrary to the SED hydrodynamic prediction. These results can only be

understood when these RTILs, in particular, those with the long chain lengths, are considered to be structured liquid rather than a continuum, as assumed in the SED theory. The results suggest that the microviscosity around the probe molecule is lower than the bulk viscosity of the medium.

These results can also be analyzed from another angle. As $C_{rot} = \tau_r$ (expt)/τ_r(theo), it is a measure of the association of the solute with the solvent molecules or a ratio of the actual hydrodynamic volume to the stick hydrodynamic volume. Other factors remaining same, an increase in the size of the solvent molecule due to an increase in the alkyl chain length is expected to increase the C_{rot} value. However, this is not the case here (Table 6.2). The C_{rot} values indicate a lesser degree of association with increase in the size of the solvent. This can only be explained if there occurs a phase separation into hydrophobic and hydrophilic domains with increase in the size of the solvent and localization of the probe molecule in the nonpolar domain.

Table 6.2. Rotational Relaxation Time of C153 in Different ILs at Isothermal (40 ^{0}C) and Isoviscous (η = 130 cP) Condition

ILs	Viscosity[a] (cP)	$<\tau_{rot}>$[b] (T = 40 ^{0}C)	C_{rot}[c]	Viscosity[d] (cP)	$<\tau_{rot}>$[b] (Isoviscous)	C_{rot}[c]
$[Mor_{1,2}][Tf_2N]$	82	4.3	0.55	130	5.9	0.46
$[Mor_{1,4}][Tf_2N]$	157	5.9	0.39		5.5	0.45
$[Mor_{1,6}][Tf_2N]$	180	6.4	0.37		5.4	0.44
$[Mor_{1,8}][Tf_2N]$	214	6.2	0.30		4.7	0.39

[a]At 40 ^{0}C, estimated from the plots shown in Fig. 3. [b]Average rotational time (ns), $<\tau_{rot}> = a_1\tau_{r1} + a_2\tau_{r2,}$ where, $a_1 + a_2 = 1$, ±5%. [c]$C_{rot} = \tau_r^{exp} / \tau_r^{stick}$. [d]Experimentally measured viscosity at 32, 43, 45 and 47 ^{0}C for $[Mor_{1,2}][Tf_2N]$, $[Mor_{1,4}][Tf_2N]$, $[Mor_{1,6}][Tf_2N]$ and $[Mor_{1,8}][Tf_2N]$, respectively.

The anisotropy decay profiles were measured and the rotational time constants are estimated (Table 6.2) also under an isoviscous condition (η = 130 cP) by heating the four RTILs to different temperatures. As can be seen from Table 6.2, C153 shows similar rotational relaxation time constant except in $[Mor_{1,8}][Tf_2N]$, where a relatively faster decay of the anisotropy is observed. The observation seems to imply that the microheterogeneous domain structure of $[Mor_{1,8}][Tf_2N]$ still persists even at a higher temperature (47 ^{0}C) and C153 is located in a region which is less viscous than the bulk viscosity of the medium (130 cP).

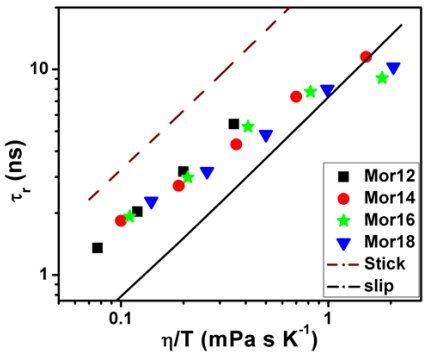

Fig. 6.8. Plot of rotational time constant (τ_r) versus η/T in different ionic liquids. The slip (solid) and stick (dash) lines are computed by using the V = 246 Å^3, f = 1.71, C = 0.24 (taken from ref. 35)

Apart from the studies carried out under isothermal and isoviscous conditions, we have measured the temperature dependence of the rotational relaxation time constant over a wide range of temperature (25 – 65 ^{0}C) in these ionic liquids. The results are depicted in Figure 6.8. The plot of τ_r versus η/T indicates that the τ_r values of C153 lie between the slip and stick boundary

condition of the SED theory. It is interesting to note, however, the deviation from the linearity in long chain containing ionic liquids. The degree of the nonlinearity in each set is evident from the fitting parameters, when the data is fit to $\tau_r = A(\eta/T)^p$.

C153 in $[Mor_{1,2}][Tf_2N]$

$$\tau_r = (14.25 \pm 0.25)\left(\frac{\eta}{T}\right)^{0.92\pm0.012} \qquad \text{(N=4, R=0.9997)}$$

C153 in $[Mor_{1,4}][Tf_2N]$

$$\tau_r = (8.80 \pm 0.17)\left(\frac{\eta}{T}\right)^{0.67\pm0.03} \qquad \text{(N=5, R=0.9959)}$$

C153 in $[Mor_{1,6}][Tf_2N]$

$$\tau_r = (7.31 \pm 0.50)\left(\frac{\eta}{T}\right)^{0.48\pm0.08} \qquad \text{(N=5, R=0.9311)}$$

C153 in $[Mor_{1,8}][Tf_2N]$

$$\tau_r = (7.20 \pm 0.30)\left(\frac{\eta}{T}\right)^{0.54\pm0.05} \qquad \text{(N=5, R=0.9777)}$$

Except for $[Mor_{1,2}][Tf_2N]$, the p values for these ionic liquids lie between 0.48 to 0.67. This is contrast to the findings of most of the rotational dynamics studies in ionic liquids, which report p values close to 1.[50-55] It is also known that the 'p' values are close to 1 for all common organic solvents except for higher n-alkanes, where this value is around 0.63.[74,75] The deviation in the plot of τ_r versus η/T from the slip boundary condition at low temperature and a decrease in the coupling constant ($C_{rot} = \tau_r/\tau_{stick}$) for long chain containing ionic liquids is similar to the rotational behavior of C153 in higher n-alkanes,[74] which was attributed to inefficient solvent packing around the rotating solute. In another study, a very

similar rotational behavior of C153 in molten salt is explained in terms of the domain structure of the medium at low temperature.[75] Considering these literature, we explain our results in terms of the heterogeneity of the ionic liquids, where a domain structure is formed by the alkyl group of the ionic liquids in one hand and charged constituents of the ionic liquids on the other.[57-64] It appears that with increase in the chain length of the ionic liquids the probe molecule prefers to reside in the nonpolar domain, formed by the alkyl group and this is why a deviation from the SED model, similar to that observed in higher n-alkanes, is observed in long chain containing ionic liquids.

Though excitation wavelength dependent study is another approach to probing the heterogeneity of the medium,[35] in the present case, an excitation wavelength dependent study (λ_{exc} = 375, 405 and 439 nm) did not show any significant variation of the rotational time constant. However, from this observation we cannot comment on the presence/absence of the heterogeneity of these ionic liquids mainly because as we could not excite at the red-edge of the absorption band of the molecule with these wavelengths. One needs to use longer wavelength excitation and carry out experiments with additional probe molecules to arrive at a definite conclusion.

6.3.2. Solvation Dynamics*:* The time-resolved emission spectra of C153, constructed from the wavelength dependent fluorescence decay profiles according to the procedure described in Chapter 2, show time-dependent shift of the emission maximum from higher energy to the lower energy (Figure 6.9) indicating slow solvent-mediated relaxation of the excited state of the probe. The total time-dependent Stokes shift estimated from the measured wavenumbers

corresponding to the fluorescence maxima at zero and infinite times, are found to be 1045, 1235, 1140 and 1360 cm^{-1} at 40 ^{0}C for $[Mor_{1,2}][Tf_2N]$ to $[Mor_{1,8}][Tf_2N]$, respectively. The ultrafast component of the dynamics, which is missed here due to the finite time-resolution of our single photon counting setup is estimated by calculating the expected time-zero spectrum using a literature procedure.[76] The missing component of the total solvent reorganization dynamics is ~ 40-60% and found to be dependent on the chain length of the cation (Table 6.3). The results suggest that at a given temperature, the missing component of the total solvent reorganization dynamics decreases with increase in the alkyl chain length of the ionic liquid.

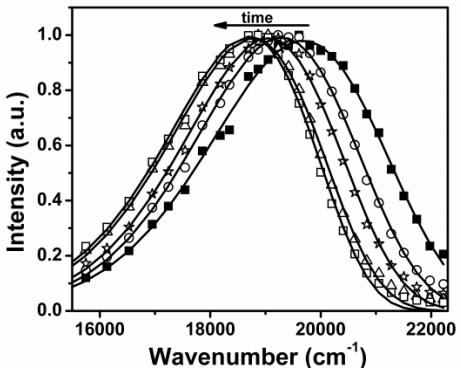

Fig. 6.9. Normalized TRES of C153 in $[Mor_{1,2}][Tf_2N]$ (at 40 ^{0}C) (■) 0 ps, (○) 100 ps, (★) 250 ps, (Δ) 1000 ps, (◇) 2000 ps.

The time constant of the observable, slow component of the solvent reorganization dynamics is estimated by measuring the peak frequencies of the spectra at various times (t = 0, t and ∞) and then analyzing the time-dependence of the spectral shift correlation function, C(t), defined as

$$C(t) = [\bar{\nu}(t) - \bar{\nu}(\infty)]/[\bar{\nu}(0) - \bar{\nu}(\infty)] \quad (6.2)$$

The time dependent decay of C(t) was found to be better described by a bi-exponential function of the form, $C(t) = \alpha_1 \exp(-t/\tau_1) + \alpha_2 \exp(-t/\tau_2)$, τ_1 and τ_2 are the solvent relaxation time and α_1 and α_2 are the normalized pre-exponential factors. Representative plots of the data and bi-exponential fits to those are shown in Figure 6.10. The individual fast and slow components of the dynamics along with the average values of the solvent relaxation times are collected in Table 6.3. It is evident that both the fast and slow components of the dynamics depend on the chain length of the cation and with increasing viscosity of the medium the dynamics becomes slow. It can also be seen (Table 6.3) that the average solvent relaxation time increases with the increase of the substituted alkyl chain length i.e. viscosity of the medium. The correlation between average solvation time and the viscosity of the RTILs is illustrated in Figure 6.11.

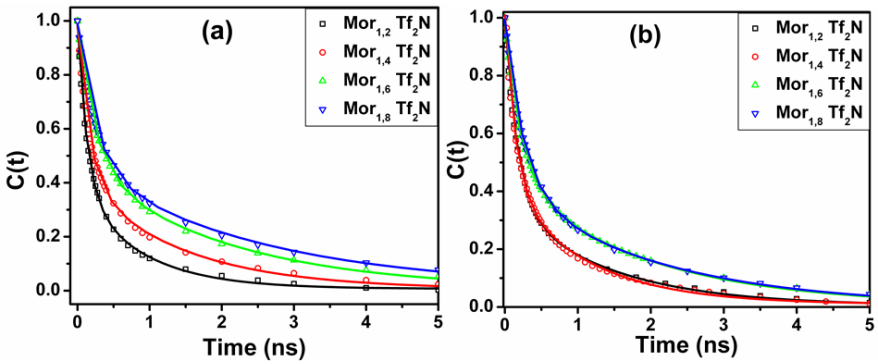

Fig. 6.10. Decay of the spectral shift corelation function, C(t), in different ILs at (a) isothermal (40 ^{0}C) and (b) isoviscous (η = 130 cP) condition. Solid lines represent the bi-exponential fits to the data points.

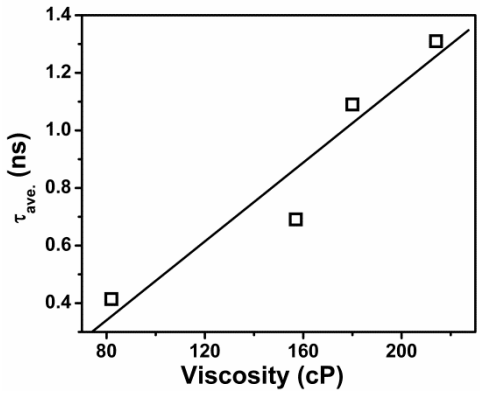

Fig. 6.11. Viscosity dependence of the average solvation time in the ILs. The data points presented here were collected at 40 ^{0}C. Solid line represents the linear fit to the data points.

Table 6.3. Solvent Relaxation Parameters Estimated from the TRES of C153 at Isothemal Condition (40 ^{0}C)

RTILs	Viscosity [a] (cP)	Relaxation Data[b]			$\bar{\nu}(0)$ (cm^{-1})	Observed Shift ($\Delta\bar{\nu}$) (cm^{-1})	Miss. Com.[d]
		τ_1 (a_1)	τ_2 (a_2)	τ_{sol} [c]			
$Mor_{1,2}Tf_2N$	82	0.14 (0.62)	0.87 (0.38)	0.41	19685	1045	60%
$Mor_{1,4}Tf_2N$	157	0.17 (0.58)	1.42 (0.42)	0.69	20015	1235	50%
$Mor_{1,6}Tf_2N$	180	0.24 (0.53)	2.05 (0.47)	1.09	20020	1140	52%
$Mor_{1,8}Tf_2N$	214	0.25 (0.53)	2.50 (0.47)	1.31	20250	1360	43%

[a]At 40 ^{0}C, estimated from the plots shown in Fig. 3. [b]Using $C(t) = a_1\exp(-t/\tau_1) + a_2\exp(-t/\tau_2)$ where τ_1 and τ_2 are in ns . [c]Average solvation time (ns), $\tau_{sol} = a_1\tau_1 + a_2\tau_2$, where, $a_1 + a_2 = 1$, ±5%. The numbers in the parenthesis indicate the weighted amplitude. [d]Calculated according to ref. 76.

Under an isoviscous condition (η = 130 cP), the extent of the missing or ultrafast component of the solvent reorganization dynamics is found similar in all

RTILs, i.e. no effect of the chain length is observable on this component (Table 6.4). However, of the two time-resolvable components of the solvation dynamics, the shorter component does not vary significantly with the RTILs, but the longer component depends on the chain length of the cation. In fact, the latter is slower by a factor of ~2 in $[Mor_{1,6}][Tf_2N]$ and $[Mor_{1,8}][Tf_2N]$ compared to $[Mor_{1,2}][Tf_2N]$ and $[Mor_{1,4}][Tf_2N]$. Consequently, despite of having an identical viscosity the average solvation time of C153 in long chain length containing RTILs is much higher than in short-chain containing solvents.

Table 6.4. Solvent Relaxation Parameters Estimated from the TRES of C153 under an Isoviscous Condition (η = 130 cP)

RTILs (T/ ^{0}C)[a]	η[b] (cP)	Relaxation Data[c]			Missing Comp.[e]
		τ_1 (a_1)	τ_2 (a_2)	$<\tau_{sol}>$[d]	
$Mor_{1,2}Tf_2N$ (32)	130	0.17 (0.64)	1.39 (0.36)	0.58	53%
$Mor_{1,4}Tf_2N$ (43)		0.15 (0.59)	1.12 (0.41)	0.55	51%
$Mor_{1,6}Tf_2N$ (45)		0.22 (0.55)	1.88 (0.45)	0.97	55%
$Mor_{1,8}Tf_2N$ (47)		0.25 (0.58)	2.04 (0.42)	1.00	49%

[a] Temperature at which the experiments were performed. [b]Experimentally measured viscosity values. [c]Using $C(t) = a_1\exp(-t/\tau_1) + a_2\exp(-t/\tau_2)$ where τ_1 and τ_2 are in ns. [d]Average solvation time (ns), $\tau_{av} = a_1\tau_1 + a_2\tau_2$, where, $a_1 + a_2 = 1$, ±5%. The numbers in the parenthesis indicate the weighted amplitude. [e]Calculated according to ref. 76.

Maroncelli and his coworkers[35] observed that $<\tau_{solv}>$ of a large number of ionic liquids is dependent on the size of the constituent cation (R_+) as $<\tau_{solv}> \propto (\eta/T)^p R_+^q$ (where p = 1, q = 4 and R_+ = radius of the cation). On examination of the dependence of the average solvation time on the size of the cation according

to the given equation, we found that the plot of $<\tau_{solv}>$ versus $(\eta/T)^1R_+^4$ gives nice correlation (R^2 = 0.958) compared to the $<\tau_{solv}>$ versus (η/T) plot (R^2 = 0.825) under isothermal condition. However, a plot of $<\tau_{solv}>$ versus $(\eta/T)^1R_+^4$ with the isoviscous condition results, gives a rather poor correlation (R^2 = 0.724). Thus, it is evident that the solvation time of a probe molecule is governed not only by the bulk viscosity and size of the large ion when the organized structure of the medium comes into the picture.

6.4. Conclusion

Some of the physicochemical characteristics of four morpholinium RTILs with different alkyl chain length attached to the cation have been probed by studying the fluorescence behavior of C153 as a function of the excitation wavelength and temperature. The excitation wavelength and temperature dependent studies seem to suggest that these N-alkyl-N-methylmorpholinium RTILs are more structured and heterogeneous than the imidazolium ILs. Time-resolved fluorescence anisotropy measurements reveal that C153 is located in an environment, whose viscosity is different from the bulk viscosity of the ionic liquid. While the solvation reorganization dynamics under the isothermal condition is found to be similar to that in imidazolium RTILs, these measurements under an isoviscous condition suggest that the slow component of the dynamics is not necessarily dictated by the viscosity of the medium alone. Overall, a more organized domain structure of these N-alkyl-N-methylmorpholinium RTILs, particularly for the long chain containing ones, is indicated in this study.

References and Notes

(1) Hallett, J. P.; Welton, T. *Chem. Rev.* **2011**, *111*, 3508.
(2) Dupont, J. *Acc. Chem. Res.* **2011**, *44*, 1223.
(3) Plechkova, N. V.; Seddon, K. R. *Chem. Soc. Rev.* **2008**, *37*, 123.
(4) Ionic Liquids (Special issue on ionic liquids) *Acc. Chem. Res.* **2007**, *40*, 1077.
(5) The Physical Chemistry of Ionic Liquids (special issue on ionic liquids). *J. Phys. Chem. B* **2007**, *111*, 4639.
(6) Physical Chemistry of Ionic Liquids (Special issue on ionic liquids). *Phys. Chem. Chem. Phys.* **2010**, *12*, 1629.
(7) Hough, W. L.; Rogers, R. D. *Bull.Chem. Soc. Japan* **2007**, *80*, 2262.
(8) Kobrak, M. N. The Chemical Environment of Ionic Liquids: Links between Liquid Structure, Dynamics, and Solvation *Advances in Chemical Physics*; Rice, S. A., Ed.; John Wiley & Sons, Inc., 2008; Vol. 139; pp 83.
(9) Weingärtner, H. *Angew. Chem. Int. Ed.* **2008**, *47*, 654.
(10) Castner, E. W. Jr.; Wishart, J. F. *J. Chem. Phys.* **2010**, *132*, 120901.
(11) Samanta, A. *J. Phys. Chem. B* **2006**, *110*, 13704.
(12) Samanta, A. *J. Phys. Chem. Lett.* **2010**, *1*, 1557.
(13) Kim, K. S.; Choi, S.; Demberelnyamba, D.; Lee, H.; Oh, J.; Lee, B. B.; Mun, S. J. *Chem. Comm.* **2004**, 828.
(14) Galinski, M.; Stepniak, I. *J. Appl. Electrochem.* **2009**, *39*, 1949.
(15) Lava, K.; Binnemans, K.; Cardinaels, T. *J. Phys. Chem. B* **2009**, *113*, 9506.
(16) Brigouleix, C.; Anouti, M.; Jacquemin, J.; Caillon-Caravanier, M.; Galiano, H.; Lemordant, D. *J. Phys. Chem. B* **2010**, *114*, 1757.
(17) Yu, W.; Peng, H.; Zhang, H.; Zhou, X. *Chinese J. Chem.* **2009**, *27*, 1471.
(18) Samanta, A.; Fessenden, R. W. *J. Phys. Chem. A* **2000**, *104*, 8577.
(19) Chapman, C. F.; Maroncelli, M. *J. Phys. Chem.* **1991**, *95*, 9095.
(20) Karmakar, R.; Samanta, A. *J. Phys. Chem. A* **2002**, *106*, 4447.

(21) Lakowicz, J. R. *Principles of Fluorescence Spectroscopy*, Third Edition ed.; Springer Science, New York, 2006.

(22) Fleming, G. R. *Chemical Applications of Ultrafast Spectroscopy*; Oxford University Press, 1986.

(23) Bagchi, B.; Oxtoby, D. W.; Fleming, G. R. *Chem. Phys.* **1984**, *86*, 257.

(24) Maroncelli, M.; Fleming, G. R. *J. Chem. Phys.* **1987**, *86*, 6221.

(25) Karmakar, R.; Samanta, A. *J. Phys. Chem. A* **2002**, *106*, 6670.

(26) Karmakar, R.; Samanta, A. *J. Phys. Chem. A* **2003**, *107*, 7340.

(27) Chakrabarty, D.; Harza, P.; Chakraborty, A.; Seth, D.; Sarkar, N. *Chem. Phys. Lett.* **2003**, *381*, 697.

(28) Arzhantsev, S.; Ito, N.; Heitz, M.; Maroncelli, M. *Chem. Phys. Lett.* **2003**, *381*, 278.

(29) Ingram, J. A.; Moog, R. S.; Ito, N.; Biswas, R.; Maroncelli, M. *J. Phys. Chem. B* **2003**, *107*, 5926.

(30) Ito, N.; Arzhantsev, S.; Heitz, M.; Maroncelli, M. *J. Phys. Chem. B* **2004**, *108*, 5771.

(31) Ito, N.; Arzhantsev, S.; Maroncelli, M. *Chem. Phys. Lett.* **2004**, *396*, 83.

(32) Saha, S.; Mandal, P. K.; Samanta, A. *Phys. Chem. Chem. Phys.* **2004**, *6*, 3106.

(33) Mandal, P. K.; Samanta, A. *J. Phys. Chem. B* **2005**, *109*, 15172.

(34) Paul, A.; Samanta, A. *J. Phys. Chem. B* **2007**, *111*, 4724.

(35) Jin, H.; Baker, G. A.; Arzhantsev, S.; Dong, J.; Maroncelli, M. *J. Phys. Chem. B* **2007**, *111*, 7291.

(36) Chowdhury, P. K.; Halder, M.; Sanders, L.; Calhoun, T.; Anderson, J. L.; Armstrong, D. W.; Song, X.; Petrich, J. W. *J. Phys. Chem. B* **2004**, *108*, 10245.

(37) Mukherjee, P.; Crank, J. A.; Sharma, P. S.; Wijeratne, A. B.; Adhikary, R.; Bose, S.; Armstrong, D. W.; Petrich, J. W. *J. Phys. Chem. B* **2008**, *112*, 3390.

(38) Adhikari, A.; Sahu, K.; Dey, S.; Ghosh, S.; Mandal, U.; Bhattacharyya, K. *J. Phys. Chem. B* **2007**, *111*, 12809.

(39) Funston, A. M.; Fadeeva, T. A.; Wishart, J. F.; Castner, E. W. Jr. *J. Phys. Chem. B* **2007**, *111*, 4963.

(40) Khara, D. C.; Samanta, A. *Ind. J. Chem.* **2010**, *49A*, 714.
(41) Shim, Y.; Kim, H. J. *J. Phys. Chem. B* **2008**, *112*, 11028.
(42) Kobrak, M. N.; Znamenskiy, V. *Chem. Phys. Lett.* **2004**, *395*, 127.
(43) Halder, M.; Headley, L. S.; Mukherjee, P.; Song, X.; Petrich, J. W. *J. Phys. Chem. A* **2006**, *110*, 8623.
(44) Kashyap, H. K.; Biswas, R. *J. Phys. Chem. B* **2008**, *112*, 12431.
(45) Kashyap, H. K.; Biswas, R. *J. Phys. Chem. B* **2010**, *114*, 254.
(46) Kashyap, H. K.; Biswas, R. *Ind. J. Chem. Sec. A* **2010**, *49*, 685.
(47) Muramatsu, M.; Nagasawa, Y.; Miyasaka, H. *J. Phys. Chem. A* **2011**, *115*, 3886.
(48) Fukazawa, H.; Ishida, T.; Shirota, H. *J. Phys. Chem. B* **2011**, *115*, 4621.
(49) Maroncelli, M.; Zhang, X. X.; Liang, M.; Roy, D.; Ernsting, N. P. *Faraday Discussions* **2012**, *154*, 409.
(50) Khara, D. C.; Samanta, A. *Phys. Chem. Chem. Phys.* **2010**, *12*, 7671.
(51) Dutt, G. B. *J. Phys. Chem. B* **2010**, *114*, 8971.
(52) Dutt, G. B. *Ind. J. Chem. Sec. A* **2010**, *49*, 127.
(53) Karve, L.; Dutt, G. B. *J. Phys. Chem. B* **2011**, *115*, 725.
(54) Karve, L.; Dutt, G. B. *J. Phys. Chem. B* **2012**, *116*, 1824.
(55) Fruchey, K.; Fayer, M. D. *J. Phys. Chem. B* **2010**, *114*, 2840.
(56) Das, S. K.; Sarkar, M. *J. Phys. Chem. B* **2012**, *116*, 194.
(57) Lopes, J.; Padua, A. A. H. *J. Phys. Chem. B* **2006**, *110*, 3330.
(58) Wang, Y. T.; Voth, G. A. *J. Phys. Chem. B* **2006**, *110*, 18601.
(59) Xiao, D.; Rajian, J. R.; Li, S. F.; Bartsch, R. A.; Quitevis, E. L. *J. Phys. Chem. B* **2006**, *110*, 16174.
(60) Triolo, A.; Russina, O.; Bleif, H. J.; Di Cola, E. *J. Phys. Chem. B* **2007**, *111*, 4641.
(61) Iwata, K.; Okajima, H.; Saha, S.; Hamaguchi, H. *Acc. Chem. Res.* **2007**, *40*, 1174.
(62) Yamaguchi, T.; Miyake, S.; Koda, S. *J. Phys. Chem. B* **2010**, *114*, 8126.
(63) Annapureddy, H. V. R.; Kashyap, H. K.; Biase, P. M. D.; Margulis, C. J. *J. Phys. Chem. B* **2010**, *114*, 16838.

(64) Russina, O.; Triolo, A.; Gontrani, L.; Caminiti, R. *J. Phys. Chem. Lett.* **2012**, *3*, 27.

(65) Reichardt, C. *Solvents and Solvent Effects in Organic Chemistry*, Second ed.; VCH Verlagsgesellschaft, 1988.

(66) Reichardt, C. *Green chem.* **2005**, *7*, 339.

(67) Dobek, K. *J. Fluoresc* **2011**, *21*, 1547.

(68) Santhosh, K.; Banerjee, S.; Rangaraj, N.; Samanta, A. *J. Phys. Chem. B* **2010**, *114*, 1967.

(69) Demchenko, A. P. *Luminescence* **2002**, *17*, 19.

(70) Mandal, P. K.; Paul, A.; Samanta, A. *J. Photochem. Photobiol. A: Chem.* **2006**, *182*, 113.

(71) Mandal, P. K.; Sarkar, M.; Samanta, A. *J. Phys. Chem. A* **2004**, *108*, 9048.

(72) As the $<\tau_{sol}>$ values of C153 in morpholinium ILs (0.41 – 1.31 ns, Table 3) are estimated at 40 ^{0}C, whereas the excitation wavelength dependence (Fig. 4) is studied at 25 ^{0}C, it is necessary to make necessary correction of the solvation time from its temperature dependence before comparison. Using the viscosity dependence of $<\tau_{sol}>$ (Fig. 10) and known viscosity of these ILs at 25 ^{0}C, one can obtain the $<\tau_{sol}>$ values at 25 ^{0}C. These values range between 2.8–3.9 ns, which are still significantly lower than the long fluorescence lifetime (τ_f = 4.8–5.2 ns) of C153.

(73) Ghatak, C.; Rao, V. G.; Ghosh, S.; Mandal, S.; Sarkar, N. *J. Phys. Chem. B* **2011**, *115*, 12514.

(74) Horng, M.-L.; Gardecki, J. A.; Maroncelli, M. *J. Phys. Chem. A* **1997**, *101*, 1030.

(75) Guchhait, B.; Gazi, H. A. R.; Kashyap, H. K.; Biswas, R. *J. Phys. Chem. B* **2010**, *114*, 5066.

(76) Fee, R. S.; Maroncelli, M. *Chem. Phys.* **1994**, *183*, 235.

Chapter 7

Rotational Dynamics of Dipolar and Nonpolar solutes in N-alkyl-N-methylmorpholinium Ionic Liquids

Rotational dynamics of dipolar solutes, AP, and PRODAN and nonpolar solute, anthracene have been studied by using time-resolved fluorescence anisotropy techniques in a series of N-alkyl-N-methylmorpholinium RTILs to explore the microscopic physicochemical properties of these RTILs. The experimental results obtained in this study are also analyzed in terms of commonly used Stokes-Einstein-Debye (SED) hydrodynamic model. The analysis of rotational time constant according to SED model reveals that AP, PRODAN and anthracene rotate in three different regimes; stick, between stick and slip, and slip to sub slip boundary conditions, respectively. These observations have been attributed to the heterogeneous structure of these RTILs.

7.1. Introduction

Understanding of the physicochemical properties of the RTILs is essential for better utilization of these substances in different applications.[1-7] The N-alkyl-N-methylmorpholinium ionic liquids, which are found to be more cost effective compared to the commonly used imidazolium and pyrrolidium salts, have come into prominence, though their physicochemical properties are yet to be explored carefully.[8-12] The results of our previous study (Chapter 6) reveals that these

morpholinium RTILs are more heterogeneous than the other existing RTILs which are so far being explored. In this chapter, we have studied the rotational dynamics of dipolar and nonpolar solutes to obtain a better understanding of the physicochemical properties of these morpholinium ionic liquids.

As rotational motion of a solute provides useful information on its microenvironment in an unknown medium, the dynamics of rotational diffusion of several fluorescent molecules have been studied by measuring the extent of fluorescence depolarization as a function of time to investigate the structures of various RTILs, which are found to be heterogeneous at the microscopic level,[13-38] and also to study the influence of the various constituents of the RTILs on the rotational dynamics of the probe molecules.[22,39-52] These studies have provided considerable insight into the nature of interaction between the solute and the ionic constituents of various RTILs thus shedding light on the microenvironments of these promising, but complex media. We have recently explored a series of N-alkyl-N-methylmorpholinium ionic liquids comprising different alkyl chain length by studying the steady-state and time-resolved fluorescence behavior of C153 in these media.[12] A comparison of the fluorescence response of C153 in these and imidazolium ionic liquids seems to suggest that the morpholinium ionic liquids are more structured than the imidazolium ones. Considering that it is possible to obtain considerable insight into the structural organization of the RTILs by studying the rotational dynamics of molecular systems, we probe the organized environments of a series of relatively less explored but promising morpholinium ionic liquids by monitoring the rotational diffusion of two dipolar and one

nonpolar probe molecules using time-resolved fluorescence anisotropy measurements.

In this context, we note that there are only a limited number of studies, where the effect of the chain length of one of the constituents of the RTILs on the rotational dynamics is studied.[22,41,42,46,48] Maroncelli and co-workers[48] studied the rotational dynamics of C153 in several ammonium ionic liquids comprising different chain length of the cation. Other than the expected influence of viscosity of the RTILs no other factor was found to influence the rotational dynamics of the solute. Fruchey and Fayer[22] studied the rotational dynamics of negatively charged (sodium 8-methoxypyrene-1,3,6-sulfonate, MPTS), and neutral (perylene) molecules in a series of N-alkyl-N-methylimidazolium ionic liquids. They observed superstick behavior of the charged molecule, MPTS, due to its strong hydrogen bonding interaction with the imidazolium cation of the ionic liquids and slip to sub slip behavior of the neutral molecule, perylene. The rotational dynamics of perylene in the octyl chain containing ionic liquid is found to be similar to that in paraffine oil. Dutt[46] also studied the rotational dynamics of a charged probe (R110) and a neutral probe (DMDPP) in different N-alkyl-N-methylimidazolium ionic liquids. While he found that rotational time constants of R110 shift towards the stick boundary condition with increase in alkyl chain length of the ionic liquids due to specific hydrogen bonding interaction between the solute and RTILs, no influence of the alkyl chain length of cation was found on the rotational dynamics of DMDPP. Recently, Das and Sarkar[42] have also studied the rotational dynamics of two neutral solutes (AP and C153) in imidazolium ionic liquids comprising anions with different alkyl chain length.

They found AP rotation to follow the stick boundary condition due to its specific interaction with the RTILs, whereas C153 rotation changes from slip to sub slip behavior with increase in the alkyl chain length of the anion. The latter was explained on the basis of increase in size of the RTIL with respect to the solute. Very recently, Gangamallaiah and Dutt[41] have studied the rotational dynamics of neutral (9-phenylanthracene, 9-PA) and charged (both cationic, R110 and anionic, fluorescein, FL) molecules in several 1-alkyl-3-methylimidazolium ionic liquids to study the effect of the alkyl chain length on the rotational dynamics of the solute. However, they did not observe any effect of the alkyl chain length on the solutes rotation; the neutral probe was found to follow the slip boundary condition and the ionic probes followed close to stick boundary condition according to the SED model.

In this work, we have chosen three specific neutral solutes (two dipolar molecules, namely, AP, PRODAN and one nonpolar molecule, anthracene, (Chart 7.1) to explore the physicochemical properties of these less explored, but promising morpholinium ionic liquids by studying the rotational dynamics. AP was selected due its specific hydrogen bonding ability to enter into the hydrogen bonding interaction with hydrogen bond donors/accepters.[42,51] PRODAN and anthracene, which have comparable volume, are chosen due to their preference to different environments of an organized assembly consisting of polar and nonpolar domains.[53,54] While most of the measurements have been performed by exciting the molecules at wavelength corresponding to the peak of the first absorption maximum, the experiments on dipolar probes have also been carried out by exciting them at a wavelength, which corresponds to the red-edge of the first

absorption band with a view to probing the heterogeneity of the media from another direction.

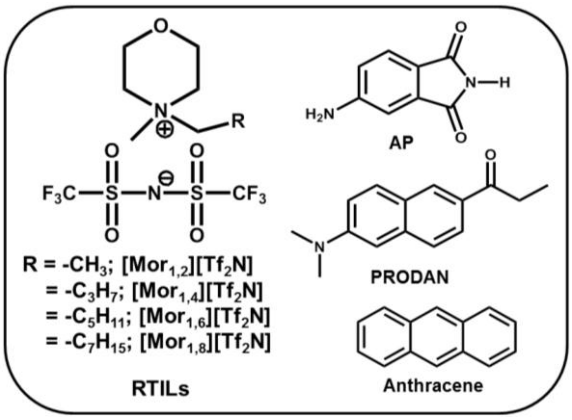

Chart 7.1. Chemical formula and abbreviations of the RTILs and probe molecules

7.2. Results and Discussion

The time-resolved fluorescence anisotropy measurements have been performed over a temperature range of 25 – 65 ^{0}C except in the case of $[Mor_{1,2}][Tf_2N]$ for which the study was carried out in the temperature range of 35 – 65 ^{0}C. In addition, the measurements on the two dipolar probes AP and PRODAN, are carried out using two different excitation wavelengths (375 and 439 nm). The rotational relaxation times are estimated from the single or bi-exponential fit to the anisotropy decay profiles (depending on the quality of the fit judged by the χ^2 values and plot of residuals). In the latter case, the average value of the two time constants, was used as the two rotational time of the probe molecule. It is to be noted that except in $[Mor_{1,2}][Tf_2N]$, the rotational time constants were obtained from the bi-exponential to the anisotropy decay profiles.

AP. The rotational relaxation times of AP in four ionic liquids at various temperatures for two different excitation wavelengths are presented in Table 7.1. The results show that at any given temperature, the rotational relaxation time increases with increase in the alkyl chain length of the cation and decreases with increase in temperature. This trend is understandable considering that the viscosity of the RTILs increases with increase in the alkyl chain length of the cation and decreases with increase in temperature.

The rotational times measured by exciting the sample at the red edge of the first absorption band (439 nm) show a similar trend. It is interesting to note, however, the difference in the rotational time constants for two different excitations, which though is negligible in $[Mor_{1,2}][Tf_2N]$, clearly noticeable in the

longest chain length containing RTIL, $[Mor_{1,8}][Tf_2N]$, particularly near the room temperature (Figure 7.1).

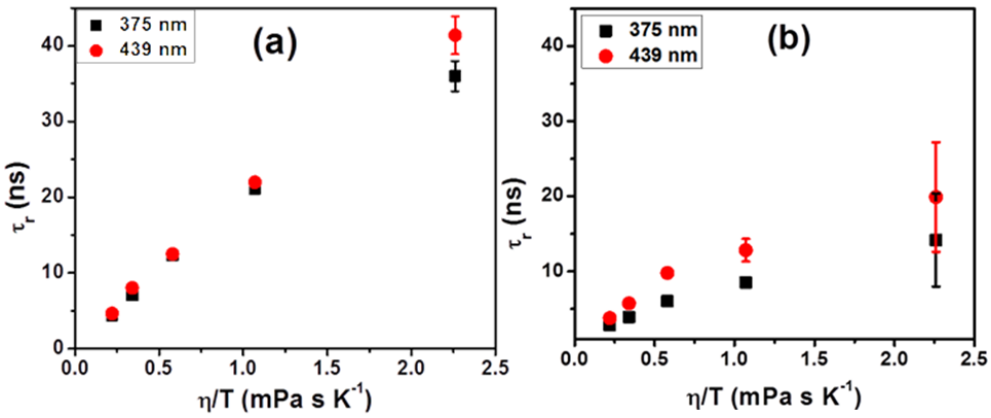

Figure 7.1. Excitation wavelength dependence of τ_r with η/T for AP (a) and PRODAN (b) in $[Mor_{1,8}][Tf_2N]$.

PRODAN. The measured rotational time constants of PRODAN in four different ionic liquids at various temperatures for two different excitation wavelengths are collected in Table 7.1. The effect of temperature and alkyl chain length on the rotational time constants of PRODAN is very similar to that observed for AP, i.e. the rotational time increases with increase in the chain lengths of the alkyl group and decreases with increase in temperature of the medium. However, unlike AP, PRODAN does not show appreciable variation of the rotational time with change of the alkyl chain length of the cation.

For PRODAN, excitation at 439 nm also gives a higher rotation time constant compared to 375 nm excitation. While the overall trend of variation of

the rotational time with alkyl chain length of the cation and temperature is found similar to that observed for AP, the variation of the rotational time of PRODAN with excitation wavelength is found more pronounced than in the other case (Figure 7.1).

Table 7.1. Rotational relaxation times[a] of the probes in four morpholium RTILs as a function of temperature and excitation wavelength

ILs	Tempr. (K)	Viscosity (cP)	Rotational relaxation time in ns				
			AP		PRODAN		Anthracene
			λ_{ex} = 375 nm	λ_{ex} = 439 nm	λ_{ex} = 375 nm	λ_{ex} = 439 nm	λ_{ex} = 375 nm
$[Mor_{1,2}][Tf_2N]$	308	147	6.35	7.02	5.62	6.10	1.54
	318	85	3.76	4.25	4.20	4.26	0.90
	328	52	2.33	2.73	2.78	2.88	0.55
	338	34	1.52	1.71	1.94	2.05	0.36
$[Mor_{1,4}][Tf_2N]$	298	503	24.49	28.53	8.77	8.96	4.25
	308	236	12.11	12.80	8.17	8.87	2.27
	318	126	6.44	7.92	5.83	6.27	1.44
	328	72	3.73	4.45	3.81	4.17	0.98
	338	45	2.29	2.41	2.35	2.62	0.74
$[Mor_{1,6}][Tf_2N]$	298	578	32.07	36.30	8.70	9.26	3.31
	308	269	16.50	20.94	7.35	8.05	2.40
	318	142	9.50	10.46	6.21	6.91	1.59
	328	80	5.35	6.00	3.70	4.26	1.11
	338	48	3.26	3.77	2.49	2.84	0.78
$[Mor_{1,8}][Tf_2N]$	298	673	36.0	41.40	14.18	19.90	3.25
	308	327	21.10	21.98	8.56	12.83	2.03
	318	183	12.31	12.50	6.06	9.80	1.36
	328	113	7.03	8.03	3.94	5.74	0.86
	338	76	4.37	4.64	2.84	3.80	0.62

[a]± 5-35%, τ_f of AP, PRODAN and anthracene in ILs are measured to be around 18, 4 and 3.5 ns respectively.

Anthracene. Rotational dynamics of the nonpolar solute, anthracene, in these RTILs is found to be quite interesting and very different from those of the dipolar probes, AP and PRODAN. Instead of an increase in rotational time constant, a decrease is observed with increase in viscosity of the ionic liquids as the length of the alkyl chain attached to the cation is increased (Table 7.1). The effect of temperature on the rotational dynamics is, however, found to be similar to that observed for the two dipolar solutes.

In order to understand the rotational dynamics of the solutes we have analyzed our experimental results in terms of Stokes-Einstein-Debye (SED) hydrodynamic theory, which is the most commonly used model of rotational diffusion. According to this theory, the reorientation time (τ_r^{SED}) of a non-interacting solute in a solvent continuum of viscosity η is given by

$$\tau_r^{SED} = \frac{V_h \eta}{k_B T} \qquad (7.1)$$

Where, V_h is the hydrodynamic volume of the solute, which is a product of the van der Waals volume (V) of the molecule, its shape factor (*f*) and boundary condition parameter (C), k_B is the Boltzmann constant and T is the absolute temperature of the system. The shape factor (*f*), introduced by Perrin to take into account the nonspherical shape of a solute, is a function of the axial ratio of the semi axes and is greater than 1. For a spherical solute, *f = 1*. The boundary condition parameter, C is unity when the size of the rotating solute is much bigger than the solvent molecule. This represents the stick boundary condition. However, in the case of solute having a size smaller or comparable to the solvent molecule,

C is given by 0 <*C*< 1. It is to be noted that τ_r^{SED}, given by equation (7.1), is a measure of the mechanical or hydrodynamic friction experienced by the solute molecule. The axial lengths, van der Waals volumes and the shape factors for the probe molecules used in this study are taken from literature[49] and the boundary conditions are calculated according to reported procedure.[40,44] These values are collected in the Table 7.2.

The analysis of the experimental results in terms of Stokes-Einstein-Debye (SED) hydrodynamic model reveals that AP changes from the stick to superstick behavior with increase in alkyl chain length of the RTILs, which is highlighted in Figure 7.2. The rotational dynamics of AP on excitation at longer wavelength also follows a similar change from the stick to superstick behavior (Figure 7.2b).

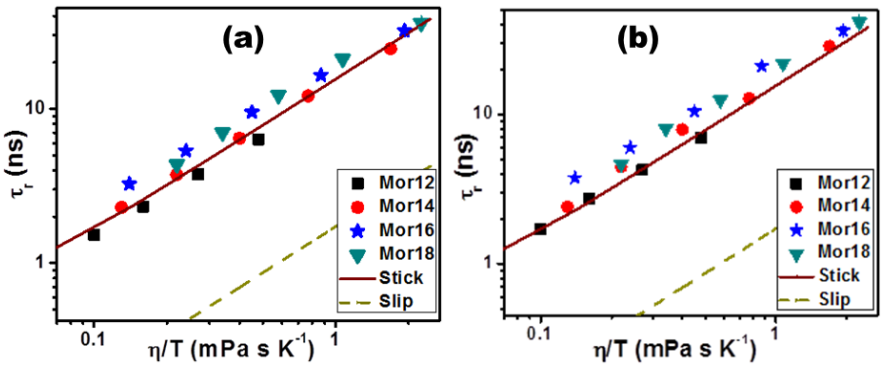

Figure 7.2. Plot of τ_r of AP versus η/T of different ionic liquids. The lines represent the stick (solid) and slip (dash) boundary conditions, computed according to the SED hydrodynamic model (λ_{ex} = 375 and 439 nm for a and b, respectively).

Table 7.2. Dimension,[a] van der Waals volume,[a] shape factor (f),[a] and boundary condition parameter (C_{slip}) of the probe molecules calculated from the SED hydrodynamic theory

Probe	Axial radii /Å^3	Volume/Å^3	*f*	C_{slip}
AP	5 x 3.5 x 1.8	134	1.6	0.11
PRODAN	7.7 x 3.9 x 1.8	227	2.4	0.19
Anthracene	5.9 x 3.9 x 1.8	175	1.3	0.29

[a]values are taken from ref. 49

Figure 7.3 shows that the rotational relaxation times of PRODAN lie between the slip and stick boundary conditions. One also observes a gradual shift towards the slip to sub slip boundary condition at low temperature with increase in alkyl chain length of the cation. At higher temperature, however, the rotational time constants vary linearly with *η/T* irrespective of the alkyl chain length of the cation. The excitation wavelength dependent rotational constants also show a similar behavior (Figure 7.3b).

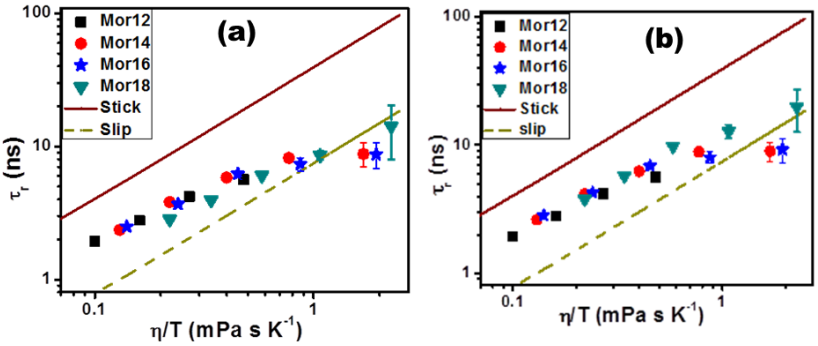

Figure 7.3. Plot of τ_r of PRODAN versus *η/T* of different ionic liquids. The lines represent the stick (solid) and slip (dash) boundary conditions, computed according to the SED hydrodynamic model (λ_{ex} = 375 and 439 nm for a and b, respectively).

The rotational time constants of anthracene do not lie between the slip and stick boundary conditions of the SED hydrodynamic model (Figure 7.4). The rotational relaxation time shifts from the slip to sub slip regime with increase in the chain length of alkyl group of the cation. Another interesting point to note is that at higher temperatures the rotational time constants lie on the slip boundary line in all ionic liquids except in $[Mor_{1,8}][Tf_2N]$, where the values are far apart from the slip boundary line.

In case of deviation of the rotational relaxation dynamics from the slip boundary condition of the SED model, quasi-hydrodynamic models like Gierer-Wirtz (GW) and Dote-Kivelson-Schwartz (DKS) are used to explain the experimental results.[55-58] In the present case, we attempt to analyze our results in terms of the GW theory,[59] which assumes the solvent to be made of concentric shells of spherical particles surrounding the spherical solute. The boundary condition parameter (C_{GW}) is calculated by considering how the angular velocity of the solvent molecules in successive shells surrounding the solute decreases as a function of the distance away from it. The expression for C_{GW} is given by[41]

$$C_{GW} = \sigma C_0 \qquad (7.2)$$

where, σ is the sticking factor, given by[49]

$$\sigma = [1 + 6(\frac{V_s}{V_p})^{1/3} C_0]^{-1} \qquad (7.3)$$

and C_0 is given by

$$C_0 = \left\{ \frac{6\left(\frac{V_s}{V_p}\right)^{1/3}}{\left[1+2\left(\frac{V_s}{V_p}\right)^{\frac{1}{3}}\right]^4} + \frac{1}{\left[1+4\left(\frac{V_s}{V_p}\right)^{\frac{1}{3}}\right]^3} \right\}^{-1} \qquad (7.4)$$

In these equations, V_s and V_p are the van der Walls volume of the solvent and solute, respectively. In the present case, a volume of 421 $Å^3$ (obtained from Edwards volume increment method[60]) was used as V_s for $[Mor_{1,8}][Tf_2N]$. The computed rotational time constant according to the GW model shows that the experimental rotational time constant for anthracene follows neither slip nor GW boundary condition, but it lies between the two (Figure 7.4).

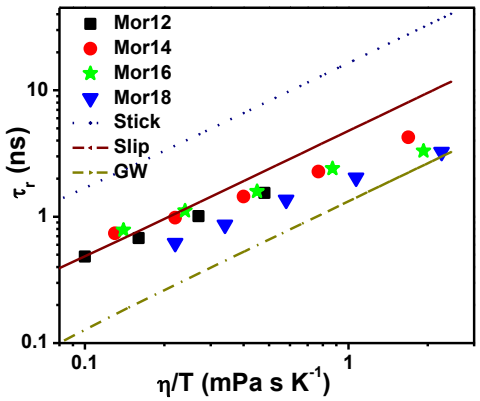

Figure 7.4. Plot of τ_r of anthracene versus *η/T* of different ionic liquids. The computed lines represent the stick (dot) and slip (solid) boundary conditions, according to SED hydrodynamic model. The third line (dash dot) represents the quashihydrodynamic Gierer-Wirtz model (λ_{ex} = 375 nm).

The above analysis reveals that the rotational dynamics of three neutral solutes are quite different in any given RTIL. This difference in the rotational

relaxation behavior of the solutes can be due to the difference in the nature of interaction between the solute and solvent. However, a detailed analysis of the results, as described below, suggests otherwise.

Both the stick and superstick rotational dynamics of AP in conventional solvents and ionic liquids are known, when AP is hydrogen bonded with the solvent molecule.[42,51,61] In the present case, hydrogen bonding interaction of the N-H proton of AP with the F atom of $[Tf_2N]^-$ and/or O atom of the morpholinium cation can contribute to the stick and superstick behavior of the rotational diffusion of AP. Figure 7.5., which depicts the variation of the coupling constants (C_{rot}) with the van der Waals volumes of RTILs, shows that the increase (49 %) of the C_{rot} is not very different from the increase (32 %) in van der Waals volume of ionic liquids for a change of the alkyl group from ethyl to octyl of cation, thus supporting strong hydrogen bonding interaction between AP and the RTILs. In this context, it is to be noted that a similar recent study in imidazolium ionic liquids shows no regular variation of C_{rot} with increase in the chain length attached to the cation despite specific hydrogen bonding interaction between the solutes and RTILs.[41] Our observation of a steady variation of the coupling constant with alkyl chain length of cation is, however, similar to that reported by others.[22,46] The linearity of the τ_r values with η/T in different RTILs that can be judged from the p values by fitting the data to $\tau_r = A(\eta/T)^p$, indicates strong hydrogen bonding between AP and RTILs still persists even at higher temperatures.

$[Mor_{1,2}][Tf_2N]$: $\tau_r = (12.41 \pm 0.05)\left(\frac{\eta}{T}\right)^{0.91\pm0.001}$ (N=4, R=1)

$[Mor_{1,4}][Tf_2N]$: $\tau_r = (15.17 \pm 0.07)\left(\frac{\eta}{T}\right)^{0.92\pm0.01}$ (N=5, R=0.9998)

$[Mor_{1,6}][Tf_2N]$: $\tau_r = (18.41 \pm 0.11)\left(\frac{\eta}{T}\right)^{0.85\pm0.01}$ (N=5, R=0.9998)

$[Mor_{1,8}][Tf_2N]$: $\tau_r = (18.73 \pm 0.61)\left(\frac{\eta}{T}\right)^{0.82\pm0.05}$ (N=5, R=0.9944)

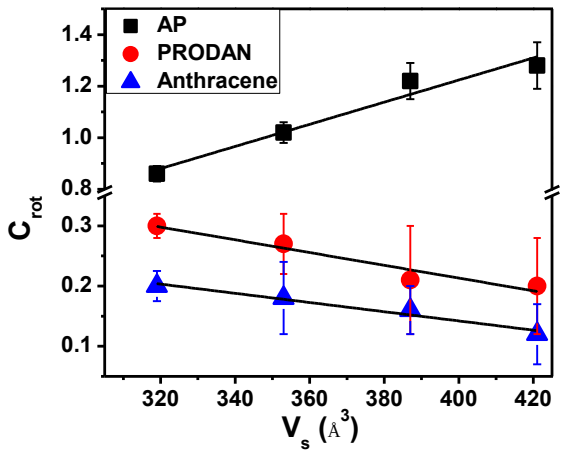

Figure 7.5. Plot of rotational coupling constant ($C_{rot,}$ 308 K) versus van der Waals volume (V_s) of the RTILs, (λ_{ex} = 375 nm). The solid lines represent linear fit to the data points.

In case of PRODAN, even though the time constants lie between the slip and stick boundary conditions, the rotational time constants gradually shift

towards the slip and sub-slip boundary condition at low temperatures with increase in the alkyl chain length of the cation. However, at higher temperature, the effect of the alkyl chain length on rotational dynamics is not observable. The plot in Figure 7.5 shows a steady decrease in the coupling constant with increase in van der Waals volumes of the RTILs. This behavior clearly indicates that the nature of interaction of PRODAN with the RTILs changes with change in the alkyl chain length of the cation. This is possible only if there is a phase separation of the RTIL into hydrophilic and hydrophobic domains with increase in alkyl chain length and the probe molecule relocates itself in the hydrophobic domain.[12] In addition to the decrease of the coupling constants with increase in the alkyl chain length of cation, a deviation from the linearity of the τ_r values with η/T is evident from the degree of nonlinearity (the value of the p parameter) of $\tau_r = A(\eta/T)^p$.

$[Mor_{1,2}][Tf_2N]$: $\tau_r = (9.2 \pm 0.6)\left(\frac{\eta}{T}\right)^{0.64\pm0.05}$ (N=4, R=0.9888)

$[Mor_{1,4}][Tf_2N]$: $\tau_r = (7.58 \pm 0.6)\left(\frac{\eta}{T}\right)^{0.41\pm0.1}$ (N=5, R=0.8829)

$[Mor_{1,6}][Tf_2N]$: $\tau_r = (7.13 \pm 0.5)\left(\frac{\eta}{T}\right)^{0.40\pm0.07}$ (N=5, R=0.9078)

$[Mor_{1,8}][Tf_2N]$: $\tau_r = (8.26 \pm 0.11)\left(\frac{\eta}{T}\right)^{0.66\pm0.02}$ (N=5, R=0.9982)

In the present case, the degree of nonlinearity is quite large and the 'p' values lie between 0.40 and 0.66. Generally the fitting parameter 'p' for a large number of molecules studied both in RTILs and conventional solvents is close to unity,[39,40,43-46,55] except in higher n-alkanes where it is around 0.63.[55] The τ_r vs η/T plots and the degree of nonlinearity in long chain containing RTILs are quite similar to the rotational dynamics of a solute in higher n-alkanes.[55] This suggests that PRODAN is mostly surrounded by the alkyl groups of the RTILs. It should be noted in this context that at temperature around $1.2T_g$, the conventional solvents become heterogeneous and a poor 'p' value ($0.25 \leq p \leq 0.75$) was observed.[62-65] The poor degree of linearity near room temperature, which is an indication of the departure from the SED hydrodynamic model, is similar to that observed previously for C153 in these RTILs.[12] The only difference is that the degree of nonlinearity is much more prominent for PRODAN compared to C153. Therefore, the present results substantiate the domain structure of these RTILs. PRODAN seems to locate itself mainly at the hydrophobic domain in long chain length containing RTILs. The association of PRODAN with the alkyl moieties creates void space through which the molecule can rotate with little hindrance, leading to a faster rotational relaxation near room temperature. A similar rotational dynamics of PRODAN in RTILs comprising different chain lengths at higher temperatures (Figure 7.3) indicates that the domain structure of the RTILs is perturbed/lost under this condition.

In case of anthracene, as the experimental rotational time constants lie between the computed slip line of the SED model and the GW boundary line, the results cannot be explained by either SED or GW model. Moreover, the coupling constants are found decrease steadily with increase in the van der Waals volumes of the RTILs (Figure 7.5), on observation similar to that made in the case of PRODAN as well. A steady decrease of the C_{rot} values suggests that the nature of interaction between anthracene and RTILs varies with the alkyl chain length of the cation. This can only be explained considering separation of the medium into hydrophobic and hydrophilic domains with anthracene positioning itself in the hydrophobic domain of the RTILs, where it experiences less friction due to not so tight packing by the alkyl chain of the cation. A similar picture emerges when one inspects the 'p' values of $\tau_r = A(\eta/T)^p$.

[$Mor_{1,2}$][Tf_2N]: $\tau_r = (2.66 \pm 0.02)\left(\frac{\eta}{T}\right)^{0.74\pm0.005}$ (N=4, R=0.9999)

[$Mor_{1,4}$[Tf_2N]: $\tau_r = (2.62 \pm 0.05)\left(\frac{\eta}{T}\right)^{0.72\pm0.03}$ (N=5, R=0.9969)

[$Mor_{1,6}$][Tf_2N]: $\tau_r = (2.40 \pm 0.46)\left(\frac{\eta}{T}\right)^{0.52\pm0.03}$ (N=5, R=0.9899)

[$Mor_{1,8}$][Tf_2N]: $\tau_r = (1.89 \pm 0.030)\left(\frac{\eta}{T}\right)^{0.67\pm0.02}$ (N=5, R=0.9972)

The low 'p' values in hexyl and octyl chains containing ionic liquids also indicate that anthracene, like PRODAN, resides in the nonpolar domain formed by these long alkyl groups.

The excitation wavelength dependent measurements on AP and PRODAN also indicate the microheterogeneous nature of these RTILs. It can be seen from Table 7.1, the rotational relaxation time in $[Mor_{1,8}][Tf_2N]$ is higher by 15% for AP and 40% for PRODAN for long wavelength excitation (439 nm) near room temperature (25 ^{0}C). Figure 7.1 shows that the excitation wavelength dependence of the rotational time constants of AP in $[Mor_{1,8}][Tf_2N]$ is clearly observable near the room temperature, whereas in the case of PRODAN, it is observable even at higher temperatures. These results can be understood as follows. A longer wavelength (439 nm) excitation, leads to preferential excitation of more (better) solvated molecules from the more polar region of the medium. These highly solvated molecules clearly experience more friction, thus exhibiting a longer rotational time compared to those located in the nonpolar domain that are preferentially excited at shorter wavelength (375 nm) excitation. A more prominent excitation wavelength dependence of PRODAN, which is observable over a longer temperature range, is indicative of a wider distribution of this molecule in different regions of the RTILs (compared to the other system) and persistence of the domain structure even at higher temperature.

A comparison of the present findings with those on rotational diffusion in imidazolium ionic liquids comprising alkyl chains of different lengths is quite pertinent here. While in one work, a similar coupling constant and linear dependence of the rotational time τ_r values on η/T with increase in alkyl chain length of the imidazolium ion indicate that the chain length hardly influences the physical properties of these RTILs, or the changed properties hardly affects the solute rotation,[41] in another study, a change in physicochemical properties of

these liquids with alkyl chain length of the cation was evident from the variation of the coupling constant values.[22,42] In our work, we could observe a steady change of the coupling constants and a high degree of nonlinearity of the τ_r values on η/T with increase in the alkyl chain length of the Nalkyl-N-methylmorpholinium cation, which not only indicate the changed physicochemical properties of these RTILs with variation of the alkyl group, but also establish the heterogeneous nature of these liquids that is more clearly evident in higher alkyl chain containing liquids.

7.3. Concluding Remark

Rotational dynamics of dipolar and nonpolar solutes in a series of N-alkyl-N-methylmorpholinium ionic liquids reveals their location in distinct environments of these media, depending on the nature of the solute. The stick to superstick behavior of AP, which is attributed to its H-bonding interaction with the constituent ions of the ionic liquids, reflects the most polar environment of the media. The slip to sub slip behavior of the nonpolar solute, anthracene, depicts the most nonpolar region of the ionic liquids formed largely by the alkyl group of the cation. On the other hand, the dipolar solute, PRODAN, which exhibits rotational time constant in between the slip and stick behavior, seems to distribute itself in both the regions. Excitation wavelength dependence of the rotational times of the dipolar probes also supports the heterogeneous environment of these RTILs. Overall, the present results provide further insight into the microheterogeneous structure of these ionic liquids, formed by the segregation of the alkyl chains on one hand and the charged components on the other. Apart from that these study

also reveals that the selection of the solute is an important factor for proper understanding the physicochemical properties of the complex medium such as ionic liquids.

References

(1) Samanta, A. *J. Phys. Chem. Lett.* **2010**, *1*, 1557.

(2) Kobrak, M. N. The Chemical Environment of Ionic Liquids: Links Between Liquid Structure, Dynamics, and Solvation In *Advances in Chemical Physics*; Rice, S. A., Ed.; John Wiley & Sons, Inc., 2008; Vol. 139; pp 83.

(3) Huang, M. M.; Weingärtner, H. *Chem Phys Chem* **2008**, *9*, 2172

(4) Castner, E. W.Jr.; Wishart, J. F. *J. Chem. Phys.* **2010**, *132*, 120901.

(5) Samanta, A. *J. Phys. Chem. B* **2006**, *110*, 13704.

(6) Daschakraborty, S.; Biswas, R. *J. Chem. Phys.* **2012**, *137*, 114501.

(7) Mandal, P. K.; Saha, S.; Karmakar, R.; Samanta, A. *Current Science* **2006**, *90*, 301.

(8) Kim, K. S.; Choi, S.; Demberelnyamba, D.; Lee, H.; Oh, J.; Lee, B. B.; Mun, S. J. *Chem. Comm.* **2004**, 828

(9) Lava, K.; Binnemans, K.; Cardinaels, T. *J. Phys. Chem. B* **2009**, *113*, 9506.

(10) Brigouleix, C.; Anouti, M.; Jacquemin, J.; Caillon-Caravanier, M.; Galiano, H.; Lemordant, D. *J. Phys. Chem. B* **2010**, *114*, 1757.

(11) Yu, W.; Peng, H.; Zhang, H.; Zhou, X. *Chinese J. Chem.* **2009**, *27*, 1471.

(12) Khara, D. C.; Samanta, A. *J. Phys. Chem. B* **2012**, *116*, 13430.

(13) Russina, O.; Triolo, A.; Gontrani, L.; Caminiti, R. *J. Phys. Chem. Lett.* **2012**, *3*, 27.

(14) Patra, S.; Samanta, A. *J. Phys. Chem. B* **2012**, *116*, 12275.

(15) Kashyap, H. K.; Hettige, J. J.; Annapureddy, H. V. R.; Margulis, C. J. *Chem. Commun.* **2012**, *48*, 5103.

(16) Aoun, B.; Goldbach, A.; González, M. A.; Kohara, S.; Price, D. L.; Saboungi, M. L. *J. Chem. Phys.* **2011**, *134*, 104509.

(17) Yamaguchi, T.; Miyake, S.; Koda, S. *J. Phys. Chem. B* **2010**, *114*, 8126.

(18) Urahata, S. M.; Ribeiro, M. C. C. *J. Phys. Chem. Lett.* **2010**, *1*, 1738.

(19) Shimomura, T.; Fujii, K.; Takamuku, T. *Phys. Chem. Chem. Phys.* **2010**, *12*, 12316.

(20) Russina, O.; Gontrani, L.; Fazio, B.; Lombardo, D.; Triolo, A.; Caminiti, R. *Chem. Phys. Lett.* **2010**, *493*, 259.

(21) Hardacre, C.; Holbrey, J. D.; Mullan, C. L.; Youngs, T. G. A.; Bowron, D. T. *J. Chem. Phys.* **2010**, *133*, 074510.

(22) Fruchey, K.; Fayer, M. D. *J. Phys. Chem. B* **2010**, *114*, 2840.

(23) Bodo, E.; Gontrani, L.; Caminiti, R.; Plechkova, N. V.; Seddon, K. R.; Triolo, A. *J. Phys. Chem. B* **2010**, *114*, 16398.

(24) Annapureddy, H. V. R.; Kashyap, H. K.; Biase, P. M. D.; Margulis, C. J. *J. Phys. Chem. B* **2010**, *114*, 16838.

(25) Xiao, D.; Jr., L. G. H.; Li, S.; Bartsch, R. A.; Quitevis, E. L.; Russina, O.; Triolo, A. *J. Phys. Chem. B* **2009**, *113*, 6426.

(26) Habasaki, J.; Ngai, K. L. *J. Chem. Phys.* **2008**, *129*, 194501.

(27) Wang, Y.; Jiang, W.; Yan, T.; Voth, G. A. *Acc. Chem. Res.* **2007**, *40*, 1193.

(28) Triolo, A.; Russina, O.; Bleif, H.-J.; Bleif, H.-J.; Cola, E. D. *J. Phys. Chem. B* **2007**, *111*, 4641.

(29) Rebelo, L. P. N.; Lopes, J. N. C.; Esperanca, J. M. S. S.; Guedes, H. J. R.; Lachwa, J.; Najdanovic-Visak, V.; Visak, Z. P. *Acc. Chem. Res.* **2007**, *40*, 1114.

(30) Iwata, K.; Okajima, H.; Saha, S.; Hamaguchi, H.-O. *Acc. Chem. Res.* **2007**, *40*, 1174.

(31) Xiao, D.; Rajian, J. R.; Li, S.; Bartsch, R. A.; Quitevis, E. L. *J. Phys. Chem. B* **2006**, *110*, 16174.

(32) Wang, Y.; Voth, G. A. *J. Phys. Chem. B* **2006**, *110*, 18601.

(33) Shigeto, S.; Hamaguchi, H. O. *Chem. Phys. Lett.* **2006**, *427*, 329.

(34) Lopes, J. C.; Gomes, M. F. C.; Padua, A. A. H. *J. Phys. Chem. B* **2006**, *110*, 16816.

(35) Lopes, J. A. C.; Padua, A. A. H. *J. Phys. Chem. B* **2006**, *110*, 3330.

(36) Hu, Z.; Margulis, C. J. *Proc. Natl. Acad. Sci. U. S. A.* **2006**, *103*, 831.

(37) Wang, Y.; Voth, G. A. *J. Am. Chem. Soc.* **2005**, *127*, 12192.

(38) Daschakraborty, S.; Biswas, R. *J. Chem. Sci.* **2012**, *124*, 763.

(39) Karve, L.; Dutt, G. B. *J. Phys. Chem. B* **2012**, *116*, 1824.

(40) Karve, L.; Dutt, G. B. *J. Phys. Chem. B* **2012**, *116*, 9107.

(41) Gangamallaiah, V.; Dutt, G. B. *J. Phys. Chem. B* **2012**, *116*, 12819.
(42) Das, S. K.; Sarkar, M. *J. Phys. Chem. B* **2012**, *116*, 194.
(43) Karve, L.; Dutt, G. B. *J. Phys. Chem. B* **2011**, *115*, 725.
(44) Khara, D. C.; Samanta, A. *Phys. Chem. Chem. Phys.* **2010**, *12*, 7671.
(45) Dutt, G. B. *Ind. J. Chem.* **2010**, *49A*, 705.
(46) Dutt, G. B. *J. Phys. Chem. B* **2010**, *114*, 8971.
(47) Mali, K. S.; Dutt, G. B.; Mukherjee, T. *J. Chem. Phys.* **2008**, *128*, 054504.
(48) Jin, H.; Baker, G. A.; Arzhantsev, S.; Dong, J.; Maroncelli, M. *J. Phys. Chem. B* **2007**, *111*, 7291.
(49) Ito, N.; Arzhantsev, S.; Maroncelli, M. *Chem. Phys. Lett.* **2004**, *396*, 83.
(50) Ito, N.; Arzhantsev, S.; Heitz, M.; Maroncelli, M. *J. Phys. Chem. B* **2004**, *108*, 5771.
(51) Ingram, J. A.; Moog, R. S.; Ito, N.; Biswas, R.; Maroncelli, M. *J. Phys. Chem. B* **2003**, *107*, 5926.
(52) Das, S. K.; Sahu, P. K.; Sarkar, M. *J. Phys. Chem. B* **2013**, *113*, 636.
(53) Zvaigzne, A. I.; Wolfe, J.; William E. Acree, J. *J. Chem. Eng. Data* **1994**, *39*, 541.
(54) *Reviews in Fluorescence*; Geddes, C. D.; Lakowicz, J. R., Eds.; Springer: New York, 2005, pp 199.
(55) Horng, M. L.; Gardecki, J. A.; Maroncelli, M. *J. Phys. Chem. A* **1997**, *101*, 1030.
(56) Anderton, R. M.; Kauffman, J. F. *J. Phys. Chem.* **1994**, *98*, 12117.
(57) Roy, M.; Doraiswamy, S. *J. Chem. Phys.* **1993**, *98*, 3213.
(58) Ben-Amotz, D.; Drake, J. M. *J. Chem. Phys.* **1988**, *89*, 1019.
(59) Gierer, A.; Wirtz, K. *Z. Nuturforsch. A* **1953**, *8*, 532.
(60) Edward, J. T. *J. Chem. Educ.* **1970**, *47*, 261.
(61) Paul, A.; Samanta, A. *J. Phys. Chem. B* **2007**, *111*, 4724.
(62) Guchhait, B.; Gazi, H. A. R.; Kashyap, H. K.; Biswas, R. *J. Phys. Chem. B* **2010**, *114*, 5066.

(63) Faetti, M.; Giordano, M.; Leporini, D.; Pardi, L. *Macromolecules* **1999**, *32*, 1876.

(64) Andreozzi, L.; Faetti, M.; Giordano, M.; Leporini, D. *J. Phys. Chem. B* **1999**, *103*, 4097.

(65) Andreozzi, L.; Schino, A. D.; Giordano, M.; Leporini, D. *Europhys. Lett.* **1997**, *38*, 669.

Chapter 8

Concluding Remarks

This chapter summarizes the results of the investigations delineated in the thesis. The scope of further studies based on the findings of the present work is also outlined.

8.1. Overview

The work embodied in this thesis has been undertaken with the primary objective of exploring the photophysical processes of some select organic solutes in RTILs. Excited state dynamics, charge transfer, solute rotation and solvation dynamics have been studied in these media for two specific reasons. Firstly, to explore the influence of the RTILs on the photophysical process which are difficult to understand in conventional solvents. Secondly, to understand the physicochemical properties of some new RTILs by studying the photophysical response of some well-studied organic solutes. Several instrumental techniques and methodologies, namely, IR and NMR spectroscopy for characterization, cone and plate viscometer, UV-visible absorption, steady-state and time-resolved fluorescence, room temperature and low temperature phosphorescence have been employed to carry out this work. The objectives of the various projects undertaken and the results obtained from these investigations have been outlined below.

The excited state dynamics of BA in several conventional organic solvents reveals that the two anthryl moieties of BA are decoupled, i.e. perpendicular to each other, in the ground state. In nonpolar solvents, BA emits from the

decoupled state upon photoexcitation. However, in polar medium the molecule emits from a planar conformer due to photoinduced conformational change in the excited state. The excited state relaxation process is very fast and can be followed only using a setup with an ultra-fast time resolution.

In the present study, we have used highly viscous nature of the ionic liquids to slow down the excited state dynamics such that it can be followed with the TCSPC time resolution. The excited dynamics of bianthryl (BA) has been studied in three imidazolium ionic liquids differing in their polarity and viscosity using steady-state and time-resolved fluorescence spectroscopy techniques. The steady-state emission spectra indicate that BA emits mainly from the relaxed CT state. Even though the dynamics of LE $\rightarrow$ CT transformation is quite fast in viscous ionic liquids, we could capture the early stage of the formation CT state from the LE state by using a time-resolved fluorescence study in our TCSPC setup. Following the formation of the CT state, a solvation process was could be observed. The average solvation time obtained in the present study is found to be quite similar to that obtained in earlier study, where ideal solvation probes were used.

The photophysical behavior of benzil, which is studied extensively in conventional organic solvents, is quite interesting. It undergoes excited state conformational relaxation process in both singlet and triplet states. Benzil exhibits room temperature phosphorescence, which is rarely observed for common organic molecule. It undergoes reverse intersystem crossing process $T_1 \rightsquigarrow S_1$ state by either the triplet-triplet annihilation (P-type) process or a thermally activated (E-type) process depending on the concentration of benzil in the solution. Relaxed

skew conformer of benzil and emission from a higher excited state (S_2) has been also observed. In this work, UV-visible absorption, steady-state and delayed emission of benzil have been studied in three imidazolium ionic liquids differing in their viscosity and polarity to understand the influence of the high viscosity, low solubility of the dissolved gases and microheterogeneous nature of the ionic liquids on these photophysical processes of benzil.

Steady-state absorption spectra of benzil indicate that the two carbonyl groups are more decoupled in these ionic liquids in comparison to the conventional organic solvents. Room temperature phosphorescence spectra, even in degassed condition, indicate the low solubility of oxygen in these ionic liquids. In the present study, E-type delayed fluorescence has been observed and rate of reverse intersystem crossing is found to be governed by the polarity of the ionic liquids. The excitation wavelength dependent phosphorescence spectra at liquid nitrogen temperature (77 K) reveal the presence of multiple conformers of benzil in the ground state.

In order to understand the physicochemical properties of RTILs the fluorescence behavior of a large number of neutral solutes has been studied. In the present study, we have explored the steady-state and time-resolved fluorescence behavior of charged solutes, anionic, ANS and cationic, EB in one imidazolium ionic liquid, to understand the influence of electrostatic forces in ionic liquid.

Steady-state emission spectra of ANS and EB are found to be similar to the respective spectra in conventional organic solvents. Rotational dynamics of charged solutes in imidazolium ionic liquid suggests that van der Waals and specific interactions between the solute and ionic liquid play more important role

in directing the rotational dynamics of solute rather than the electrostatic interaction. The rotational dynamics of the charged solutes have been found to be similar in RTIL and isoviscous conventional solvent. Solvation dynamics studies also did not reveal any difference in solvation time obtained from the previous studies where neutral solutes were used as a solvation probe.

RTILs based on the N, N′-dialkylimidazolium salts have thus far been the most widely studied because of their attractive physical properties. However, considering the high cost of industrial scale synthesis of these salts, the focus seems to be shifting gradually towards other less expensive alternatives such as the morpholinium RTILs, which are not only cheap and easy to develop, but also possess good physicochemical characteristics.

A series of N-alkyl-N-methylmropholinium RTILs have been explored by monitoring the temperature dependent steady-state and time-resolved fluorescence behavior of C153. The spectral data reveals that the polarity of the RTILs decreases with increase in the alkyl chain length of the cation. Excitation wavelength dependent emission spectra of C153 in these media indicate that these ionic liquids are more heterogeneous than the imidazolium, ammonium, phosphonium and pyrrolidinium ionic liquids. Temperature dependent rotational and solvation dynamics studies also suggest more structured nature of these RTILs.

The rotational dynamics of solute provides valuable information on the interaction between the solute and solvent and sheds considerable light on the physicochemical properties of the medium.

Rotational dynamics of two dipolar solutes (**AP** and **PRODAN**) and a nonpolar solute (**anthracene**) have been studied by measuring the time-resolved fluorescence anisotropy of the systems in a series of N-alkyl-N-methylmorpholinium ionic liquids to understand the physicochemical properties of RTILs. The results obtained in this study have been analyzed in terms of Stokes-Einstein-Debye (SED) model, which confirms the heterogeneity of these RTILs that is indicated in the previous chapter. This study also reveals distribution of the probes in distinct regions, which differ in their environments, depending on the nature of the solutes.

8.2. Future scope and challenges

The dual physicochemical properties, high viscosity and polarity of the RTILs have been utilized to study the photoinduced excited state conformation dynamics of bianthryl and benzil. It was expected that the high viscosity of the RTILs would slow down the excited state dynamics which would allow us to follow the dynamics despite the limited time resolution of the instrument. However, the present study reveals that these processes are quite fast even in these viscous media. Recently, the domain structure of the RTILs has been established more firmly. Perhaps, the fast dynamics in a viscous media is a reflection of the microviscosity being much lower than the bulk viscosity. This is an aspect that needs a more detailed and deeper investigation.

Solvation and rotational dynamics of charged solutes in imidazolium ionic liquid reveals that the van der Waals and specific interactions between the solute and ionic liquids play much more important roles in dictating the rotation of a

solute rather than the electrostatic interaction. The reason for this behavior is however not very clear at this moment. A better understanding of this aspects requires more thorough and extensive investigation involving the charged solutes and RTILs by other techniques such as Fluorescence Correlation Spectroscopy (FCS), Time-resolved Electron Spin Resonance (Tr-EPR) spectroscopy etc.

The steady-state and time-resolved fluorescence behavior of some well-studied fluorophores in a series of N-alkyl-N-methylmorpholinium ionic liquids reveals that the morpholinum ionic liquids are more structured compared to the other ionic liquids, so far explored. However, the exact structure of these ionic liquids is hardly known. In order to have a clear understanding of the structural features of these ionic liquids it is necessary to study these ionic liquids by other techniques. Small and Wide Angle X-ray (SWAX), Fluorescence Correlation Spectroscopy (FCS), Time-resolved Electron Spin Resonances (Tr-EPR) spectroscopy, neutron scattering, Raman Scattering, optical Kerr effect, can provide a more detailed and clear picture on the structural features of these ionic liquids.